



Imagerie de la microcirculation cérébrale par vidéomicroscopie Sidestream Dark Field : application à l'étude de l'oedème péritumoral dans les méningiomes intracrâniens

Moncef Berhouma

► To cite this version:

Moncef Berhouma. Imagerie de la microcirculation cérébrale par vidéomicroscopie Sidestream Dark Field : application à l'étude de l'oedème péritumoral dans les méningiomes intracrâniens. Biotechnologie. Université de Lyon, 2020. Français. NNT : 2020LYSE1310 . tel-03617208

HAL Id: tel-03617208

<https://theses.hal.science/tel-03617208v1>

Submitted on 23 Mar 2022

HAL is a multi-disciplinary open access archive for the deposit and dissemination of scientific research documents, whether they are published or not. The documents may come from teaching and research institutions in France or abroad, or from public or private research centers.

L'archive ouverte pluridisciplinaire **HAL**, est destinée au dépôt et à la diffusion de documents scientifiques de niveau recherche, publiés ou non, émanant des établissements d'enseignement et de recherche français ou étrangers, des laboratoires publics ou privés.

N°d'ordre NNT :
2020LYSE1310



THESE de DOCTORAT DE L'UNIVERSITE DE LYON

Opérée au sein de

L'Université Claude Bernard Lyon 1

ECOLE DOCTORALE INTERDISCIPLINAIRE SCIENCE SANTE

N°205

Spécialité de doctorat : SCIENCES

Soutenue publiquement le 07 Décembre 2020, par :

Moncef BERHOUMA

Imagerie de la microcirculation cérébrale par
vidéomicroscopie Sidestream Dark Field : Application à
l'étude de l'œdème péritumoral dans les méningiomes
intracrâniens

Devant le jury composé de :

Marie-Reine LOSSER, Professeur, CHU Nancy, Rapporteur

Emmanuel GAY, Professeur, CHU Grenoble, Rapporteur

Anne-Claire LUKASZEWICZ, Professeur, CHU Lyon, Examinateuse

Jacques GUYOTAT, Praticien Hospitalier, CHU Lyon, Examinateur

François COTTON, Professeur, CHU Lyon, Directeur

Vivien SZABO, Chercheur, CHU Montpellier, Invité

Université Claude Bernard – LYON 1

Administrateur provisoire de l'Université	M. Frédéric FLEURY
Président du Conseil Académique	M. Hamda BEN HADID
Vice-Président du Conseil d'Administration	M. Didier REVEL
Vice-Président du Conseil des Etudes et de la Vie Universitaire	M. Philippe CHEVALLIER
Vice-Président de la Commission de Recherche	M. Jean-François MORNEX
Directeur Général des Services	M. Pierre ROLLAND

COMPOSANTES SANTE

Département de Formation et Centre de Recherche en Biologie Humaine	Directrice : Mme Anne-Marie SCHOTT
Faculté d'Odontologie	Doyenne : Mme Dominique SEUX
Faculté de Médecine et Maïeutique Lyon Sud - Charles Mérieux	Doyenne : Mme Carole BURILLON
Faculté de Médecine Lyon-Est	Doyen : M. Gilles RODE
Institut des Sciences et Techniques de la Réadaptation (ISTR)	Directeur : M. Xavier PERROT
Institut des Sciences Pharmaceutiques et Biologiques (ISBP)	Directrice : Mme Christine VINCIGUERRA

COMPOSANTES & DEPARTEMENTS DE SCIENCES & TECHNOLOGIE

Département Génie Electrique et des Procédés (GEP)	Directrice : Mme Rosaria FERRIGNO
Département Informatique	Directeur : M. Behzad SHARIAT
Département Mécanique	Directeur M. Marc BUFFAT
Ecole Supérieure de Chimie, Physique, Electronique (CPE Lyon)	Directeur : Gérard PIGNAULT
Institut de Science Financière et d'Assurances (ISFA)	Directeur : M. Nicolas LEBOISNE
Institut National du Professorat et de l'Education	Administrateur Provisoire : M. Pierre CHAREYRON
Institut Universitaire de Technologie de Lyon 1	Directeur : M. Christophe VITON
Observatoire de Lyon	Directrice : Mme Isabelle DANIEL
Polytechnique Lyon	Directeur : Emmanuel PERRIN
UFR Biosciences	Administratrice provisoire : Mme Kathrin GIESELER
UFR des Sciences et Techniques des Activités Physiques et Sportives (STAPS)	Directeur : M. Yannick VANPOULLE
UFR Faculté des Sciences	Directeur : M. Bruno ANDRIOLETTI

DEDICACE

REMERCIEMENTS

RESUME

Constituant un réseau vasculaire primordial situé entre les versants artériel et veineux, la microcirculation cérébrale est impliquée principalement dans le couplage entre l'activité neuronale et la régulation du débit sanguin cérébral, mais intervient également dans diverses situations pathologiques telles l'hémorragie sous-arachnoïdienne ou au sein de l'environnement immédiat des tumeurs cérébrales. L'imagerie de la microcirculation cérébrale repose essentiellement sur des techniques macroscopiques pré-opératoires (IRM, TDM, PET...). Une étude plus fine à l'échelle microscopique et surtout per-opératoire pourrait permettre de mieux comprendre la physiopathologie de certaines situations cliniques (œdème péritumoral par exemple) et de monitorer le débit sanguin cérébral local lors de certaines interventions neurochirurgicales (malformations vasculaires...). Diverses technologies ont été développées pour une utilisation per-opératoire mais beaucoup restent limitées par leur résolution temporelle et/ou spatiale, leur coût, leur possibilité ou non de proposer une évaluation quantitative et enfin leur intégration dans le processus chirurgical. Parmi ces technologies, seule la vidéomicroscopie permet une étude à la fois morphologique et semi-quantitative de la microcirculation. Après avoir rappelé les notions fondamentales de la microcirculation cérébrale et les méthodes actuelles de son imagerie, nous avons appliqué la vidéomicroscopie per-opératoire à l'étude de l'œdème péritumoral dans les méningiomes intracrâniens afin d'essayer de mieux en comprendre la pathogénie. Nous conclurons sur les perspectives qu'ouvre cette technique d'imagerie per-opératoire en neurochirurgie.

Mots clés :

Débit sanguin cérébral ; Imagerie ; Méningiome ; Microcirculation ; Monitoring per-opératoire ; Œdème péritumoral ; Vidéomicroscopie

Caractères : 1697

ABSTRACT

Cerebral microcirculation represents a primordial network embedded between the arterial and venous beds, and is mainly involved in the coupling of neuronal activity and cerebral blood flow regulation, as well as in some pathological conditions such as subarachnoid hemorrhage and in the peritumoral environment of brain tumors. Imaging of cerebral microcirculation mainly relies on pre-operative macroscopic technologies (MRI, CT-Scan, PET...). A more accurate microscopic and intraoperative technology for microcirculation imaging may help better understanding the pathogenesis of specific pathological conditions (peritumoral edema...) or assist for the monitoring of local cerebral blood flow during specific neurosurgical procedures (vascular malformations...). Several technologies have been developed for the intraoperative microcirculation imaging but remain limited by their temporal/spatial resolution, cost, ability to provide quantitative measurements or their integration in the surgical workflow. Among these technologies, only videomicroscopy provides a morphological imaging of microcirculation as well as semi-quantitative measurements. After a reminder of the key notions of cerebral microcirculation and available imaging technologies, we present an application of videomicroscopy in the peritumoral edema in meningiomas and we discuss the perspectives of use in neurosurgery.

Keywords :

Cerebral blood flow; Imaging; Intra-operative monitoring; Meningioma; Microcirculation; Peri-tumoral edema; Videomicroscopy

Characters : 1389

Table des matières

I - INTRODUCTION	12
II - MICROCIRCULATION ET DEBIT SANGUIN CEREBRAL.....	14
II.1 - LA MICROCIRCULATION CEREBRALE	14
II.2 - LA BARRIERE HEMATO-ENCEPHALIQUE	15
II.3 - REGULATION DU DEBIT SANGUIN CEREBRAL.....	20
III - MONITORING PER-OPERATOIRE DU DEBIT SANGUIN CEREBRAL ET IMAGERIE DE LA MICROCIRCULATION EN NEUROCHIRURGIE.....	32
IV - PATHOGENIE DE L'ŒDEME PERITUMORAL DANS LES MENINGIOMES INTRA- CRANIENS	78
V - ANOMALIES DE LA MICROCIRCULATION DANS L'ŒDEME PERI-TUMORAL : APPLICATION PEROOPERATOIRE DE LA VIDEOMICROSCOPIE SIDESTREAM DARK FIELD AUX MENINGIOMES INTRACRANIENS	95
VI - SYNTHESE - PERSPECTIVES	113

ABBREVIATIONS

SDF : Sidestream dark field imaging

DSC : Débit sanguin cérébral

PPC : Pression de perfusion cérébrale

RVC : Résistance vasculaire cérébrale

PIC : Pression intracrânienne

PAM : Pression artérielle moyenne

IRM : Imagerie par résonance magnétique

TDM : Tomodensitométrie

PET-Scan : tomographie par émission de positons

I - INTRODUCTION

La microcirculation cérébrale représente un réseau vasculaire essentiel interposé entre les artéries et les veinules cérébrales, impliqué principalement dans les échanges avec le parenchyme cérébral. Son étude participe à la compréhension des phénomènes complexes de couplage entre l'activité neuronale et la régulation du débit sanguin cérébral (DSC), mais également du rôle de la microcirculation dans diverses situations pathologiques telles l'ischémie, les tumeurs cérébrales ou les hémorragies méningées. L'étude de la microcirculation repose principalement sur l'imagerie de perfusion basée sur l'imagerie par résonance magnétique (IRM), la tomodensitométrie (TDM) ou encore la tomographie d'émission de positons (PET-Scan). Durant les 2 dernières décennies, ces techniques se sont perfectionnées en particulier grâce à l'amélioration significative de leurs résolutions temporelle et spatiale. Néanmoins, ces dernières ne permettent pas une étude fine à l'échelle de la microcirculation et ne sont pas facilement utilisables en per-opératoire. Or l'imagerie et la surveillance (monitoring) de la microcirculation lors d'un geste neurochirurgical sont essentiels pour tenter de réduire la morbidité et la mortalité opératoire dans diverses pathologies en particulier vasculaires (anévrismes artériels, malformations artéioveineuses, anastomoses vasculaires) et tumorales (cartographie cérébrale des zones fonctionnelles par exemple). Diverses technologies ont été développées pour une utilisation per-opératoire mais beaucoup restent limitées par leur résolution temporelle et/ou spatiale, leur coût, leur possibilité ou non de proposer une évaluation quantitative et enfin leur intégration dans le processus chirurgical : Technologies laser (laser doppler flowmetry, laser speckle contrast imaging), vidéomicroscopie (sidestream dark field imaging, orthogonal polarized spectral imaging), microscopie confocale,

spectroscopie infrarouge, échographie fonctionnelle, IRM per-opératoire, doppler, thermographie,...

Parmi ces technologies, seule la vidéomicroscopie permet d'obtenir une imagerie morphologique de la microcirculation (densité vasculaire par mm²) en plus de fournir des informations semi-quantitatives sur la perfusion cérébrale dans le champ étudié. Dans ce travail, nous rappellerons dans un premier temps les notions essentielles concernant la microcirculation cérébrale et la régulation du débit sanguin cérébral. Nous détaillerons ensuite les différentes technologies permettant une imagerie per-opératoire de la microcirculation en approfondissant pour chacune d'entre elles les points forts et les limites. Nous nous intéresserons spécifiquement à la vidéomicroscopie sidestream dark field imaging (SDF), avec une étude de faisabilité pour l'étude de la microcirculation au sein de l'œdème péritumoral dans les méningiomes intracrâniens. En effet, dans cette pathologie, la présence d'un œdème péritumoral n'est pas rare touchant entre 38 et 67% des méningiomes intracrâniens, impactant ainsi la morbidité des patients et compliquant leur prise en charge. La pathogénie de cet œdème, toujours débattue, est multifactorielle incluant de possibles perturbations microcirculatoires. Ces dernières ont été étudiées macroscopiquement en IRM de perfusion et en PET-Scan, mais à notre connaissance aucune preuve à l'échelle microscopique n'a été apportée jusque-là *in vivo*. Nous émettons donc l'hypothèse qu'il existe bien des anomalies de la microcirculation dans l'œdème péritumoral incluant à la fois des anomalies de densité vasculaire que des anomalies de perfusion cérébrale. Nous conclurons enfin sur les perspectives qu'offrent ces technologies peropératoires pour la compréhension de la physiopathologie de la microcirculation cérébrale et pour la réduction de la morbidité chirurgicale.

II - MICROCIRCULATION ET DEBIT SANGUIN CEREBRAL

II.1 - La microcirculation cérébrale

La microcirculation se définit comme un réseau très étendu, dense et complexe de petits vaisseaux de moins de 200 µm de diamètre¹ comprenant artéries, veinules et capillaires (5 à 8 µm de diamètre). Outre le transport des substrats vitaux aux tissus et l'évacuation de leurs déchets, ce réseau joue un rôle majeur dans la régulation de l'hémodynamique et la résistance vasculaires, l'hémostase, l'inflammation et l'immunité.[1] Au niveau cérébral, les artères piales forme un réseau anastomotique très riche au sein des espaces sous-arachnoïdiens à la surface du cerveau. A ce niveau, il existe également des anastomoses physiologiques artérioveineuses généralement inférieures à 12 m de diamètre.

Les artères piales donnent naissances aux artères intracérébrales qui pénètrent le parenchyme cérébral dont elles sont séparées par une simple couche de cellules piales fibroblaste-like et une membrane dérivée des astrocytes appelée *glia limitans* formant ainsi la membrane externe des espaces péri-vasculaires de Virchow-Robin. Les artères intracérébrales se divisent ensuite en artéries pré-capillaires puis en capillaires. Au niveau des artères intracérébrales, la paroi vasculaire est essentiellement formée des cellules musculaires lisses. Au niveau capillaire, les péricytes, formant une grande partie de la paroi vasculaire, communiquent avec les cellules endothéliales via des connexions synapse-like (connexines et cadhérines). Outre les péricytes, les pieds astrocytaires viennent englober la paroi vasculaire (Figure 1). L'ensemble de ces cellules vasculaires (cellules endothéliales, péricytes, cellules musculaires lisses), les cellules gliales (astrocytes, microglie et oligodendrocytes), la membrane basale et les neurones forment l'unité neurovasculaire. Cette dernière constitue une barrière hautement

¹ Le diamètre pris en compte dans la définition de la microcirculation est très variable selon les publications variant de 20 à 200 µm

spécialisée au niveau cérébral assurant l'homéostasie et contrôlant la perméabilité vasculaire : la barrière hémato-encéphalique (BHE).

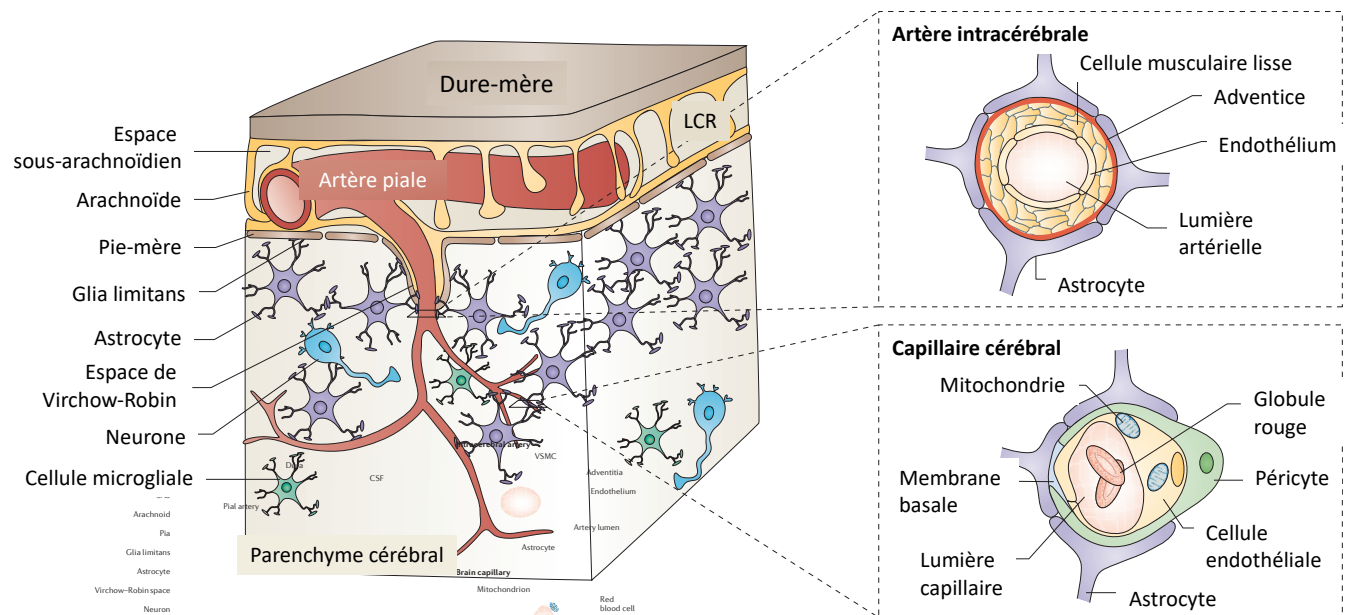


Figure 1 : Architecture de la microcirculation cérébrale (adapté de Zlokovic [2])

II.2 - La barrière hémato-encéphalique

La BHE représente une barrière biologique séparant le parenchyme cérébral de la circulation sanguine. Elle est essentiellement constituée des cellules endothéliales avec leurs jonctions intercellulaires, mais également des péricytes et des pieds astrocytaires (Figure 2) :

- a) **Cellules endothéliales** : Au niveau des capillaires cérébraux, ces cellules possèdent un phénotype particulier qui les distingue des cellules endothéliales d'autres organes : épaisseur uniforme de leur cytoplasme, présence de jonctions intercellulaires (jonctions serrées et jonctions adhérentes), présence d'une lame basale continue, un faible niveau

d'endocytose, une surface chargée négativement, l'expression de plusieurs récepteurs et transporteurs membranaires, et une forte concentration de mitochondries.

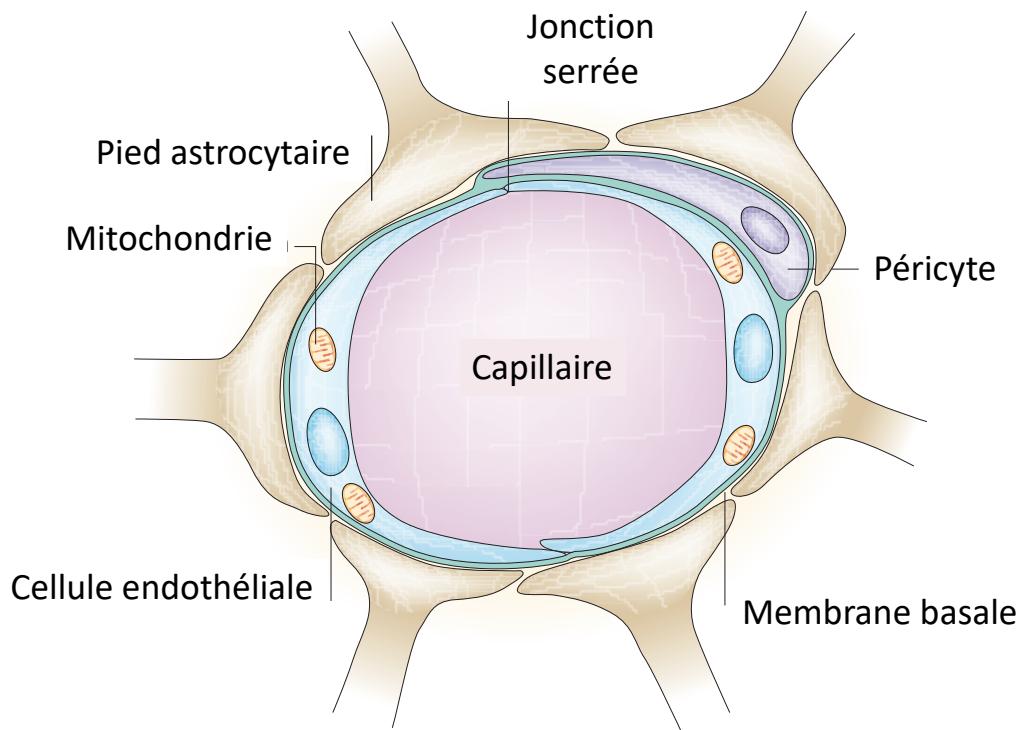


Figure 2 : Organisation cellulaire de la BHE (adapté de Loscher & Potschka, 2005). [3]

b) Les jonctions intercellulaires : Ces structures limitent considérablement la perméabilité vasculaire. On distingue les jonctions serrées (Tight junctions – TJ) et les jonctions adhérentes (Adherent junctions – AJ) (Figure 3).

Les jonctions serrées sont concentrées dans les régions apicales des cellules endothéliales, constituant des complexes protéiques transmembranaires et intracytoplasmiques. Il existe plusieurs types de

jonctions serrées : Les claudines, famille de 24 protéines reliées entre elles et formant de multiples boucles extracellulaires renforçant ainsi l'étanchéité ; l'occludine, constituée de 2 boucles extracellulaires et trois domaines intracytoplasmiques ancrés au cytosquelette par les zonula occludens (ZO) ; la molécule d'adhésion jonctionnelle (JAM) impliqués dans la migration transmembranaire des leucocytes ; et différentes protéines accessoires participant au complexe jonctionnel (zonula occludens 1 à 3 et cinguline).

Les jonctions adhérentes sont situées en dessous des jonctions serrées et comprennent des glycoprotéines transmembranaires de la famille des cadhérines, reliées solidement au cytosquelette à l'aide des protéines α -caténine et β -caténine.

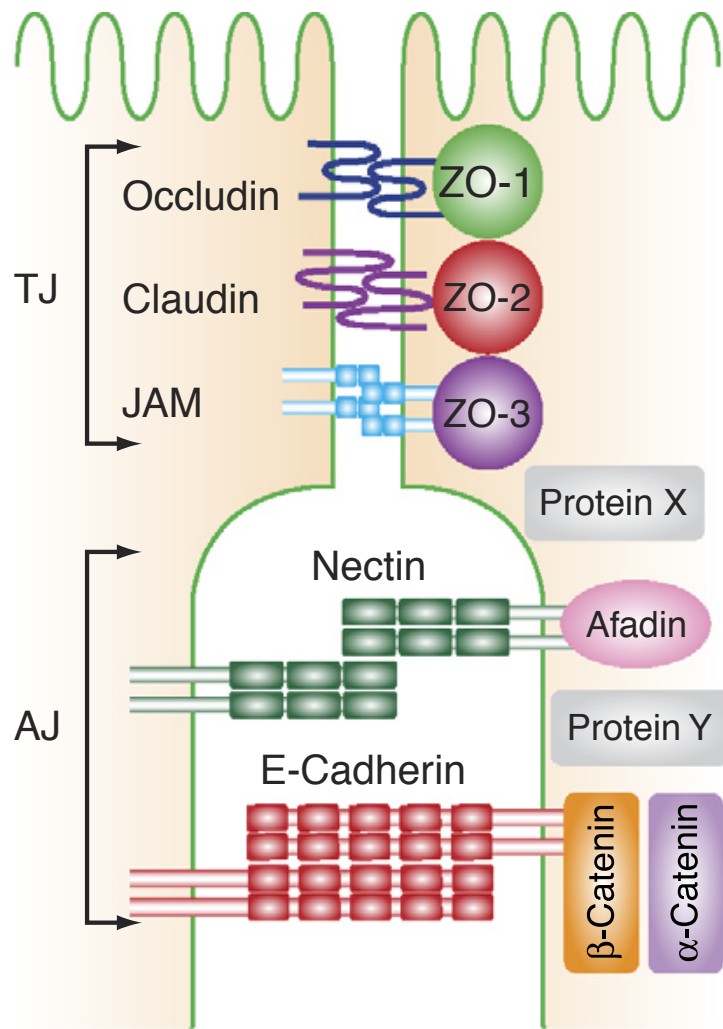


Figure 3 : Schématisation des jonctions adhérentes (AJ) et des jonctions serrées (TJ) entre les cellules endothéliales cérébrales (Miyoshi & Takai, 2005). [4]

c) **Les péricytes :** Encore dénommées cellules de Rouget, les péricytes englobent les cellules endothéliales en s'accrochant à des protéines de la membrane basale. Ils jouent un rôle clé dans la régulation du diamètre capillaire et donc du DSC, mais également lors de la vasculogenèse et l'angiogenèse.

- d) La membrane basale :** Produite par les cellules endothéliales, elle est constituée de collagène, d'élastine, de fibronectine, de protéoglycans et de laminine. Elle s'organise en 3 couches superposées : Une couche produite par les cellules endothéliales, une couche produite par les astrocytes et une couche intermédiaire faite de collagène. La membrane basale sert principalement à l'ancre et l'organisation des différentes cellules de la BHE.
- e) Les astrocytes :** Outre un rôle physique dans la constitution de la BHE, ces cellules gliales sont richement connectées aux neurones et aux autres capillaires régionaux et participent à l'élimination de différents neurotransmetteurs présents dans l'espace extracellulaire. Les astrocytes jouent également un rôle primordial dans la régulation du DSC local notamment par la production de NO.

La BHE forme ainsi une interface de 12 à 18 m² entre le lit vasculaire cérébral et le système nerveux central. La passage para-cellulaire étant très restreint, la BHE contrôle le passage des substances par différentes modalités distinctes selon la nature de la substance (Figure 4) : (i) La diffusion passive, basée sur un gradient de concentration, est limitée aux petites molécules liposolubles (certains médicaments par exemple) ; (ii) La diffusion par des transporteurs protéiques membranaires spécifiques et saturables, d'influx et d'efflux ; (iii) La transcytose par récepteur membranaire spécifique particulièrement pour l'insuline et la transferrine ; (iv) La transcytose adsorptive pour des molécules plus larges chargées positivement (albumine,...).

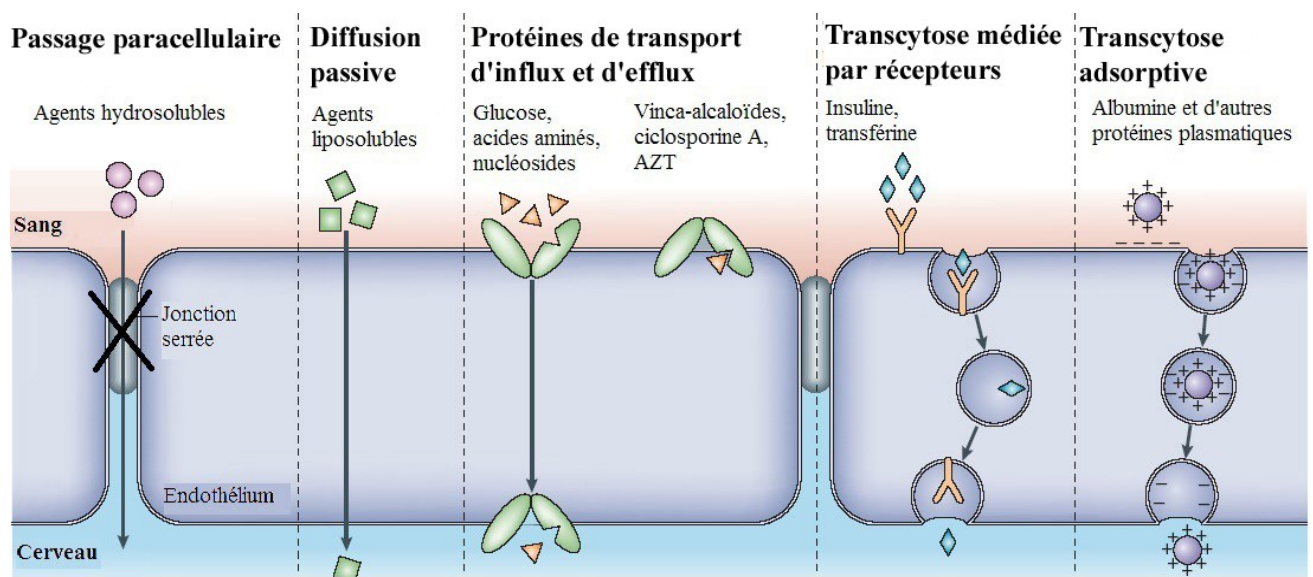


Figure 4 : Modes de passage à travers la BHE (adapté de Abbott et al. 2006).
[5]

II.3 - Régulation du débit sanguin cérébral

Par rapport à la circulation extra-cérébrale, la circulation cérébrale repose sur certaines particularités :

- L'absence de réserves d'oxygène et de glucose dans le cerveau le rend particulièrement dépendant des apports extérieurs, expliquant l'importance du DSC par rapports aux autres organes. Le DSC moyen est estimé à 50 ml/100g/min représentant 15% du débit cardiaque (Substance grise 80 ml/100g/min – Substance blanche 20 ml/100g/min). Par ailleurs la consommation cérébrale de dioxygène (O_2) représente 20 % de la consommation totale de l'organisme, soit 3,5 ml/100g/min.
- Le DSC dépend directement de la pression de perfusion cérébrale (PPC = PAM - PIC) et de la résistance vasculaire cérébrale (RVC) :

$$DSC = \frac{PPC}{RVC}$$

La RVC est fonction de la PIC, de l'état structurel anatomique des vaisseaux, de la viscosité sanguine et du tonus vasculaire cérébral. Dans les conditions normales, la RVC dépend principalement du tonus vasculaire cérébral. Quatre facteurs interviennent dans la régulation de la RVC et donc du DSC : Un facteur métabolique, un facteur humorale, un facteur nerveux, et un facteur myogène.

a) Facteur métabolique

Il s'agit du contrôle du DSC par l'activité neuronale, ou couplage débit/métabolisme illustré par la relation linéaire entre le DSC dans une région cérébrale déterminée et la consommation en glucose (Figure 5) [6] et en dioxygène (Figure 6) [7].

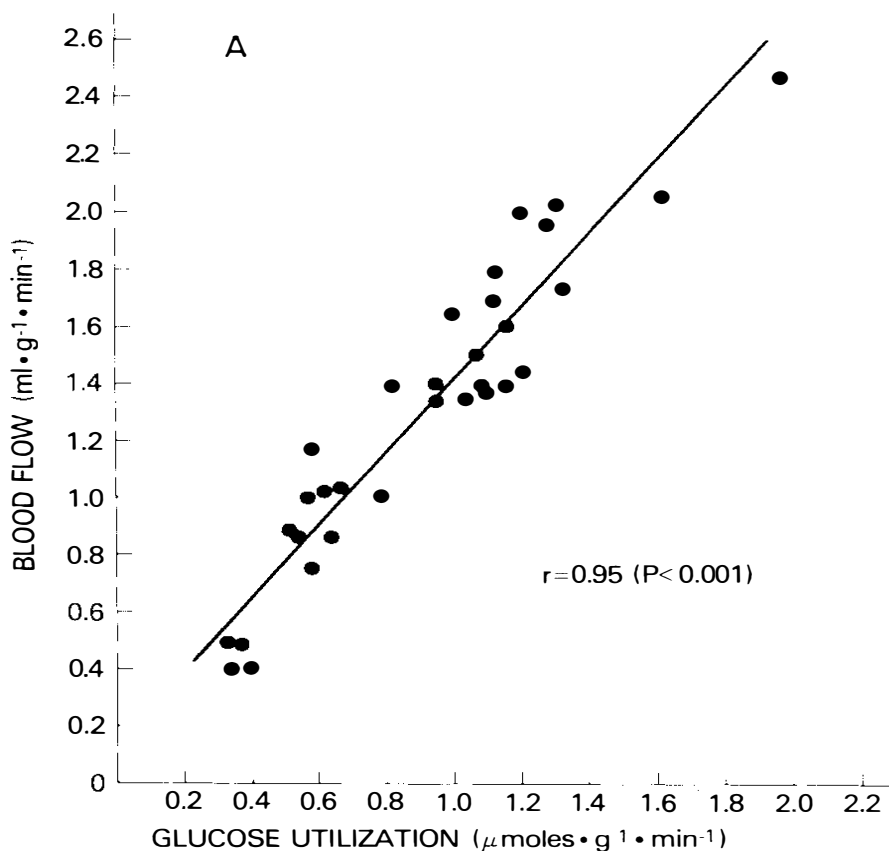


Figure 5 : Relation entre l'utilisation locale de glucose et le DSC local (Technique d'autoradiographie selon la méthode du 2-déoxyglucose de Sokoloff L., 1981) [6]

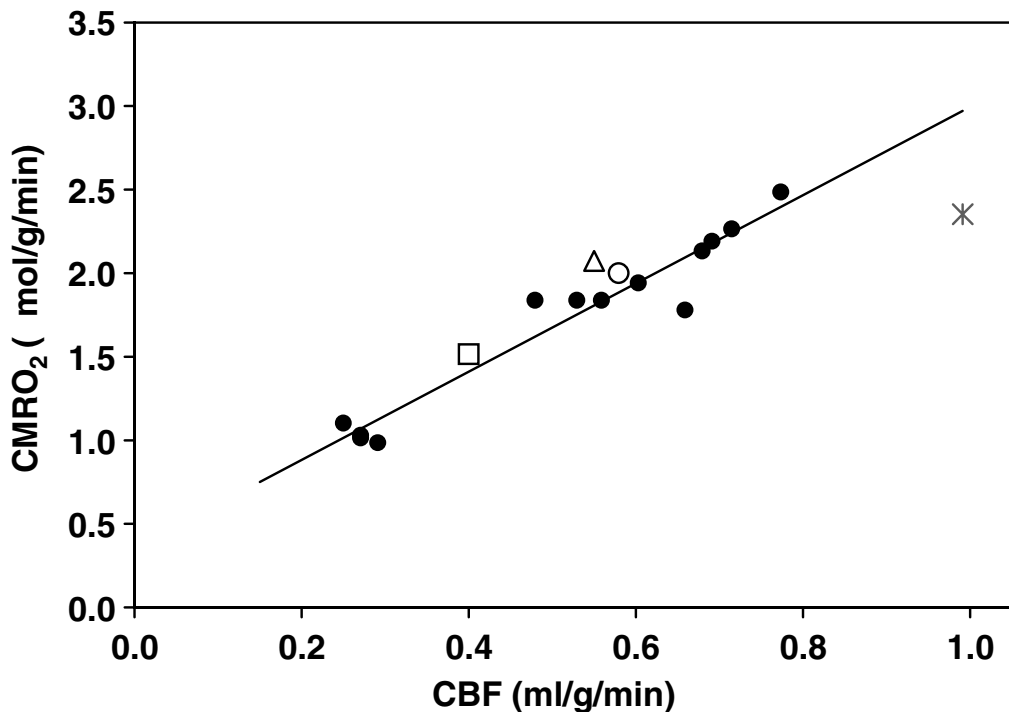


Figure 6 : Relation linéaire entre le DSC (CBF) et la consommation locale en dioxygène (CMRO₂) (Zhu et al., 2007). [7]

Le mécanisme de ce couplage débit/métabolisme est complexe et basé essentiellement sur trois processus distincts mais concomitants et coordonnés :

- i. Le couplage neurovasculaire : Cette hyperhémie fonctionnelle traduit une adaptation instantanée du diamètre des artéries cérébrales aux besoins accrus en nutriments secondaires à une

activité neuronale. Le rôle des astrocytes est majeur dans ce couplage en particulier par une augmentation brutale de leur concentration intracytosolique en calcium à l'origine d'une vasodilatation locale (Figure 7). [8]

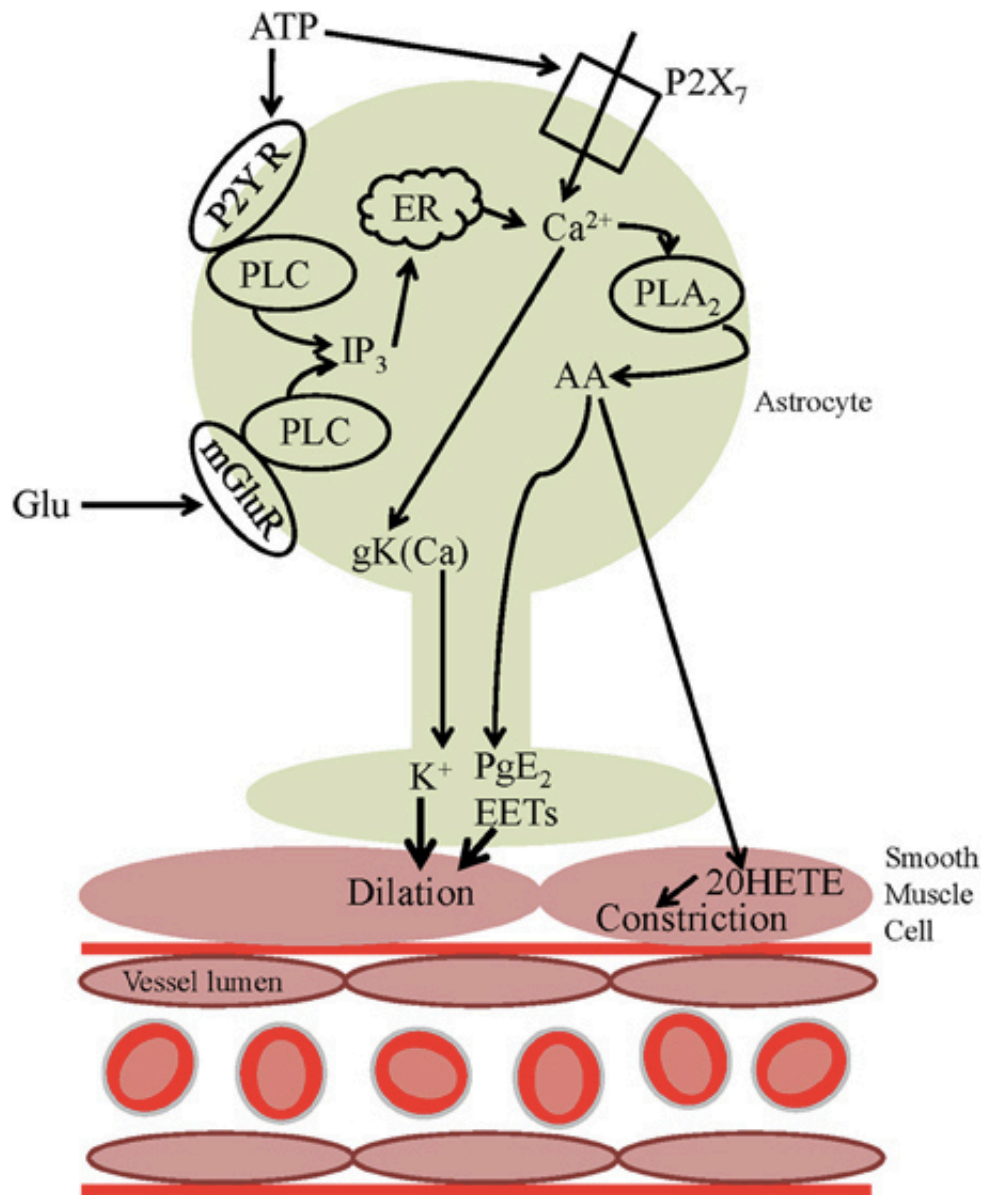


Figure 7 : Voies de signalisation astrocytaire calcium-dépendante. La libération de glutamate par les neurones active la phospholipase C (PLC) via le récepteur métabotropique à glutamate (mGluR) augmentant la concentration intracytosolique de calcium. Cette dernière active à son tour la phospholipase A2 (PLA2) provoquant la libération d'acide arachidonique (AA) métabolisé en PgE₂ et EETs. Ces derniers entraînent une dilatation par augmentation du K⁺. De plus, l'ATP active les récepteurs P2Y₇ qui stimulent également la PLA2 et la libération d'AA. AA provoque une contraction via 20HETE. Les voies sont schématisées dans l'astrocyte (en vert) et leurs effets sur la cellule musculaire lisse (en rouge) sont indiqués.

prostaglandines E2 (PgE2) et acides epoxyeicosatriénoïques (EETs), tous deux secrétés par le pied astrocytaire pour diffuser vers les muscles lisses artériolaires provoquant une vasodilatation par activation des canaux potassiques. Une voie alternative a été décrite impliquant l'adénosine triphosphate (ATP) qui peut activer la voie descendante vasoactive calcique soit via le récepteur P2Y et la voie PLC soit via le récepteur P2X7 agissant directement sur la concentration intracytosolique de calcium. A l'inverse, l'AA peut être sécrété directement à partir de l'astrocyte pour être métabolisé dans la cellule musculaire lisse en acide 20-hydroxyéicosatétraénoïque (20HETE), vasoconstricteur par inhibition des flux potassiques. Outre l'activation de la voie PLA2-AA, l'augmentation de la concentration intracytosolique de calcium peut directement activer les canaux BKCa et conséquemment la libération de K+, élément vasodilatateur. [8]

ii. La vasodilatation dépendante du flux : Celle-ci est induite par une augmentation des forces de cisaillement (*shear stress*) sur les parois vasculaires, secondaire à l'augmentation du débit sanguin.[9] Ces forces dépendent du débit sanguin dans le vaisseau en question, de la viscosité du sang et du diamètre vasculaire. La vasodilatation dépendante du flux résulte d'une réponse des cellules endothéliales aux forces de cisaillement sous la forme principalement d'une sécrétion de NO (Figure 8) et accessoirement de l'activateur tissulaire de plasminogène (t-Pa) et de prostacycline PGI2. La transformation d'un stimulus mécanique en une réponse biochimique au sein des cellules endothéliales est un mécanisme encore non élucidé, probablement complexe impliquant des récepteurs à activité tyrosine kinase, des récepteurs couplés à une protéine G, des canaux ioniques, des protéines d'adhérence, et le

glycocalyx.[10] La vasodilatation dépendante du flux peut intervenir dans tout l'arbre vasculaire mais prédomine clairement dans les artéries et les capillaires, et fait donc suite à l'augmentation du débit sanguin lui-même induit par l'activité neuronale (couplage neuro-vasculaire).

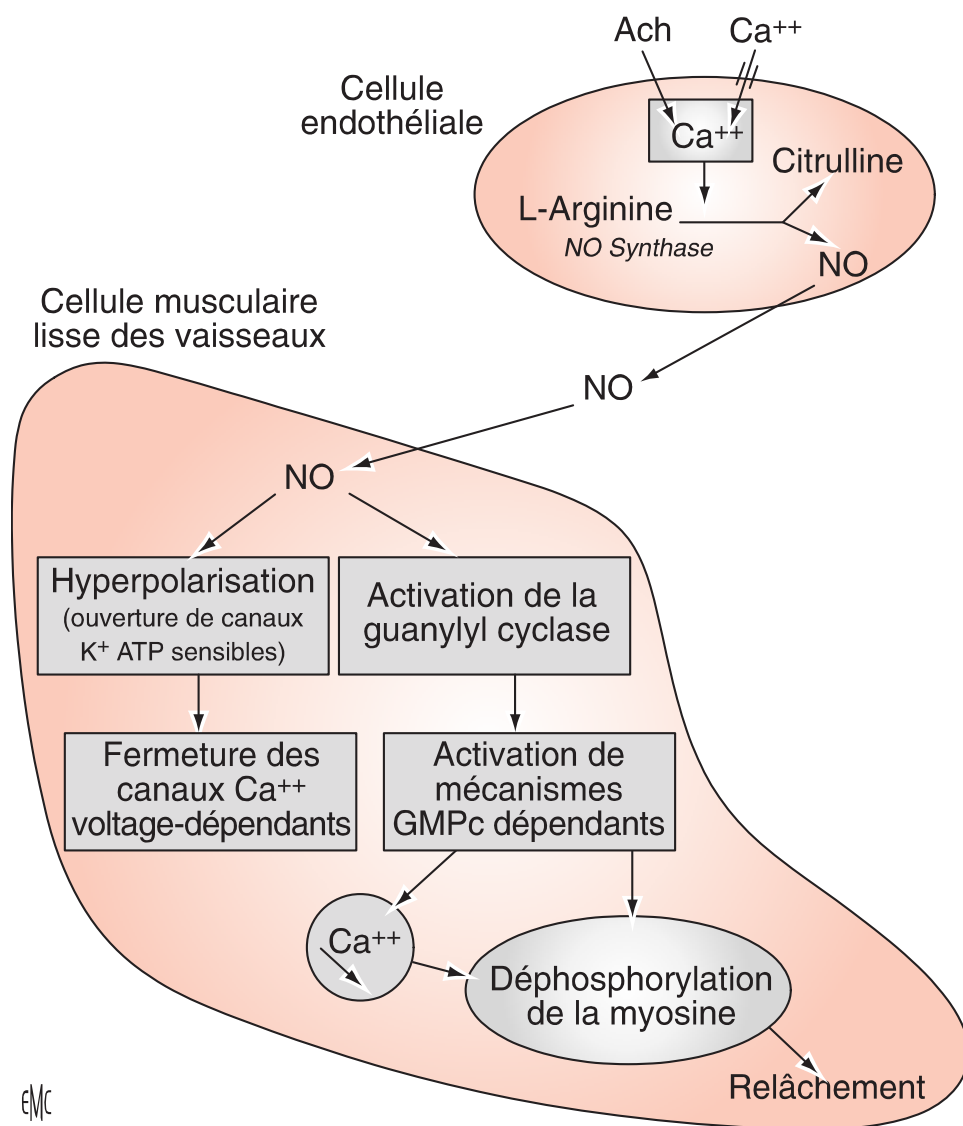


Figure 8 : Synthèse et mécanisme d'action du NO lors de la vasodilatation dépendante du flux. L'activation de la NO-Synthase par l'acétylcholine et

le calcium dans la cellule endothéiale provoque la sécrétion de NO puis l'activation de la guanylyl cyclase dans la cellule musculaire lisse et in fine la diminution de la concentration de calcium et une vasodilatation (Dupui & Géraud, 2006). [11]

iii. La vasodilatation rétrograde propagée : Cette vasodilatation se développe dans le sens opposé au flux sanguin donc en amont et à distance de la zone d'activation neuronale. Le mécanisme de cette vasodilatation reste débattu : La vasodilatation induite par l'activité neuronale lors du couplage neurovasculaire serait à l'origine d'un courant hyperpolarisant longitudinal diffusant le long des cellules endothéliales des artéries intra-parenchymateuses aux artères piales, occasionnant ainsi une diminution des résistances vasculaires cérébrales. Cette vasodilatation à distance permettrait de protéger les zones cérébrales non hyperactives.

b) Facteur humoral

Ce facteur correspond à l'effet de diverses substances circulantes sur le DSC : L'aldostérone, l'adrénaline, le CO₂ et l'O₂. Il existe une très forte sensibilité de l'ensemble de l'arbre artériel encéphalique (des artères extra-cérébrales aux artéries intra-parenchymateuses) au CO₂. La variation de 1 mm Hg de la PaCO₂ est à l'origine d'une variation très rapide (30 secondes à 2 minutes) dans le même sens du DSC de 1 à 2 ml/100g/min. Il existe plusieurs hypothèses pathogéniques pour tenter d'expliquer l'effet vasomoteur du CO₂. La conception commune repose sur l'hydratation du CO₂ en ions bicarbonates (HCO₃) et hydrogènes (H⁺) sous l'effet de

l'anhydrase carbonique, le tout déterminant le pH du liquide interstitiel cérébral : L'acidose interstitielle entraîne une hyperpolarisation des cellules musculaires lisses par activation des canaux potassiques, à l'origine d'une vasodilatation. L'alcalose produit une vasoconstriction par le phénomène inverse. L'implication du NO dans la réponse vasomotrice au CO₂ a été démontrée par les études d'inhibition de la NO synthase : L'administration de substances inhibant la NO synthase entraîne une atténuation franche de la réaction de vasodilatation secondaire à une hypercapnie. [12]

En contraste, l'effet de la PaO₂ sur la vasomotricité reste très modeste. L'hyperoxémie n'a quasiment aucun effet sur le DSC. Seule l'hypoxémie majeure (inférieure à 60 mm Hg) a un effet d'augmentation du DSC de 0,5 à 2,5 % par 1% de PaO₂ en isocapnie. Cet effet prédomine clairement sur la circulation carotidienne par rapport à la circulation vertébro-basilaire. [13] En dehors des gaz du sang, l'adrénaline peut jouer un rôle sur la régulation du DSC. Elle agirait directement sur les cellules endothéliales en y activant les récepteurs β-adrénergiques et en stimulant la production locale de NO. [14]

c) Facteur nerveux

L'innervation des vaisseaux cérébraux est riche, et on peut distinguer une innervation extrinsèque et une innervation intrinsèque (Figure 9).

- i. Innervation extrinsèque : Elle comprend le contingent sensitif du nerf trijumeau et le système nerveux autonome avec ses composantes sympathique et parasympathique. Les corps cellulaires des neurones du système nerveux sympathique sont localisés dans le ganglion cervical supérieur et à moindre

proportion dans le ganglion stellaire, avec une co-médiation par la noradrénaline et le neuropeptide Y. Ceux du système nerveux parasympathiques sont situés dans les ganglions sphéopalatin et otique, avec une co-médiation par l'acétylcholine et le Vasoactive-intestinal peptide. Les neuromédiateurs du système trigéminal sont la substance P, la CGRP (Calcitonine gene-related peptide), la neurokinine A et le pituitary adenylate-cyclase activating polypeptide (PACAP). Dans les conditions physiologiques, le système sympathique n'intervient pas sur la vasomotricité cérébrale mais en cas d'hypertension artérielle ce système provoque une vasoconstriction « protectrice » cérébrale. Le blocage du système parasympathique entraîne quant à lui une potentialisation des effets de l'autorégulation cérébrale.

- ii. Innervation intrinsèque : Elle est caractérisée par des corps cellulaires de neurones situés dans le tronc cérébral avec des axones projetant sur les pieds astrocytaires en regard des artéries intracérébrales. Ces neurones sont cholinergiques (noyau basal de Meynert et noyau fastigial), sérotoninergiques (raphé médian) et noradrénergiques (locus coeruleus). La grande majorité de ces neurones projettent sur les artéries corticales et accessoirement les artéries intracérébrales via des inter-neurones GABAergiques et glutamatergiques.

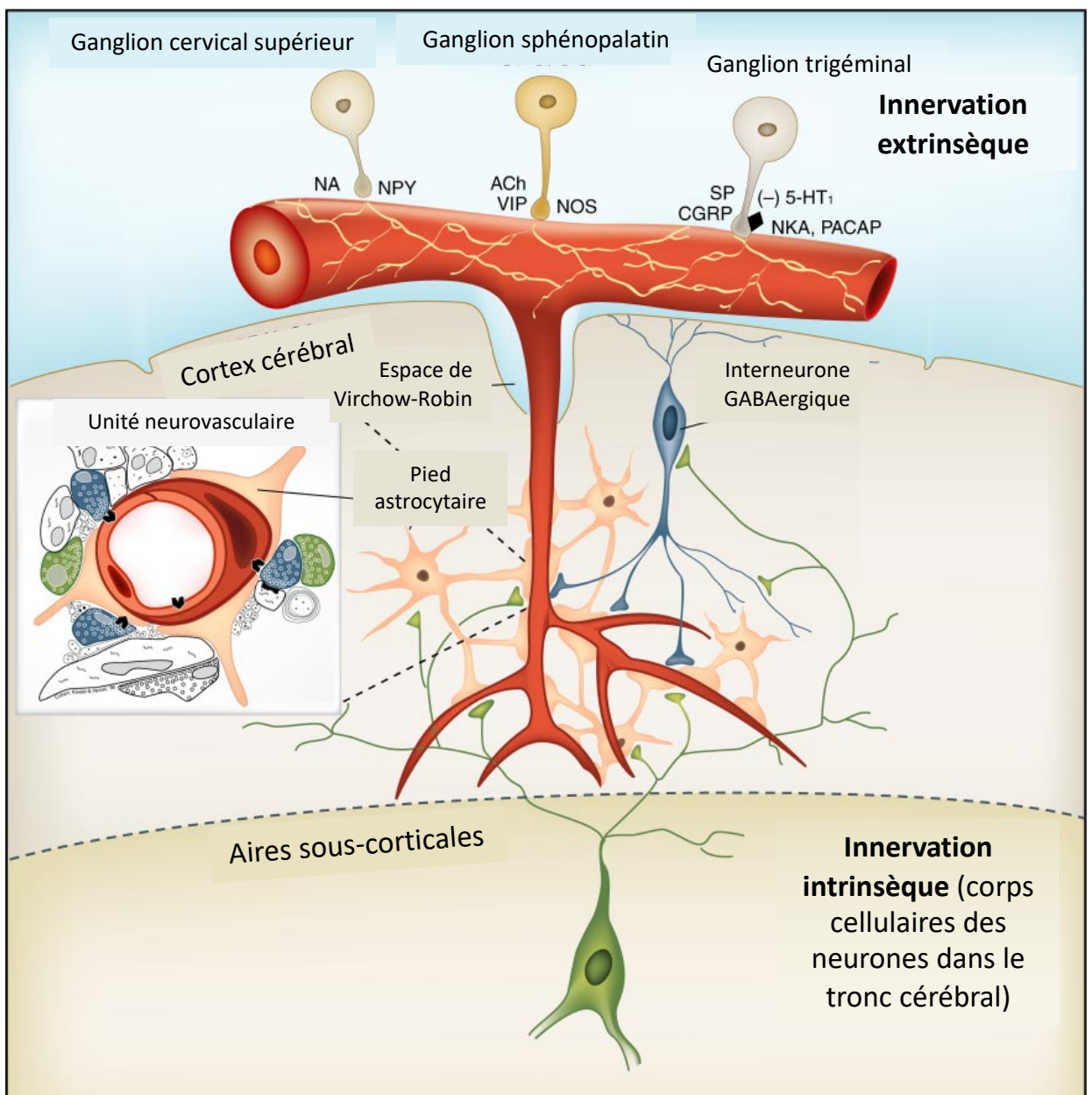


Figure 9 : Innervation des vaisseaux cérébraux. NA : Noradrénaline, NPY : Neuropeptide Y, ACh : Acétylcholine, VIP : Vasoactive intestinal peptide, SP : Substance P, CGRP : Calcitonin gene-related peptide, 5-HT : Sérotonine, NKA :Neurokinine, PACAP :Pituitary adenylate-cyclase activating polypeptide (adapté de Hamel 2006). [15]

d) Facteur myogène

Connu également sous le nom d'effet Bayliss, il correspond à la réponse des cellules musculaires lisses à un changement de la pression artérielle : Vasodilatation en cas de baisse de la pression artérielle et vasoconstriction en cas d'élévation de la pression artérielle. L'effet Bayliss mettrait en jeu les canaux TRP (*transient receptor potential channel*) des cellules musculaires lisses. [16]

Les vaisseaux cérébraux, à l'instar des vaisseaux rénaux et mésentériques, possèdent la propriété d'adapter activement leur diamètre (et donc les RVC) aux variations de la PPC afin de maintenir un DSC stable. Ce phénomène, appelé autorégulation cérébrale, constitue un mécanisme de protection cérébrale contre l'ischémie et l'hémorragie. L'autorégulation cérébrale est efficace pour une PAM entre 50 et 160 mm Hg. Cette conception classique, décrite initialement par Lassen en 1959 [17] et communément enseignée, a été remise en cause récemment : En compilant 41 études sur le sujet, Willie et al. (2014) [18] ont montré que l'indépendance entre le DSC et la PAM n'était que relative, avec un plateau bien plus étroit que dans la conception classique de Lassen. Dans cette nouvelle conception, les capacités de régulation du DSC sont bien plus importantes lors de l'hypertension que lors de l'hypotension artérielle tel que le démontre l'angle de la pente (Figure 10). Plus que la valeur absolue de PAM, c'est surtout la vitesse d'évolution des chiffres de PAM qui semble conditionner les mécanismes d'autorégulation du DSC. [19] Ces mécanismes demeurent incomplètement élucidés, mettant en jeu principalement les facteurs myogène et nerveux extrinsèque tant sympathique que parasympathique. [20]

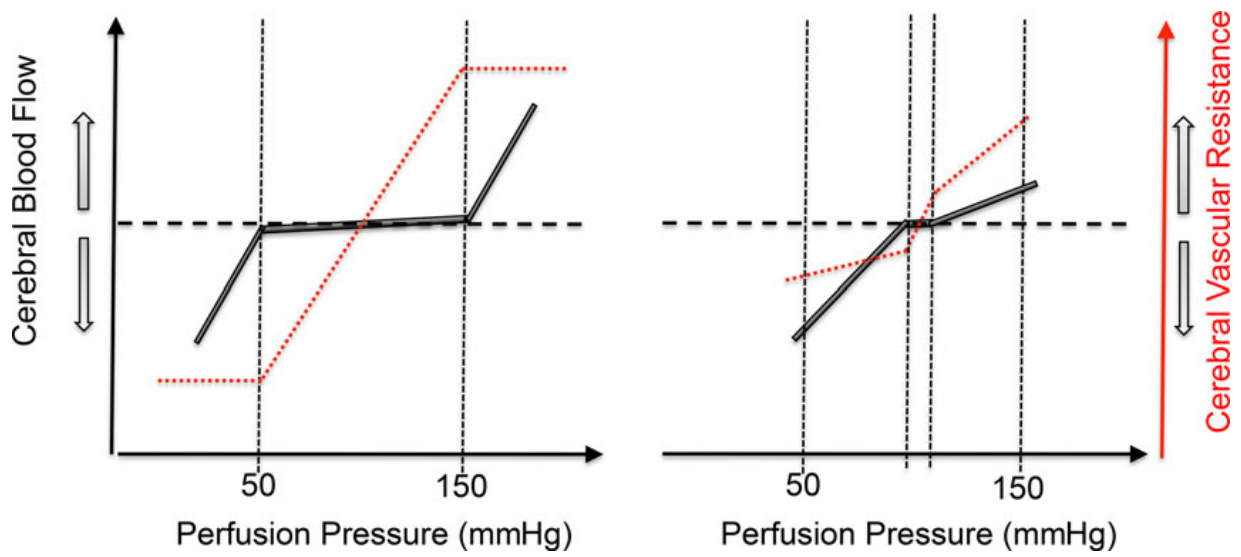


Figure 10 : Autorégulation du DSC. Conception classique de Lassen (gauche). Conception récente (Willie et al.) avec une plus grande sensibilité du DSC aux modifications de la PAM résultant en un plateau bien plus étroit en réalité (Willie et al. 2014). [13]

III - MONITORING PER-OPERATOIRE DU DEBIT SANGUIN CEREBRAL ET IMAGERIE DE LA MICRO CIRCULATION EN NEUROCHIRURGIE

Article soumis le 15/09/2020 – Clinical Neurology and Neurosurgery

Résumé

Le contrôle strict du DSC est un facteur clé en neurochirurgie aussi bien en per- qu'en péri-opératoire : Le DSC assure entre autres l'apport vital en oxygène et en substrats énergétiques au parenchyme cérébral. Le monitoring peropératoire du DSC en neurochirurgie permet de réduire le risque de complications à type d'hypo- ou d'hyperperfusion secondaires soit à des événements systémiques (instabilité hémodynamique, hémorragie, hypo- ou hypercapnie,...) ou à des contraintes chirurgicales (clippage d'un vaisseau, écartement cérébral,...). Ce monitoring est également un outil précieux pour aider à la cartographie corticale fonctionnelle.

Différentes technologies ont été développées dans ce domaine spécifique : Techniques laser (*laser doppler flowmetry, laser speckle contrast imaging*), vidéomicroscopie (*orthogonal polarized spectral imaging, sidestream dark field imaging*), IRM peropératoire, thermographie, angiographie à l'infracyanine, et l'échographie fonctionnelle. Ces technologies, pourtant bien explorées dans leur utilisation en dehors du bloc opératoire, posent le problème de leur intégration au *workflow* au cours d'un geste neurochirurgical. Une technologie optimale de monitoring peropératoire du DSC doit répondre à des critères particuliers : Excellentes résolutions spatiale et temporelle, intégration au microscope opératoire, monitoring quantitatif en temps réel, facilité d'utilisation et sans contact avec le cerveau si possible. Dans ce travail, nous proposons une revue exhaustive des technologies actuellement disponibles en précisant pour chacune leurs qualités propres et avantages, mais également leurs limitations.

INTRAOPERATIVE CEREBRAL BLOOD FLOW MONITORING IN NEUROSURGERY: A COMPREHENSIVE REVIEW OF CONTEMPORARY TECHNOLOGIES AND EMERGING PERSPECTIVES

Moncef Berhouma^{1,2,3}, Jorn FIESTRA^{2,4}, Thomas WAECHLI^{2,4},
Thiebaud PICART¹, Chloe DUMOT¹, Isabelle PELISSOU-GUYOTAT¹, Omer
EKER^{3,5}, Jacques GUYOTAT¹, Baptiste BALANCA^{6,7}, Stephane
MARINESCO⁷, Anne-Claire LUKASZEWCZ⁶, Ivan RADOVANOVIC²,
Fran ois COTTON^{3,8}

1 - Department of neurosurgical oncology and vascular neurosurgery – Pierre Wertheimer Neurological and Neurosurgical Hospital – Hospices Civils de Lyon – France

2 - Division of neurosurgery, Toronto Western Hospital, University of Toronto, Canada

3 - Creatis Lab - CNRS UMR 5220 – INSERM U1206 – Lyon 1 University – INSA Lyon – France

4 – Department of neurosurgery, Clinical Neuroscience Center, University Hospital Zurich, University of Zurich, Switzerland.

5 – Department of interventional neuroradiology - Pierre Wertheimer Neurological and Neurosurgical Hospital – Hospices Civils de Lyon – France

6 - Department of neuro-anesthesia and neuro-critical care – Pierre Wertheimer Neurological and Neurosurgical Hospital – Hospices Civils de Lyon – France

7 - Centre de Recherche en Neurosciences de Lyon - Inserm U1028 - CNRS UMR 5292 - Universit  Lyon 1

8 – Department of imaging – Centre hospitalier Lyon sud – Hospices civils de Lyon – France

Corresponding Author: **Moncef BERHOUMA MD, MSc**

Department of Neurosurgical Oncology and Vascular Neurosurgery

Pierre Wertheimer Neurological and Neurosurgical Hospital

University of Lyon – Hospices Civils de Lyon

59 Boulevard Pinel 69003 Lyon – France

Email: berhouma.moncef@gmail.com

moncef.berhouma@chu-lyon.fr

Telephone: (0033) 04.72.35.75.69

RUNNING TITLE: Intraoperative cerebral blood flow monitoring

ABSTRACT

Intraoperative monitoring of cerebral blood flow (CBF) has become an invaluable adjunct to vascular and oncological neurosurgery, reducing the risk of post-operative morbidity and mortality. Several technologies have been developed during the last two decades including laser-based techniques, videomicroscopy, intraoperative MRI, indocyanine green angiography, and thermography. Although these technologies have been thoroughly studied and clinically applied outside the operative room, current practice lacks an optimal technology that perfectly fits the workflow within the operative neurosurgical room. The different available technologies have specific strengths but suffer several drawbacks including mainly limited spatial and/or temporal resolution. An optimal CBF monitoring technology should meet particular criteria for an intraoperative use: Excellent spatial and temporal resolution, integration in the operative workflow, quantitative real-time monitoring, ease of use, and non-contact technique. We herein review the main contemporary technologies for intraoperative CBF monitoring and their current and potential future applications in neurosurgery.

KEYWORDS: Brain surgery, Cerebral blood flow, Intraoperative imaging, Laser doppler flowmetry, Laser speckle contrast imaging, Microcirculation, Sidestream dark field imaging

ABBREVIATIONS:

CBF : Cerebral blood flow

CPP : Cerebral perfusion pressure

CSF : Cerebrospinal fluid

LDF : Laser doppler flowmetry

LDI : Laser doppler imaging

LSCI : Laser speckle cell imaging

MESI : Multi-exposure speckle imaging

CCD : Charge-coupled device

CSD : Cortical spreading depolarization

AVM : arteriovenous malformation

NIRS : Near-infrared spectroscopy

BOLD : blood oxygenation-level dependent

SDF : Sidestream dark field

CLE : Confocal laser endomicroscopy

DSA : Digital subtraction angiography

ICG-VA : Indocyanine green video angiography

MDU : Microvascular doppler ultrasound

FUS : Functional ultrasound

CEU : Contrast-enhanced ultrasound

INTRODUCTION

In neurosurgery, monitoring cerebral blood flow (CBF) is a key factor for optimal intra- and peri-operative patient management. Through cerebral perfusion, CBF ensures adequate brain functioning through the delivery of oxygen and energy substrates but also the drainage of metabolic waste products. The regulation of cerebral perfusion is directly correlated to the adjustment of the intracranial volume which includes the cerebrovascular arteriovenous network and the cerebrospinal fluid (CSF) volume. Both cerebrovascular resistance and cerebral perfusion pressure (CPP = mean arterial pressure – intracranial pressure) condition the CBF (Poiseuille's law).

CBF corresponds to the volume of blood that flows per unit mass (or volume) per unit time in the brain. In adults, CBF ranges from 20 to 80 ml/(100 g min) with an average of 50 ml/(100 g min).^{1,2}

According to the following equation:

$$\text{Blood flow} = \frac{\Delta P}{R} = \frac{\Delta P \pi r^4}{8\mu L}$$

(ΔP : Pressure gradient, R : vascular resistance, r : vessel radius, L : vessel length, μ : blood viscosity)

CBF may be primarily affected by variations of vessel radius (i.e. vasodilatation, vasoconstriction), CPP, and blood viscosity (reflection of hematocrit). CBF perpetually adapts to brain metabolism variations (neurovascular coupling) while its homeostasis is rigorously maintained through potent cerebral autoregulation mechanisms.

During a neurosurgical procedure, CBF monitoring is critical to avoid both hypo- and hyper-perfusion complications either secondary to systemic events

(arterial pressure instability, post-hemorrhagic anemia, hyper- or hypocapnia...) or due to local surgical constraints (vessel clipping, brain retraction...). It is also a potentially very useful adjunct for brain mapping during tumor resection. Although a myriad of invasive and non-invasive CBF monitoring technologies are available for the pre- and post-operative periods¹⁻⁴, it is rarely available intra-operatively mostly because of the absence of an optimal technology that perfectly suits the environment within an operating room. In the current clinical practice, very few techniques have the capacity to provide real-time CBF monitoring without interfering with the surgical workflow.

Here, we review the predominantly available CBF monitoring techniques that are suitable for the intra-operative environment and we describe the benefits and disadvantages of each technique (Table 1), focusing on the characteristics that appear to be fundamental for the “ideal” CBF monitoring technology in operative neurosurgery: Excellent spatial and temporal resolution, integration in the surgical workflow, quantitative real-time monitoring, ease of use, and non-contact technique.

METHODS

A bibliographic search from March 1982 to March 2020 via Medline and Scopus databases with the keywords “cerebral blood flow”, “intraoperative” and “neurosurgery” was performed following the Preferred Reporting Items for Systematic Reviews and Meta-Analyses (PRISMA) (Figure 1). We included both animal and human studies describing CBF monitoring outside and inside the neurosurgical operative room environment. All types of study design were included. The abstracts of identified publications were reviewed, and only relevant articles were considered. There were no language restrictions. To compare the different CBF monitoring technologies, we used an ordinal scale for

each characteristic: Depth of imaging, spatial and temporal resolutions, surgical integration in the workflow, and the possibility to provide quantitative measurements.

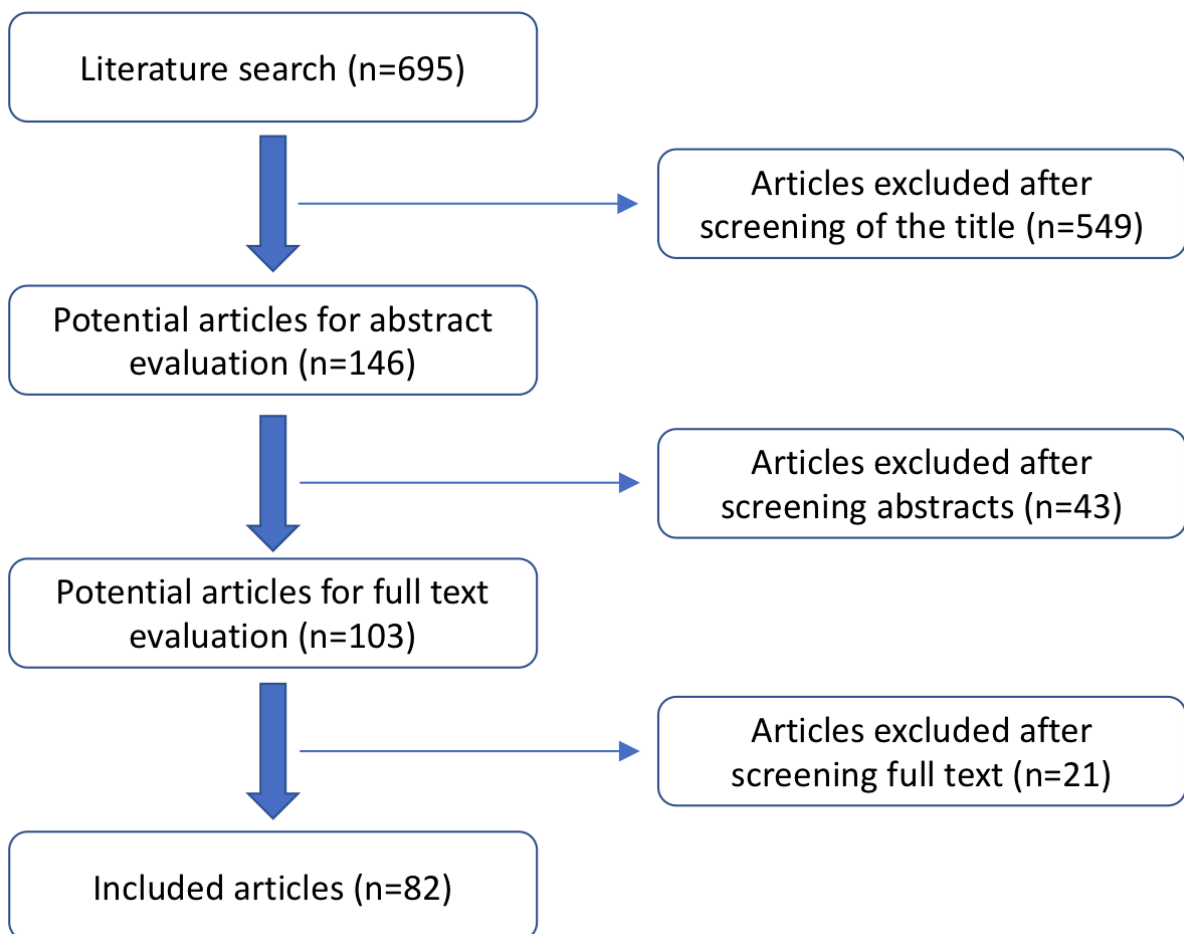


Figure 1: Flow chart of literature search strategy

LASER DOPPLER-BASED TECHNOLOGIES

Laser Doppler flowmetry (LDF) was developed in the 1970's, mainly for dermatological purposes.^{5,6} This optically based technology relies on a coherent laser light and measures the flow of fluids carrying light-scattering particles and erythrocytes within an illuminated brain tissue volume of approximately 1 mm³.⁷

The blood flow (reflection of erythrocytes' velocity and density) is indirectly estimated through the frequency shift (resulting from the Doppler effect) transmitted to incident monochromatic photons by the mobile erythrocytes within the vessels (Figure 2). LDF provides relative measurements of blood flow and requires calibration before usage. Different LDF probes have been developed including mainly cortical surface contact probes to intraparenchymal ones (mainly used in intensive care monitoring such as an ICP monitoring probe⁸) allowing either single shot measurements or continuous monitoring during specific neurosurgical procedures.

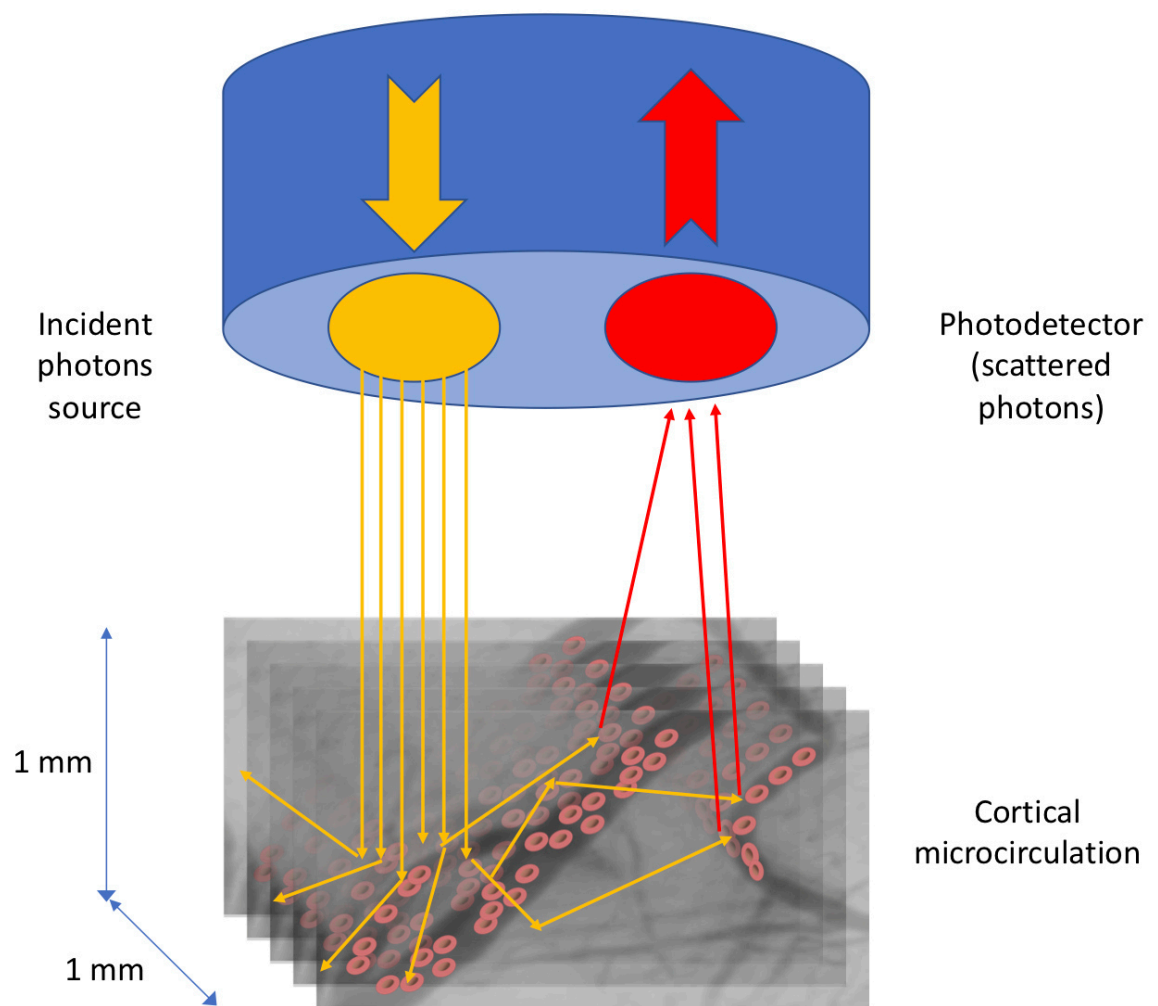


Figure 2: Laser Doppler Flowmetry. An incident photons source produces a laser light beam that infiltrates approximately 1 mm³ of brain cortex. Mobile (erythrocytes, leucocytes, etc....) and immobile (neurons, glial cells, etc....) structures scatter the incident photons resulting in a Doppler shift and an electrical signal reflecting both velocity and density of erythrocytes.

Rosenblum et al. first introduced LDF in the neurosurgical field in 1987 providing measurements of cortical peri-nidal CBF variations before and after resection of a brain arteriovenous malformation (AVM), depicting at the microcirculatory level the concept of normal perfusion pressure breakthrough.⁹ LDF has also been useful in the continuous intraoperative monitoring of CBF during revascularization bypass surgery in moyamoya disease, with the ability to predict post-operative cerebral hyperperfusion syndrome.¹⁰ More recently, Kubo et al. used LDF intraoperatively associated with middle cerebral artery pressure measurement, as a possible substitute of balloon test occlusion, during parent artery surgical occlusion for symptomatic cavernous carotid aneurysms in order to identify the critical variations of CBF and henceforth patients who require a concomitant high-flow bypass.¹¹ Surface cortical probes provide real-time information on local CBF variations, and thus can help the detection of ischemic events and cortical spreading depolarization (CSD).¹² Other than for vascular neurosurgery, LDF has been shown to be useful in functional and oncological neurosurgery¹³. With its capability in differentiating white matter from grey matter based on specific patterns of microvascular blood flow, LDF with intraparenchymal probes can help improving the safety and accuracy of deep brain stimulation procedures¹⁴. Haj-Hosseini et al. associated 5-ALA fluorescence and LDF in a unique specific stereotactic probe to optimize the capacity of

tracking intra-cerebral vessels on the trajectory of the probe and better detect tumoral tissue.¹⁵

Overall, during neurosurgical procedures, LDF offers the possibility of excellent real-time blood flow measurements and hence a good temporal resolution as compared to other intraoperative CBF monitoring technologies but suffers a poor spatial resolution due to a single point analysis. The latter raises the problem of representativity of the whole CBF compared to the local measurements provided by LDF and emphasizes the importance for choosing relevant surgical sites to obtain an exploitable measurement. This lack of representativity becomes particularly evident in the interpretation of CBF data monitored by an intraparenchymal LDF probe in ICU patients.⁸ In this choice of surgical site for LDF registration, the neurosurgeon should avoid any cortical zone that includes relatively large vessels to ensure the reliability of measurements in the analyzed brain volume. Another drawback of LDF is the high sensitivity of the probe to micromovements (brain pulsatility, cortical fluids, surgical maneuvers) leading to motion artifacts resulting in imprecise measurements.

In order to overcome these drawbacks, laser doppler imaging (LDI) has been developed. This technology is based on LDF, but a movable mirror directs the laser incident beam on different measurement points to allow scanning of a larger cortical surface. The depth of scanning is 2 to 3 times higher than LDF reaching up to 1.5 mm. Apart of being able to provide a larger surface analysis, LDI is a non-contact technology avoiding the risk of pressure artifacts. It offers a good spatial resolution with a good reproducibility, but its temporal resolution is very low compared to LDF as it does not provide real-time analysis and requires a relatively long time for both surface scanning and data processing. This drawback has limited its usefulness during neurosurgical procedures. Raabe et al. integrated LDI technology into an operative microscope enabling to analyze CBF during awake surgery with a protocol for eloquent cortex stimulation, thereby providing a real-time intraoperative functional brain monitoring¹⁶. Technologies

with faster data acquisition and processing are being investigated and may result in a LDI technology with both improved spatial and temporal resolution, in the near future.

More recently, LDF was combined to spectrophotometry (backscattering spectroscopy) in a single multiparameter probe (“oxygen-to-see or O2C”) to provide the capillary venous oxygenation and the relative hemoglobin content as a metabolic monitoring in addition to microcirculation data.¹⁷ Sommer et al evaluated the feasibility of this system in the intra-operative setting and showed its sensibility to surgical brain tissue retraction and modifications of the head position.¹⁸

LASER SPECKLE CELL IMAGING

Developed initially in 1981 for imaging of retinal blood flow¹⁹, laser speckle cell imaging (LSCI) - initially known as LASCA for laser speckle contrast analysis - relies on a light effect called laser speckle, secondary to the illumination of a biological tissue by a coherent laser beam. This effect results from the irregular backscattering of the light by the heterogeneous structure of the illuminated tissue. The resulting random speckle pattern detected by a charge-coupled device (CCD) camera (Figure 3) varies with the movement of erythrocytes, becoming more blurred in presence of a high erythrocyte flow and thus reducing the contrast. Blood flow is then deducted by the quantification of the spatial blurring of the speckle pattern over the exposure time of the CCD camera (Figure 4). Basically, the spatial blurring is quantified using the speckle contrast K:

$$K(T) = \frac{\sigma S(T)}{\langle I \rangle}$$

(T corresponds to the exposure time of the camera, σS the standard deviation and I the mean intensity of pixel values).²⁰

Even if the K value correlates to the level of motion of erythrocytes, this technique is not able to quantify the absolute blood flow.²¹ In contrast to LDF and LDI, LSCI allows faster real-time measurements of blood flow on large surfaces resulting in excellent temporal and spatial resolution, but remains limited in penetration of the brain cortex achieving a maximal depth of approximately 300 μm . Despite LSCI being a non-contact technology, it is very sensitive to movement artifacts - particularly cardiac and respiratory related motions - as well as brain shift during neurosurgical procedures. Richards et al. developed a system allowing a retrospective motion correction based on ECG filtering and physiological noise reduction, resulting in a better intraoperative accuracy of LSCI and the possibility to detect minimal CBF variations.²² Dunn et al. noted that one important limitation of LSCI results from the use of a single camera exposure time and the sensitivity of the technique to several confounding factors (illumination discrepancies and the presence of light scattered from static tissue), leading to the development of an extension of LSCI named multi-exposure speckle imaging (MESI) to improve the quantitative accuracy for measuring CBF.²³⁻²⁵ Using a more robust mathematical model, Dunn et al. showed that MESI is adapted to chronic monitoring of the blood flow and has a good correlation with in vivo blood flow values, opening new perspectives for the intra- and inter-patients' CBF comparative studies. Other parameters can be measured with optical imaging concomitantly with LSCI or MESI, including hemoglobin oxygenation and oxygen tension to better explore and understand neurovascular coupling in ischemic diseases and functional brain mapping.²⁶⁻³⁰

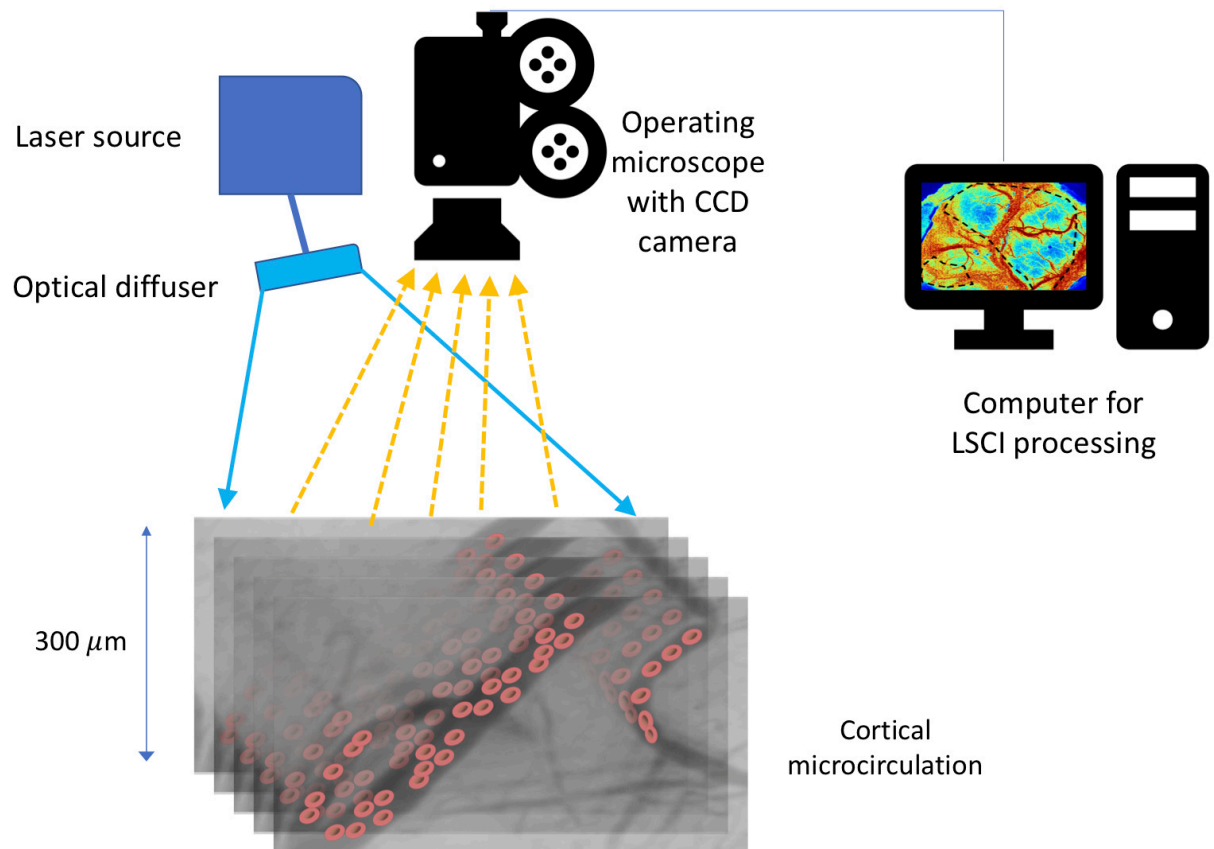


Figure 3: Laser speckle cell imaging. A coherent laser beam illuminates the most superficial heterogeneous layer of the brain cortex up to 300 μm resulting in an irregular backscattering of the light. A CCD camera, possibly integrated in the operative microscope, detects the ensuing random speckle pattern which is variable with erythrocytes' movements.

LSCI is currently gaining increased popularity in both research and clinical applications due to its aforementioned excellent spatial and temporal resolutions. Hecht et al. evaluated LSCI in 3 patients undergoing direct cerebral revascularization surgery and confirmed the ability of LSCI to provide quasi-real time relative CBF monitoring with a clear capacity to depict any minimal blood flow variations during surgery.³¹ Furthermore, Parthasarathy et al. integrated the LSCI device to the neurosurgical operating microscope to ease the surgical workflow. A filter calibrated with the electrocardiogram was also used to decrease

the pulsations-related artifacts.³² Ideguchi et al. used LSCI to better identify feeding arteries during the resection of brain tumors and AVMs, and thus reduce the risk of post-operative ischemic complications. Specifically, by using temporary arterial occlusion under LSCI monitoring, the authors were able to distinguish feeding arteries from en passage arteries and combined arteries (i.e. en passage arteries providing feeding branches to the lesion). Hecht et al explored the potential of LSCI for the prediction of infarction by monitoring 22 patients undergoing decompressive craniectomy for middle cerebral artery infarction.³⁴ By standardizing LSCI analysis parameters, the authors determined LSCI specific perfusion thresholds that not only allow the recognition of infarcted brain but mainly predict further infarctions. Klijn et al. evaluated the feasibility of LSCI in identifying eloquent brain cortex during awake glioma surgery.³⁵ They confirmed that LSCI was accurately able to detect any cortical CBF increase secondary to induced motor activity, overcoming the limitations of traditional electric stimulations mapping, i.e. the time consumption and risk of false positive responses as well as seizure activity. Woitzik et al. used LSCI intraoperatively to identify and follow the spatiotemporal progression of CSD in malignant stroke as CSDs exhibit characteristic cortical CBF patterns.³⁶

LSCI and MESI are easily accessible technologies with an excellent spatiotemporal resolution providing a quantitative monitoring of CBF. The combination of LSCI and other videomicroscopic imaging can provide a morphological assessment of the microcirculation (vessel density, proportion of perfused vessels, etc....) in addition to the quantitative monitoring of CBF.³⁷ In the upcoming years, its integration in the surgical microscope will certainly ease its regular use in vascular but also oncological neurosurgery, providing a close to quantitative real-time CBF monitoring.

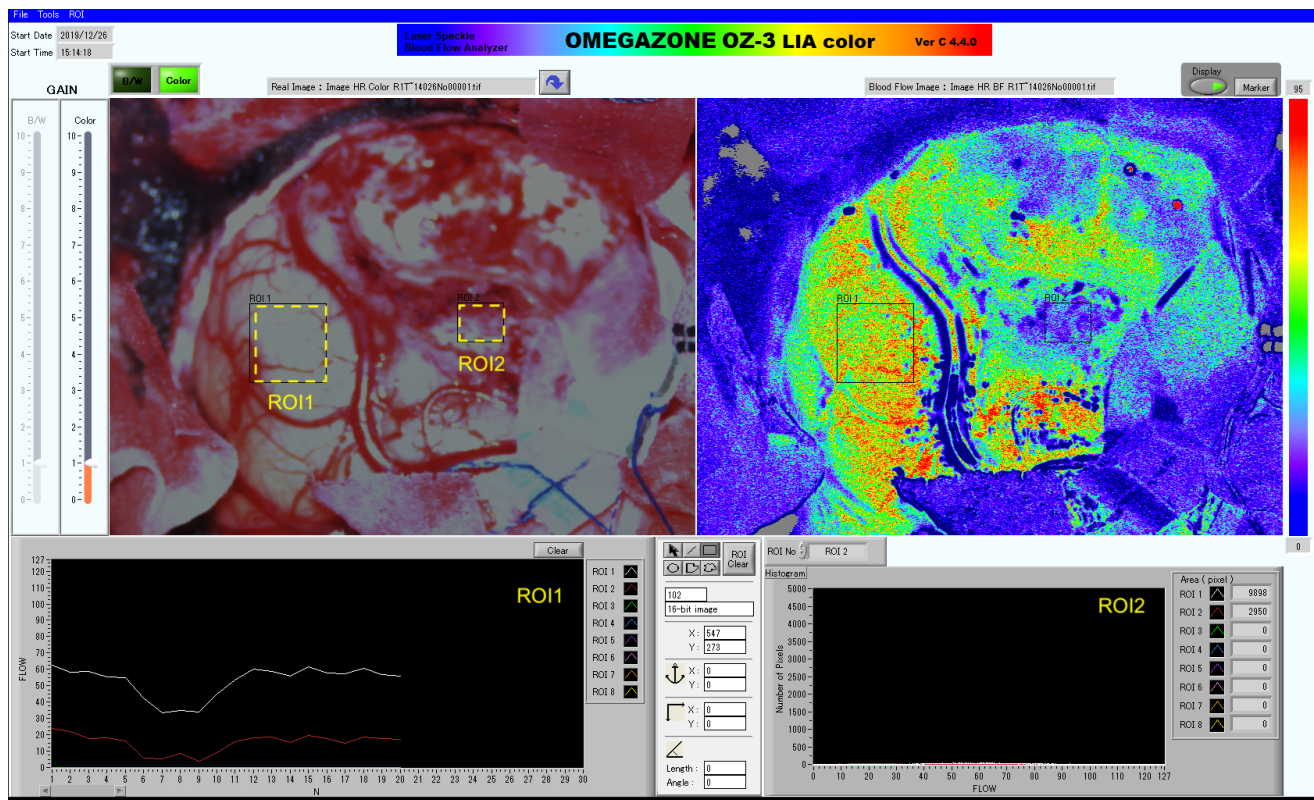


Figure 4: Example of intraoperative laser speckle cell imaging during brain glioma removal with a surgical microscope integrated LSCI device (Omegazone OZ-3, Omegawave Inc.). The difference in CBF can be measured between 2 ROIs (ROI1 corresponds to normal brain tissue, ROI2 corresponds to tumoral brain tissue). (Courtesy of Dr Jun Muto, Fujita Health University)

SIDESTREAM DARK FIELD IMAGING

Sidestream dark field (SDF) imaging is a videomicroscopy technique allowing a direct visualization of the cortical microcirculation. Originally, Slaaf et al. developed in 1987 an incident illuminator for intravital imaging of microcirculation.³⁸ In 1999 Groner et al. improved the concept by developing orthogonal polarization spectral (OPS) imaging, the precursor of sidestream dark field (SDF) technique.³⁹ This videomicroscopic technique relies on a stroboscopic

light emitting diode ring-based modality and allows a direct visualization of the cortical microcirculation (Figure 5). The hand-held device includes a light guide, a magnifying lens and a CCD video camera (Figure 6a). The illumination is ensured by a 530 to 548 nm wavelength green light specifically absorbed by hemoglobin, leading to a dark appearance of erythrocytes. SDF provides imaging of the microcirculation at a depth of approximately 530 μm and with a final on-screen magnification reaching 320 to 325 times that of the original and a field size of 1280 $\mu\text{m} \times 960 \mu\text{m}$. This technology allows measuring key microcirculatory parameters (Figure 6b), such as vessel density, vessel diameter, flow index, proportion of perfused vessels and microvasospasms.⁴⁰ The recent development of advanced analysis software permits real-time intraoperative analysis of these microcirculatory parameters by optimizing the temporal resolution. The spatial resolution, however, remains limited. As all contact technologies, SDF suffers the possibility of motion and pressure artifacts. In neurosurgery, these artifacts may be reduced by the use of a self-retaining holding arm for the probe during registration. When image acquisition is optimal, the intra-observer and inter-observer variabilities remain very limited.

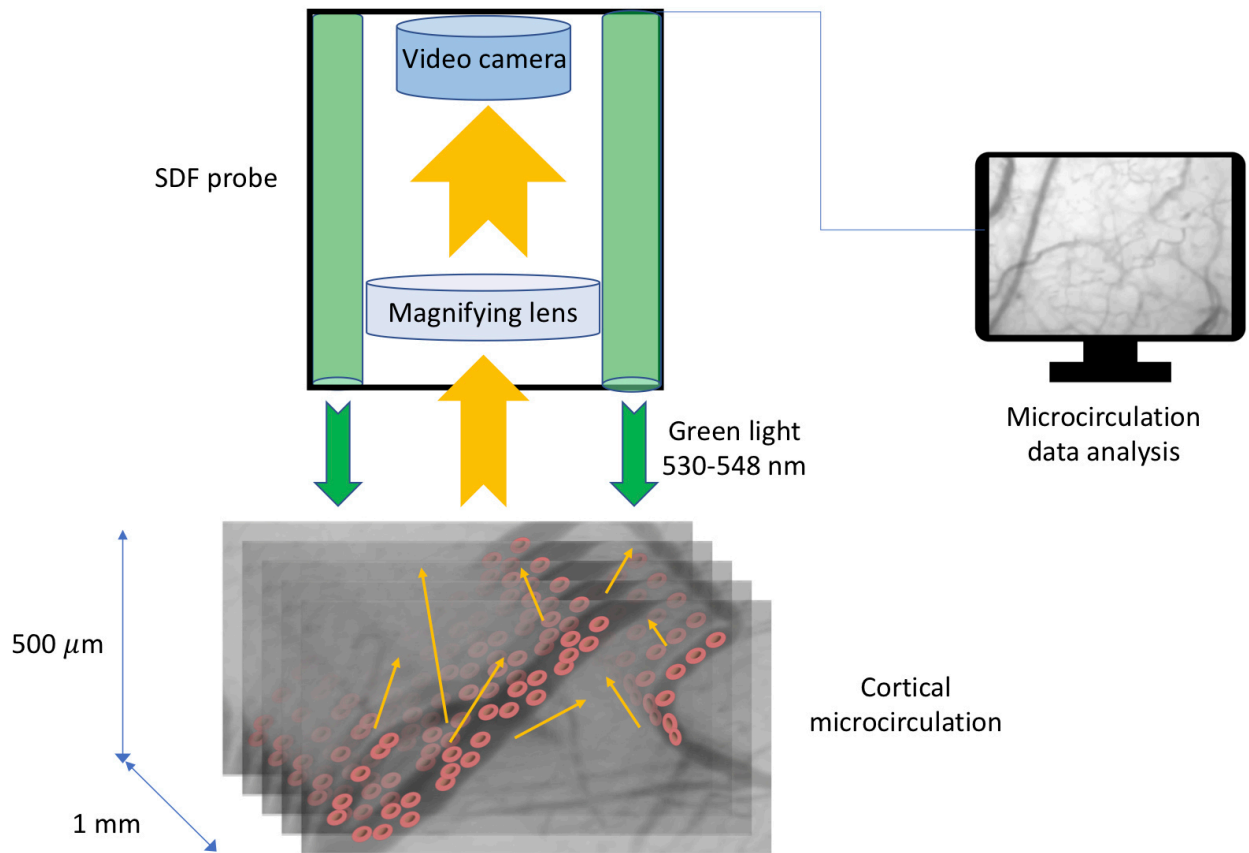


Figure 5: Sidestream dark field imaging. A stroboscopic green light (530 to 548 nm) illuminates the cortical surface up to 500 μm . This specific wavelength light is exclusively absorbed by erythrocytes and results in the display of the black vascular network in a gray background.

The development of compact portable handheld OPS and SDF devices have offered the possibility of intraoperative use in neurosurgery to monitor the microcirculation, including microvascular blood flow. In two subsequent studies, Uhl et al. monitored microcirculation during brain aneurysm surgery revealing microvascular vasospasms and decreased vascular density in patients with subarachnoid hemorrhage.^{41,42} Pennings et al. used OPS imaging to reveal arteriolar contractility in response to hypercapnia in a surgical series of

aneurysmal subarachnoid hemorrhage.⁴³ Furthermore, with OPS technology, the same group investigated the perfusion variations of the peri-nidal area during brain AVM surgery and the microvascular response to local papaverine administration during brain aneurysm surgery.^{44,45} More recently, Perez-Barcena et al. confirmed the feasibility of intraoperative SDF imaging to monitor microcirculatory parameters in traumatic brain injury and malignant stroke.^{46,47} Our group is evaluating the feasibility of SDF imaging of peri-tumoral microcirculation in intracranial meningiomas to better explore the pathogenesis of peri-tumoral edema (unpublished data). The intra-operative use of SDF imaging as a continuous real-time monitoring technology in neurosurgery remains very limited due to the poor spatial resolution (single points analysis), susceptibility to motion and pressure artifacts, and difficulties to measure high blood flow velocities.



Figures 6a: Sidestream dark field imaging. The development of a hand-held device and a real-time image analysis ease its use intra-operatively (Courtesy of MicroscanTM, Microvision Medical, Amsterdam, The Netherlands).



Figure 6b: Example of cortical SDF imaging showing the flow of erythrocytes

INDOCYANINE GREEN VIDEO ANGIOGRAPHY

Indocyanine green video angiography (ICG-VA) is an intraoperative technique using a near-infrared range fluorescent tricarbocyanine water-soluble

dye, initially developed to evaluate the cardiac output, hepatic function and ophthalmic angiography, and has been introduced in neurosurgery during the last two decades (Figures 7a and 7b).⁴⁸ ICG shows a spectral absorption at 800-805 nm and an emission peak at 835 nm, with a half-life ranging between 150 to 180 seconds. Injected intravenously at a dose of 0.2 to 0.5 mg/kg, ICG binds to alpha-1 lipoprotein and remains intravascular to be finally excreted by the liver. Repeated intravenous injections are possible at different stages of surgery to allow comparative assessments of blood flow, respecting an interval of 20-25 minutes between two injections to maintain an optimal contrast enhancement and limiting the cumulative total dose inferior to 5 mg/kg. The visualization technology is actually integrated in most operative neurosurgical microscopes without significant interruption of the workflow, providing a flow graph evaluating the time to peak (interval from the raise of the wave to the peak of signal intensity) and thus semi-quantitative evaluation of CBF. Flow maps of CBF may be obtained using the ratio between fluorescence intensity and rise time.⁴⁹ Different authors have suggested correlations between the time-intensity curve obtained with a specific software for ICG-VA and the quantitative CBF obtained by an ultrasound flowmeter, allowing in fine a quasi-quantitative blood flow assessment by ICG-VA.⁵⁰ Real-time intraoperative blood flow analysis using ICG-VA may be useful in the evaluation of flow dynamics in and around brain AVMs, aneurysm surgery to check the absence of parent vessel post-clipping stenosis and the absence of aneurysmal residue (Figures 7a and 7b), and in hemangioblastomas surgery.⁴⁹⁻⁵⁴ ICG-VA is very useful during revascularization surgery as, in addition to intraoperative evaluation of graft patency and a quantitative analysis of the relative flow through the bypass, it provides the possibility to identify an optimal recipient artery for the bypass (“flash fluorescence technique”)⁵², and even help predict the postoperative neurological outcome.^{55,56} Although ICG-VA has become a relatively low-cost widely used technique in operative rooms with a good safety profile, it still suffers some specific drawbacks compared to other

intraoperative CBF imaging techniques: (i) It doesn't allow a continuous monitoring of blood flow and requires repetitive intravenous dye injections with a minimum of 20-25 minutes between two injections; (ii) Very rare adverse reactions to the intravenous dye are possible (nausea, vomiting, pruritus, bronchospasm, allergy, myocardial infarction, epilepsy); (iii) exploration of subcortical vasculature is limited.

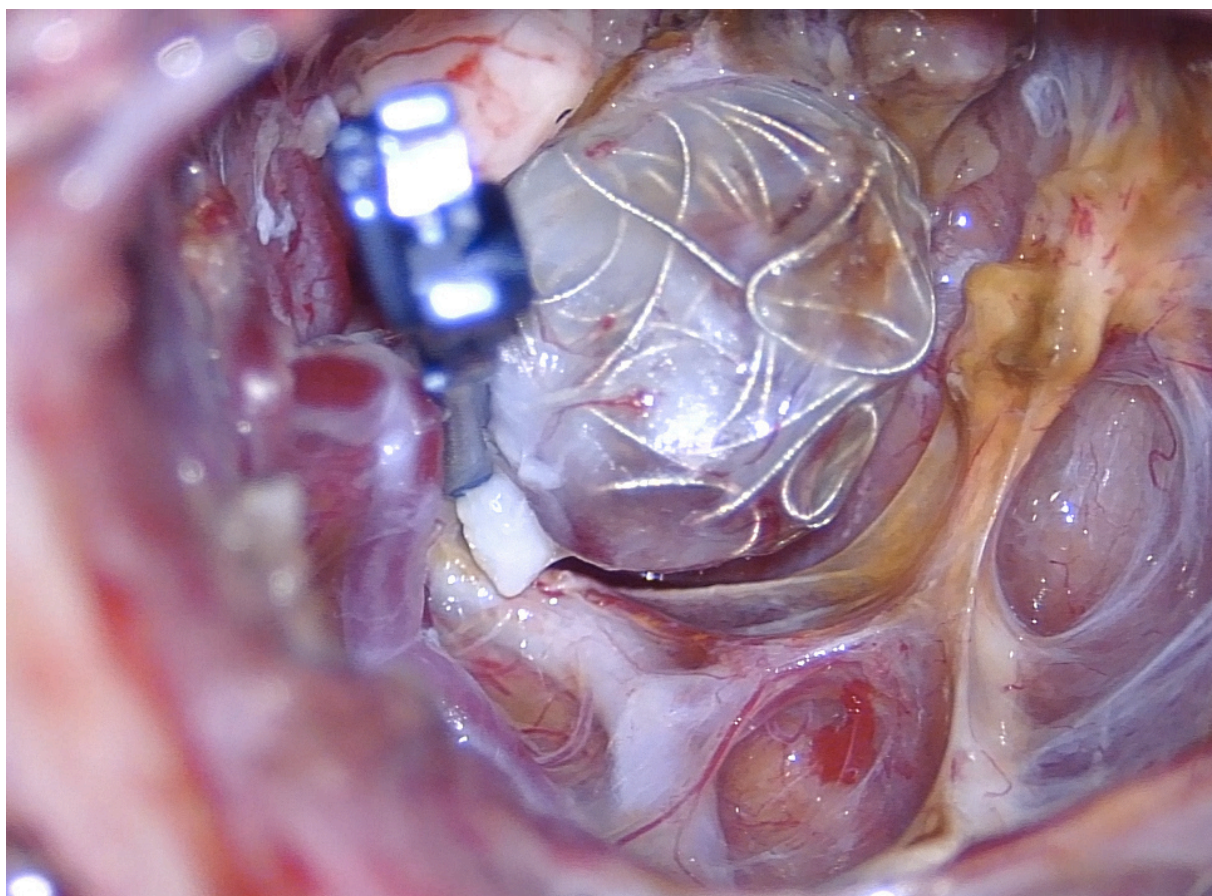


Figure 7a: Indocyanine green video angiography (ICG-VA). Right middle cerebral artery aneurysm previously coiled presenting with a significant recurrence at his neck and treated surgically by clipping.



Figure 7b: Intraoperative ICG-VA confirms the absence of aneurysmal sac residue and the qualitative preservation of the flow in the parent vessel and its branches.

DIGITAL SUBTRACTION ANGIOGRAPHY

Intraoperative digital subtraction angiography (DSA) is routinely used in neurosurgery since a few decades, particularly for complex aneurysm surgery, revascularization procedures, brain AVM resections, and dural arteriovenous fistula surgery.⁵⁷ DSA provides mainly morphological information on brain vasculature and basic dynamic alterations (flow slow-down, vasospasm...), but

does not allow absolute measurements of blood flow. Moreover, it requires a specific operating room installation and exposes the patient and the staff personnel to radiations. DSA owns its own complications: arterial dissection, thromboembolic event, allergy to contrast product, and groin hematoma. Intraoperative DSA has been largely replaced by ICG-VA due to its simplicity of use and integration in the operative microscope.

THERMAL IMAGING

Both CBF and to a lesser extent metabolic activity, result in variations of the cortical temperature.⁵⁸⁻⁶⁰ Imaging of these temperature variations (thermography) have been developed for brain tumor identification^{58,61}, cortical mapping⁵⁹ and CBF monitoring during cerebrovascular surgery.^{62,63} The combination of thermography and an intravenous cold saline bolus injection as a contrast agent has greatly improved the possibility of real-time intraoperative CBF imaging, not only on the cortical surface but also in the deeper surgical cavities.⁶² Hwang et al. used thermal imaging to depict the vascular steal phenomenon usually observed in the peri-nidal region of a brain AVM.⁶³ Muller et al. compared the thermal imaging to ICG-VA during aneurysm surgery and highlighted the possibility of imaging perfusion within the parenchyma deeper than the cortical surface.⁶² Suzuki et al. developed a multimodal device associating thermography and LSCI to help understand the part of metabolic activity and microvascular blood flow in the variations of cortical temperature with promising possibilities for the study of neurovascular and metabolic coupling.⁶⁴ Even though thermography lacks the possibility of direct quantitative absolute measurements of CBF and morphological imaging of microcirculation, its contactlessness, real-time and non-invasive characteristics, open interesting

perspectives for its development in the intraoperative imaging armamentarium in neurosurgery.

NEAR-INFRARED SPECTROSCOPY

Near-infrared spectroscopy (NIRS) is an optical technology used to measure the variations of hemoglobin concentration (oxyhemoglobin (HbO_2), deoxyhemoglobin (dHb) and total hemoglobin concentration ($\text{HbT}=\text{HbO}_2+\text{dHb}$)) via absorption spectroscopy, usually utilized as a non-invasive technique through the scalp, thus providing a reflection of CBF.⁶⁵ The cerebral oxygen saturation (ScO_2) results from the ratio HbO_2/HbT . Both ScO_2 and the concentration difference HbD (HbO_2-dHb) are correlated to CBF. NIRS may be used alone in intensive care or associated to other optical techniques such as diffuse correlation spectroscopy to monitor CBF.⁶⁶ Recently, NIRS has been adapted to be used in the operative room with an emitting light intensity 75% lower than the scalp NIRS. Fukuda et al. used intraoperative NIRS to demonstrate hemodynamic variations in cortico-cortical activity between the primary and supplementary motor cortex during epilepsy surgery.⁶⁷ By using the same intraoperative technique and direct cortical stimulations, Sato et al. were able to highlight the cortico-cortical hemodynamic variations in the language networks with a specific pattern of increase in oxyhemoglobin concomitant with a decrease in deoxyhemoglobin reflecting neurovascular coupling.⁶⁸ In their experience, the authors have been limited in their study by a reduced spatial resolution (quasi-single point analysis) in contrast with an excellent temporal resolution, with a depth sensitivity up to 30 mm from the cortical surface. Intraoperative NIRS represents an interesting seizure-free brain mapping technique⁶⁹ and a portable technology for the exploration of neurovascular coupling, but still does not

provide direct blood flow measurements with sufficient spatial and temporal resolutions as required in cerebrovascular neurosurgery.

INTRAOPERATIVE MRI

Intraoperative MRI is regularly used in oncological neurosurgery to assess the quality of tumor resection and update neuronavigation data following brain shift.⁷⁰ Intraoperative MRI usually relies on anatomical sequences as well as on functional sequences and diffusion tensor imaging for the detection of eloquent cortical and subcortical areas.⁷¹ Recently, Stadlbauer et al. evaluated a quantitative blood oxygenation-level dependent (BOLD) MR sequence intraoperatively to monitor oxygen metabolism and CBF before and after brain tumor resection depicting the beneficial effect of mass effect withdrawal on peritumoral blood flow.⁷² Moreover, Fierstra et al. demonstrated the feasibility of BOLD fMRI to intraoperatively assess cerebrovascular reactivity (CVR) using 3 cycles of apnea-induced hypercapnia on a 3-tesla MRI (Figure 8).⁷³ According to the authors, intraoperative BOLD-CVR may not only help monitoring regional and global cerebral hemodynamics during neurosurgical revascularizations surgeries⁷⁴, but also assist for detecting residual glioma with a specific CVR pattern⁷⁵. Nevertheless, intraoperative MRI requires an elaborate environment and suffers specific potential drawbacks, such as prolonged anesthetic and time of the entire procedure, specific requirements for the operating instrumentation and staff, as well as a poor temporal resolution impeding any real-time continuous monitoring of CBF, relative measurement of CBF, and the sensibility to surgical field artifacts (air, blood and hemostatic products).

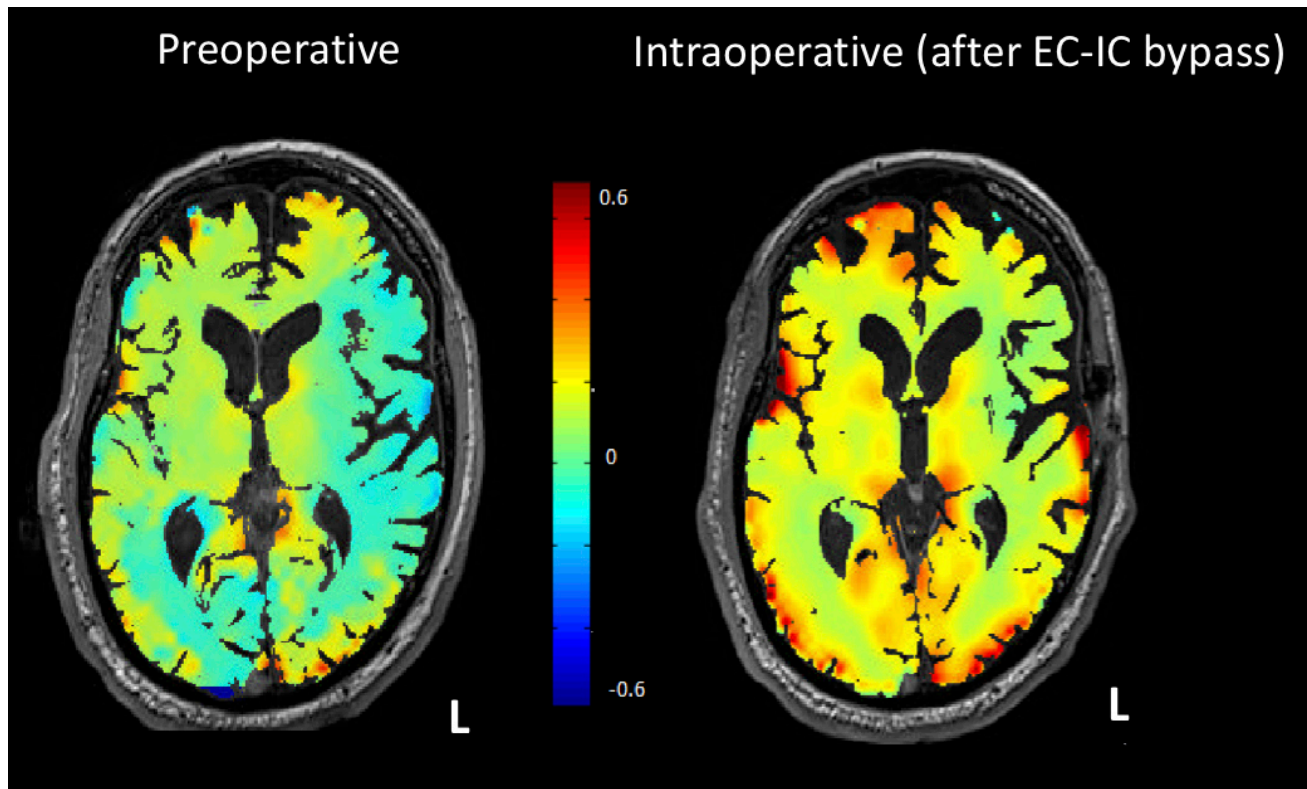


Figure 8: Example of an intraoperative BOLD-CVR study of a patient with a left-sided carotid occlusion that underwent EC-IC bypass revascularization. The BOLD-CVR image is depicted in an axial orientation with color-coding of the CVR values (ranging from red -normal/positive CVR- towards blue -impaired/negative CVR-). One can appreciate that already on this intraoperative study immediately after bypass anastomosis, CVR improvements in the left hemisphere can be seen (yellow and red areas). BOLD-CVR is calculated as %BOLD signal change/mmHg change in CO₂.

CONFOCAL LASER ENDOMICROSCOPY

Confocal laser endomicroscopy (CLE) is a high resolution and high contrast optical imaging technique based on tissue illumination by a low-power laser and detection of the fluorescence reflected from the brain tissue through a

pinhole. With a depth of exploration reaching 200 µm, CLE is used intraoperatively in neurosurgery to provide in-vivo histological diagnosis and may help in the near future to better visualize tumor borders and thus optimize the surgical resection of brain tumors.⁷⁶ Besides, CLE has the capacity to visualize the superficial microvascular network intraoperatively⁷⁷ and the movement of erythrocytes as well as flow abnormalities (thrombosis, cell rolling...) but its role for the intraoperative blood flow monitoring remains very scarce because of low spatiotemporal resolution. As an alternative to CLE, the two-photon microscopy is a fluorescence imaging technique using near-infrared excitation light and allowing a deeper brain tissue penetration (up to 1mm). However its intraoperative applicability in humans still remains restricted due to its limited temporal and spatial resolution for usage in neurosurgery.⁷⁸

ULTRASOUND-BASED TECHNOLOGIES

Microvascular doppler ultrasound (MDU) is a simple and straightforward tool regularly used in vascular neurosurgery.^{53,79} In addition to ICG-VA, MDU provides essential information on vessel patency and quality of aneurysmal sac exclusion. Nevertheless, MDU requires a direct application on the vessel to be analyzed and thus have very poor spatial resolution. It also suffers poor sensitivity to detect arterial stenosis. In contrast, flow quantification probes offer the possibility to quantify blood flow in a specific vessel, and thus represents an invaluable tool particularly during revascularization surgeries to assess the bypass and help identify vessel donor and recipient.

Several ultrasound techniques have been described for an intraoperative use in neurosurgery, predominantly as an adjunct for brain tumor resection. Contrast enhanced ultrasound (CEU) utilizes an intravenous contrast agent containing microbubbles (air or inert gas).⁸⁰ With the imaging of tumoral microvasculature,

CEU offers a better visualization of brain gliomas than standard B-mode ultrasound and may optimize the surgical resection, but does not provide any possibility of CBF monitoring. More recently, a new modality based on high-frame-rate ultrasound named functional ultrasound (FUS) has been introduced to the operative room.⁸¹ FUS allows the detection of very small variations in blood dynamics that correlate with metabolic activation of brain tissue through neurovascular coupling, and thus help optimizing the brain mapping during awake surgery for tumor removal.⁸² Even if CEU and FUS provide a valuable help for brain tumor delineation and brain mapping based on microvasculature imaging, these techniques do not provide a quantitative CBF monitoring. Both modalities offer deep penetration analysis, a large field of view and real-time imaging, but remain contact techniques with the risk of motion and pressure artifacts.

PERSPECTIVES AND CONCLUSION

Outside the operative room, CBF monitoring is widely used with a multitude of technological modalities. In contrast, for intraoperative monitoring of CBF, there is no optimal technology that is entirely suitable. Ideally, such a technology should rely on specific requirements for applications in operative neurosurgery:

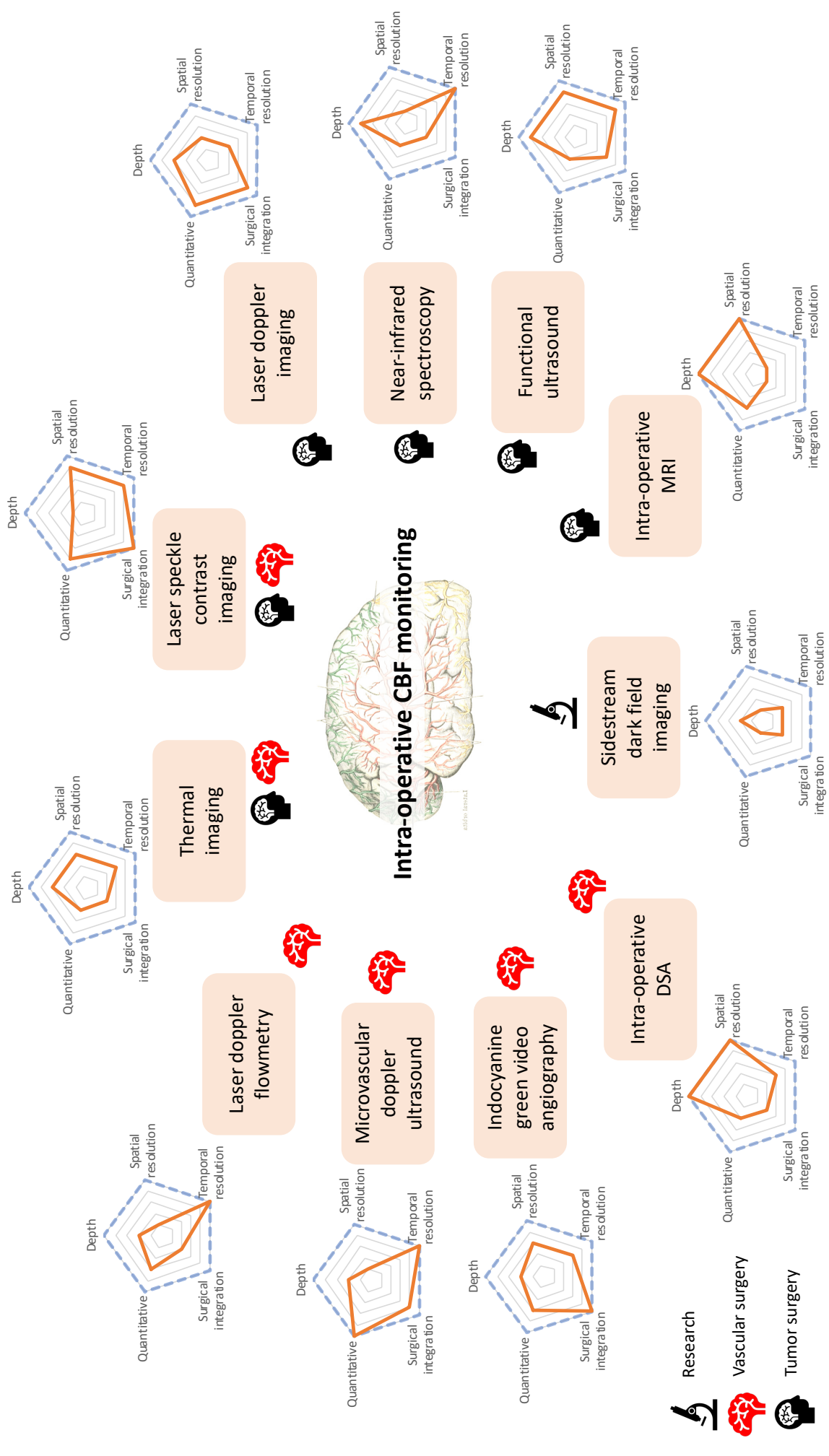
- Non-contact: Any contact with the brain tissue may lead to motion- and pressure artifacts and thus results in inaccurate CBF measurements. This is particularly significant with LDF, SDF imaging and NIRS. Nevertheless, all available technologies including non-contact devices face the issue of brain pulsations that can lead to a certain amount of motions artifacts.
- Excellent temporal resolution: permitting a real-time continuous monitoring of CBF (data acquisition and analysis) and allowing the neurosurgeon to have an immediate feed-back for any incident as well as

enabling to enforce local (clip readjustment, retractor release...) and/or systemic (optimization of blood pressure, CO₂ pressure, depth of anesthesia...) correction measures without delay.

- Excellent spatial resolution: allowing CBF imaging of large brain tissue areas to have a more regional assessment instead of a very limited focal or even single-point imaging.
- Quantitative CBF measurements: The majority of available technologies for intraoperative CBF monitoring does not provide absolute measurements of CBF but relative values and estimations, with the exception of the Doppler flowmeter which is limited to the study of only one artery at a time. This inability to provide absolute measurements makes it difficult to perform intra- and mostly inter-patient comparisons, and to define quantitative thresholds for the intra-operative decision process.
- Depth analysis: Except intraoperative MRI, DSA and NIRS, common CBF imaging technologies provide only very superficial cortical analysis (less than 1.5 mm), impeding the assessment of deep white matter and perforating microvascular blood flow. This limitation can lead to false interpretations where cortical flow is maintained while invisible deep circulation is impaired, for example when a feeding artery is temporarily clipped during an AVM surgery.
- Integration in the surgical workflow: an optimal CBF monitoring system should not significantly impact the duration of surgery and should ideally be fully integrated into the surgical microscope to avoid substantial interruptions of the workflow. Integration in the microscope makes sterile draping easier, thus minimizing the risk of infection. Simplicity of use and data comprehension are also paramount. Intraoperative MRI and DSA, despite the essential information they can provide, are quite expensive and cumbersome in that regard.

Considering all these characteristics, LSCI and MESI appear to have the best current technological profile for the intraoperative use in neurosurgery, including excellent temporal and spatial resolution, and particularly integration to the surgical microscope (Figure 9). Applications of intra-operative CBF monitoring in neurosurgery should dramatically increase in the near future because of the technical refinements that are being developed and the expanding integration in the surgical workflow. These applications will certainly exceed the field of vascular neurosurgery, which is actually manifest, to encompass neuro-oncological surgery (brain mapping, tumor identification) and functional surgery (deep brain stimulation), particularly when used in association with electrophysiological monitoring to concomitantly monitor deep brain vasculature and reduce operative morbidity. Finally, the development of hybrid solutions associating blood flow and metabolic monitoring are of great interest in brain surgery and shall help in the understanding of neurometabolic coupling mechanisms.^{18,64,66}

Figure 9: Comparative overview of cerebral blood flow monitoring technologies focusing on depth of analysis, spatial and temporal resolutions, integration to the surgical workflow and possibility of quantitative measurements.



Laser Doppler technologies		LSCI	SDF	ICG-VA	Thermal imaging	NIRS
LDF	LDI					
Depth analysis	500 µm	1-1.5 mm	530 µm	300 µm	≤ 1mm	30 mm
Contact with the brain	Yes	No	Yes	No	No	Yes
Spatial resolution	-	+	-	++	+	-
Temporal resolution	++	-	+	++	+	++
Possibility of continuous intraoperative monitoring	Yes	No	No	No	No	No
Integration in the surgical microscope	-	+	-	++	-	-
Type of analysis	Relative CBF measurements	Color coded map with relative CBF measurements	No CBF measurement	Indirect estimation of relative CBF	Morphological analysis of the vasculature	Indirect estimation of relative CBF (measurement of Hb concentration)

		perfused vessels, vessel diameter				
Applications in neurosurgery	Peri-nidal monitoring in brain AVMs Detection of CSD Optimization of deep brain electrodes placement and brain biopsies	Brain mapping Monitoring during decompressive craniectomy for stroke and brain injury	Monitoring of CBF during revascularization surgery Monitoring during decompressive craniectomy for stroke and brain injury	Brain tumor identification Identification of feeding arteries during tumor or AVM surgery	Vascular neurosurgery AVM surgery	Brain mapping Hemangioblastoma surgery
	Possibility of intra-parenchymal probe	Combination with spectrophotometry (“oxygen-to-see” probe) to provide concomitant metabolic monitoring	Recently developed incident dark field imaging may provide a better image resolution	Multi-exposure speckle imaging (MESI) for better quantitative accuracy	Possibility to use an intravenous bolus of cold saline as a contrast agent	

Table 1. Characteristics of main contemporary technologies for the intraoperative cerebral blood flow imaging in neurosurgery.

LDF: Laser Doppler flowmeter, LDI: Laser Doppler imaging, CSD: Cortical spreading depolarization, LSCI: Laser speckle-contrast imaging, SDF: Sidestream dark field, ICG-VA: Indocyanine green video angiography, NIRS: Near-infrared spectroscopy, AVM: arteriovenous malformation

Poor :-

Good : +

Excellent : ++

Authorship: All authors have critically revised the manuscript and approved its final content. Manuscript draft, analysis and interpretation of the data: MB, TP, JF, TW. Acquisition of the data: MB, SM, BB, CD, JG. Conception and design of the study: MB, JG, IPG, OE, IR, FC. Interpretation of the data: MB, ACL, FC.

Funding: None

Conflict of interest: The authors declared no potential conflicts of interest with respect to the research, authorship, and/or publication of this article.

REFERENCES

- 1 Lal C, Leahy MJ. An Updated Review of Methods and Advancements in Microvascular Blood Flow Imaging. *Microcirculation* 2016; **23**: 345–363.
- 2 Fantini S, Sassaroli A, Tgavalekos KT, Kornbluth J. Cerebral blood flow and autoregulation: current measurement techniques and prospects for noninvasive optical methods. *Neurophotonics* 2016; **3**: 031411.
- 3 Daly SM, Leahy MJ. 'Go with the flow ': a review of methods and advancements in blood flow imaging. *J Biophotonics* 2013; **6**: 217–255.
- 4 Devor A, Sakadžić S, Srinivasan VJ, Yaseen MA, Nizar K, Saisan PA *et al.* Frontiers in Optical Imaging of Cerebral Blood Flow and Metabolism. *J Cereb*

Blood Flow Metab 2012; **32**: 1259–1276.

- 5 Riva C, Ross B, Benedek GB. Laser Doppler measurements of blood flow in capillary tubes and retinal arteries. *Invest Ophthalmol* 1972; **11**: 936–944.
- 6 Stern MD, Lappe DL, Bowen PD, Chimosky JE, Holloway GA, Keiser HR *et al.* Continuous measurement of tissue blood flow by laser-Doppler spectroscopy. *Am J Physiol* 1977; **232**: H441-448.
- 7 Arbit E, DiResta GR. Application of laser Doppler flowmetry in neurosurgery. *Neurosurg Clin N Am* 1996; **7**: 741–748.
- 8 Kirkpatrick PJ, Smielewski P, Czosnyka M, Pickard JD. Continuous monitoring of cortical perfusion by laser Doppler flowmetry in ventilated patients with head injury. *J Neurol Neurosurg Psychiatry* 1994; **57**: 1382–1388.
- 9 Rosenblum BR, Bonner RF, Oldfield EH. Intraoperative measurement of cortical blood flow adjacent to cerebral AVM using laser Doppler velocimetry. *J Neurosurg* 1987; **66**: 396–399.
- 10 Kawamata T, Kawashima A, Yamaguchi K, Hori T, Okada Y. Usefulness of intraoperative laser Doppler flowmetry and thermography to predict a risk of postoperative hyperperfusion after superficial temporal artery–middle cerebral artery bypass for moyamoya disease. *Neurosurg Rev* 2011; **34**: 355–362.
- 11 Kubo Y, Koji T, Kondo R, Yoshida K, Ogasawara K. Intraoperative monitoring of cerebral cortical blood flow and middle cerebral artery pressure as a substitute for preoperative balloon test occlusion in patients with internal carotid artery aneurysms. *Acta Neurochir (Wien)* 2018; **160**: 1129–1137.
- 12 Winkler MKL, Chassidim Y, Lublinsky S, Revankar GS, Major S, Kang E-J *et al.* Impaired neurovascular coupling to ictal epileptic activity and spreading depolarization in a patient with subarachnoid hemorrhage: Possible link to blood–brain barrier dysfunction. *Epilepsia* 2012; **53**: 22–30.
- 13 Rejmstad P, Åkesson G, Åneman O, Wårdell K. A laser Doppler system for monitoring cerebral microcirculation: implementation and evaluation during neurosurgery. *Med Biol Eng Comput* 2016; **54**: 123–131.

- 14 Wårdell K, Zsigmond P, Richter J, Hemm S. Relationship Between Laser Doppler Signals and Anatomy During Deep Brain Stimulation Electrode Implantation Toward the Ventral Intermediate Nucleus and Subthalamic Nucleus. *Oper Neurosurg (Hagerstown)* 2013; **72**: ons127–ons140.
- 15 Haj-Hosseini N, Richter JCO, Milos P, Hallbeck M, Wårdell K. 5-ALA fluorescence and laser Doppler flowmetry for guidance in a stereotactic brain tumor biopsy. *Biomed Opt Express* 2018; **9**: 2284–2296.
- 16 Raabe A, Van De Ville D, Leutenegger M, Szelényi A, Hattingen E, Gerlach R *et al.* Laser Doppler imaging for intraoperative human brain mapping. *Neuroimage* 2009; **44**: 1284–1289.
- 17 Klein KU, Stadie A, Fukui K, Schramm P, Werner C, Oertel J *et al.* Measurement of cortical microcirculation during intracranial aneurysm surgery by combined laser-Doppler flowmetry and photospectrometry. *Neurosurgery* 2011; **69**: 391–398.
- 18 Sommer B, Kreuzer M, Bischoff B, Wolf D, Schmitt H, Eyupoglu IY *et al.* Combined Laser-Doppler Flowmetry and Spectrophotometry: Feasibility Study of a Novel Device for Monitoring Local Cortical Microcirculation during Aneurysm Surgery. *J Neurol Surg A Cent Eur Neurosurg* 2017; **78**: 1–11.
- 19 Briers JD, Fercher AF. Retinal blood-flow visualization by means of laser speckle photography. *Invest Ophthalmol Vis Sci* 1982; **22**: 255–259.
- 20 Dunn AK. Laser speckle contrast imaging of cerebral blood flow. *Ann Biomed Eng* 2012; **40**: 367–377.
- 21 Kazmi SMS, Richards LM, Schrandt CJ, Davis MA, Dunn AK. Expanding applications, accuracy, and interpretation of laser speckle contrast imaging of cerebral blood flow. *J Cereb Blood Flow Metab* 2015; **35**: 1076–1084.
- 22 Richards LM, Towle EL, Fox DJ, Dunn AK. Intraoperative laser speckle contrast imaging with retrospective motion correction for quantitative assessment of cerebral blood flow. *NPh* 2014; **1**: 015006.
- 23 Parthasarathy AB, Tom WJ, Gopal A, Zhang X, Dunn AK. Robust flow

- measurement with multi-exposure speckle imaging. *Opt Express* 2008; **16**: 1975–1989.
- 24 Kazmi SMS, Parthasarthy AB, Song NE, Jones TA, Dunn AK. Chronic imaging of cortical blood flow using Multi-Exposure Speckle Imaging. *J Cereb Blood Flow Metab* 2013; **33**: 798–808.
- 25 Richards LM, Kazmi SS, Olin KE, Waldron JS, Fox DJ, Dunn AK. Intraoperative multi-exposure speckle imaging of cerebral blood flow. *J Cereb Blood Flow Metab* 2017; **37**: 3097–3109.
- 26 Ponticorvo A, Dunn AK. Simultaneous imaging of oxygen tension and blood flow in animals using a digital micromirror device. *Opt Express* 2010; **18**: 8160–8170.
- 27 Jones PB, Shin HK, Boas DA, Hyman BT, Moskowitz MA, Ayata C *et al.* Simultaneous multispectral reflectance imaging and laser speckle flowmetry of cerebral blood flow and oxygen metabolism in focal cerebral ischemia. *J Biomed Opt* 2008; **13**: 044007.
- 28 Shin HK, Dunn AK, Jones PB, Boas DA, Lo EH, Moskowitz MA *et al.* Normobaric hyperoxia improves cerebral blood flow and oxygenation, and inhibits peri-infarct depolarizations in experimental focal ischaemia. *Brain* 2007; **130**: 1631–1642.
- 29 Dunn AK, Devor A, Dale AM, Boas DA. Spatial extent of oxygen metabolism and hemodynamic changes during functional activation of the rat somatosensory cortex. *Neuroimage* 2005; **27**: 279–290.
- 30 Dunn AK, Devor A, Bolay H, Andermann ML, Moskowitz MA, Dale AM *et al.* Simultaneous imaging of total cerebral hemoglobin concentration, oxygenation, and blood flow during functional activation. *Opt Lett* 2003; **28**: 28–30.
- 31 Hecht N, Woitzik J, Dreier JP, Vajkoczy P. Intraoperative monitoring of cerebral blood flow by laser speckle contrast analysis. *Neurosurgical Focus* 2009; **27**: E11.

- 32 Parthasarathy AB, Weber EL, Richards LM, Fox DJ, Dunn AK. Laser speckle contrast imaging of cerebral blood flow in humans during neurosurgery: a pilot clinical study. *J Biomed Opt* 2010; **15**: 066030.
- 33 Ideguchi M, Kajiwara K, Yoshikawa K, Goto H, Sugimoto K, Inoue T *et al.* Avoidance of ischemic complications after resection of a brain lesion based on intraoperative real-time recognition of the vasculature using laser speckle flow imaging. *J Neurosurg* 2017; **126**: 274–280.
- 34 Hecht N, Müller M-M, Sandow N, Pinczolits A, Vajkoczy P, Woitzik J. Infarct prediction by intraoperative laser speckle imaging in patients with malignant hemispheric stroke. *J Cereb Blood Flow Metab* 2016; **36**: 1022–1032.
- 35 Klijn E, Hulscher HC, Balvers RK, Holland WPJ, Bakker J, Vincent AJPE *et al.* Laser speckle imaging identification of increases in cortical microcirculatory blood flow induced by motor activity during awake craniotomy. *J Neurosurg* 2013; **118**: 280–286.
- 36 Woitzik J, Hecht N, Pinczolits A, Sandow N, Major S, Winkler MKL *et al.* Propagation of cortical spreading depolarization in the human cortex after malignant stroke. *Neurology* 2013; **80**: 1095–1102.
- 37 Nadort A, Kalkman K, van Leeuwen TG, Faber DJ. Quantitative blood flow velocity imaging using laser speckle flowmetry. *Scientific Reports* 2016; **6**: 1–10.
- 38 Slaaf DW, Tangelder GJ, Reneman RS, Jäger K, Bollinger A. A versatile incident illuminator for intravital microscopy. *Int J Microcirc Clin Exp* 1987; **6**: 391–397.
- 39 Groner W, Winkelmann JW, Harris AG, Ince C, Bouma GJ, Messmer K *et al.* Orthogonal polarization spectral imaging: A new method for study of the microcirculation. *Nat Med* 1999; **5**: 1209–1212.
- 40 De Backer D, Hollenberg S, Boerma C, Goedhart P, Büchele G, Ospina-Tascon G *et al.* How to evaluate the microcirculation: report of a round table conference. *Crit Care* 2007; **11**: R101.
- 41 Uhl E, Lehmberg J, Steiger H-J, Messmer K. Intraoperative Observation of

Human Cerebral Microcirculation. *Orthogonal Polarization Spectral Imaging* 2000; **24**: 72–81.

- 42 Uhl E, Lehmberg J, Steiger H-J, Messmer K. Intraoperative detection of early microvasospasm in patients with subarachnoid hemorrhage by using orthogonal polarization spectral imaging. *Neurosurgery* 2003; **52**: 1307–1315; discussion 1315-1317.
- 43 Pennings FA, Bouma GJ, Ince C. Direct Observation of the Human Cerebral Microcirculation During Aneurysm Surgery Reveals Increased Arteriolar Contractility. *Stroke* 2004; **35**: 1284–1288.
- 44 Pennings FA, Ince C, Bouma GJ. Continuous real-time visualization of the human cerebral microcirculation during arteriovenous malformation surgery using orthogonal polarization spectral imaging. *Neurosurgery* 2006; **59**: 167–171; discussion 167-171.
- 45 Pennings FA, Albrecht KW, Muizelaar JP, Schuurman PR, Bouma GJ. Abnormal responses of the human cerebral microcirculation to papaverin during aneurysm surgery. *Stroke* 2009; **40**: 317–320.
- 46 Pérez-Bárcena J, Goedhart P, Ibáñez J, Brell M, García R, Llinás P *et al.* Direct observation of human microcirculation during decompressive craniectomy after stroke. *Crit Care Med* 2011; **39**: 1126–1129.
- 47 Pérez-Bárcena J, Romay E, Llompart-Pou JA, Ibáñez J, Brell M, Llinás P *et al.* Direct observation during surgery shows preservation of cerebral microcirculation in patients with traumatic brain injury. *J Neurol Sci* 2015; **353**: 38–43.
- 48 Raabe A, Beck J, Gerlach R, Zimmermann M, Seifert V. Near-infrared indocyanine green video angiography: a new method for intraoperative assessment of vascular flow. *Neurosurgery* 2003; **52**: 132–139; discussion 139.
- 49 Woitzik J, Peña-Tapia PG, Schneider UC, Vajkoczy P, Thomé C. Cortical perfusion measurement by indocyanine-green videoangiography in patients undergoing hemicraniectomy for malignant stroke. *Stroke* 2006; **37**: 1549–1551.

- 50 Saito M, Saga T, Hayashi H, Noro S, Wada H, Kamada K. Quantitative Blood Flow Assessment by Multiparameter Analysis of Indocyanine Green Video Angiography. *World Neurosurg* 2018; **116**: e187–e193.
- 51 Kato N, Prinz V, Dengler J, Vajkoczy P. Blood Flow Assessment of Arteriovenous Malformations Using Intraoperative Indocyanine Green Videoangiography. *Stroke Res Treat* 2019; **2019**. doi:10.1155/2019/7292304.
- 52 Cavallo C, Gandhi S, Zhao X, Belykh E, Valli D, Nakaji P *et al.* Applications of Microscope-Integrated Indocyanine Green Videoangiography in Cerebral Revascularization Procedures. *Front Surg* 2019; **6**. doi:10.3389/fsurg.2019.00059.
- 53 Starke RM, Dumont AS. Intraoperative imaging and assessment of cerebral blood flow in cerebrovascular surgery: hybrid operating rooms, intraoperative angiography and magnetic resonance imaging, Doppler ultrasound, cerebral blood flow probes, endoscopic assistance, indocyanine green videography, and laser speckle contrast imaging. *World Neurosurg* 2014; **82**: e693-696.
- 54 Raabe A, Nakaji P, Beck J, Kim LJ, Hsu FPK, Kamerman JD *et al.* Prospective evaluation of surgical microscope—integrated intraoperative near-infrared indocyanine green videoangiography during aneurysm surgery. *Journal of Neurosurgery* 2005; **103**: 982–989.
- 55 Uchino H, Kazumata K, Ito M, Nakayama N, Kuroda S, Houkin K. Intraoperative assessment of cortical perfusion by indocyanine green videoangiography in surgical revascularization for moyamoya disease. *Acta Neurochir* 2014; **156**: 1753–1760.
- 56 Horie N, Fukuda Y, Izumo T, Hayashi K, Suyama K, Nagata I. Indocyanine green videoangiography for assessment of postoperative hyperperfusion in moyamoya disease. *Acta Neurochir* 2014; **156**: 919–926.
- 57 Fredrickson VL, Russin JJ, Strickland BA, Bakhsheshian J, Amar AP. Intraoperative Imaging for Vascular Lesions. *Neurosurg Clin N Am* 2017; **28**: 603–613.

- 58 Gorbach AM, Heiss JD, Kopylev L, Oldfield EH. Intraoperative infrared imaging of brain tumors. *J Neurosurg* 2004; **101**: 960–969.
- 59 Hoffmann N, Radev Y, Koch E, Petersohn U, Steiner G, Kirsch M. Intraoperative mapping of the sensory cortex by time-resolved thermal imaging. *Biomed Tech (Berl)* 2018; **63**: 567–572.
- 60 Shevelev IA, Tsicalov EN, Gorbach AM, Budko KP, Sharaev GA. Thermoimaging of the brain. *J Neurosci Methods* 1993; **46**: 49–57.
- 61 Kateb B, Yamamoto V, Yu C, Grundfest W, Gruen JP. Infrared thermal imaging: A review of the literature and case report. *NeuroImage* 2009; **47**: T154–T162.
- 62 Müller J, Schreiter V, Böhl E, Steiner G, Koch E, Schackert G *et al.* Application of thermography for cerebral perfusion imaging during aneurysm surgery. *Current Directions in Biomedical Engineering* 2018; **4**: 29–32.
- 63 Hwang PYK, Lewis PM, Maller JJ. Use of intracranial and ocular thermography before and after arteriovenous malformation excision. *J Biomed Opt* 2014; **19**: 110503.
- 64 Suzuki T, Oishi N, Fukuyama H. Simultaneous infrared thermal imaging and laser speckle imaging of brain temperature and cerebral blood flow in rats. *J Biomed Opt* 2018; **24**: 1–11.
- 65 Pham T, Tgavalekos K, Sassaroli A, Blaney G, Fantini S. Quantitative measurements of cerebral blood flow with near-infrared spectroscopy. *Biomed Opt Express* 2019; **10**: 2117–2134.
- 66 Baker WB, Balu R, He L, Kavuri VC, Busch DR, Amendolia O *et al.* Continuous non-invasive optical monitoring of cerebral blood flow and oxidative metabolism after acute brain injury. *J Cereb Blood Flow Metab* 2019; **39**: 1469–1485.
- 67 Fukuda M, Takao T, Hiraishi T, Aoki H, Ogura R, Sato Y *et al.* Cortico-cortical activity between the primary and supplementary motor cortex: An intraoperative near-infrared spectroscopy study. *Surg Neurol Int* 2015; **6**: 44.

- 68 Sato K, Fukuda M, Sato Y, Hiraishi T, Takao T, Fujii Y. Cortico-cortical evoked hemodynamic responses in human language systems using intraoperative near-infrared spectroscopy during direct cortical stimulation. *Neuroscience Letters* 2016; **630**: 136–140.
- 69 Qiu T, Hameed NUF, Peng Y, Wang S, Wu J, Zhou L. Functional near-infrared spectroscopy for intraoperative brain mapping. *NPh* 2019; **6**: 045010.
- 70 Ulmer S. Intraoperative perfusion magnetic resonance imaging: Cutting-edge improvement in neurosurgical procedures. *World J Radiol* 2014; **6**: 538–543.
- 71 Roder C, Charyasz-Leks E, Breitkopf M, Decker K, Ernemann U, Klose U *et al.* Resting-state functional MRI in an intraoperative MRI setting: proof of feasibility and correlation to clinical outcome of patients. *J Neurosurg* 2016; **125**: 401–409.
- 72 Stadlbauer A, Merkel A, Zimmermann M, Sommer B, Buchfelder M, Meyer-Bäse A *et al.* Intraoperative Magnetic Resonance Imaging of Cerebral Oxygen Metabolism During Resection of Brain Lesions. *World Neurosurg* 2017; **100**: 388–394.
- 73 Fierstra J, Burkhardt J-K, van Niftrik CHB, Piccirelli M, Pangalu A, Kocian R *et al.* Blood oxygen-level dependent functional assessment of cerebrovascular reactivity: Feasibility for intraoperative 3 Tesla MRI. *Magn Reson Med* 2017; **77**: 806–813.
- 74 Muscas G, Bas van Niftrik CH, Fierstra J, Piccirelli M, Sebök M, Burkhardt J-K *et al.* Feasibility and safety of intraoperative BOLD functional MRI cerebrovascular reactivity to evaluate extracranial-to-intracranial bypass efficacy. *Neurosurg Focus* 2019; **46**: E7.
- 75 Hsu Y-Y, Chang C-N, Jung S-M, Lim K-E, Huang J-C, Fang S-Y *et al.* Blood oxygenation level-dependent MRI of cerebral gliomas during breath holding. *J Magn Reson Imaging* 2004; **19**: 160–167.
- 76 Belykh E, Miller EJ, Carotenuto A, Patel AA, Cavallo C, Martirosyan NL

et al. Progress in Confocal Laser Endomicroscopy for Neurosurgery and Technical Nuances for Brain Tumor Imaging With Fluorescein. *Front Oncol* 2019; **9**. doi:10.3389/fonc.2019.00554.

- 77 Belykh E, Cavallo C, Zhao X, Lawton MT, Nakaji P, Preul MC. 312 Intraoperative Imaging of Cerebral Vasculature and Blood Flow Using Confocal Laser Endomicroscopy: New Perspectives in Precise Real-Time Brain Fluorescence Microimaging. *Neurosurgery* 2018; **65**: 126–127.
- 78 Shih AY, Driscoll JD, Drew PJ, Nishimura N, Schaffer CB, Kleinfeld D. Two-photon microscopy as a tool to study blood flow and neurovascular coupling in the rodent brain. *J Cereb Blood Flow Metab* 2012; **32**: 1277–1309.
- 79 Gruber A, Dorfer C, Standhardt H, Bavinzski G, Knosp E. Prospective comparison of intraoperative vascular monitoring technologies during cerebral aneurysm surgery. *Neurosurgery* 2011; **68**: 657–673; discussion 673.
- 80 Prada F, Perin A, Martegani A, Aiani L, Solbiati L, Lamperti M *et al.* Intraoperative contrast-enhanced ultrasound for brain tumor surgery. *Neurosurgery* 2014; **74**: 542–552; discussion 552.
- 81 Soloukey S, Vincent AJPE, Satoer DD, Mastik F, Smits M, Dirven CMF *et al.* Functional Ultrasound (fUS) During Awake Brain Surgery: The Clinical Potential of Intra-Operative Functional and Vascular Brain Mapping. *Front Neurosci* 2020; **13**. doi:10.3389/fnins.2019.01384.
- 82 Deffieux T, Demene C, Pernot M, Tanter M. Functional ultrasound neuroimaging: a review of the preclinical and clinical state of the art. *Curr Opin Neurobiol* 2018; **50**: 128–135.

TABLES

Table 1: Characteristics of main contemporary technologies for the intraoperative cerebral blood flow imaging in neurosurgery.

FIGURES

Figure 1: Flow chart of literature search strategy

Figure 2: Laser Doppler Flowmetry. An incident photons source produces a laser light beam that infiltrates approximately 1 mm^3 of brain cortex. Mobile (erythrocytes, leucocytes, etc....) and immobile (neurons, glial cells, etc....) structures scatter the incident photons resulting in a Doppler shift and an electrical signal reflecting both velocity and density of erythrocytes.

Figure 3: Laser speckle cell imaging. A coherent laser beam illuminates the most superficial heterogeneous layer of the brain cortex up to $300 \mu\text{m}$ resulting in an irregular backscattering of the light. A CCD camera, possibly integrated in the operative microscope, detects the ensuing random speckle pattern which is variable with erythrocytes' movements.

Figure 4: Example of intraoperative laser speckle cell imaging during brain glioma removal with a surgical microscope integrated LSCI device (Omegazone OZ-3, Omegawave Inc.). The difference in CBF can be measured between 2 ROIs (ROI1 corresponds to normal brain tissue, ROI2 corresponds to tumoral brain tissue). (Courtesy of Dr Jun Muto, Fujita Health University)

Figure 5: Sidestream dark field imaging. A stroboscopic green light (530 to 548 nm) illuminates the cortical surface up to $500 \mu\text{m}$. This specific wavelength light

is exclusively absorbed by erythrocytes and results in the display of the black vascular network in a gray background.

Figures 6: Sidestream dark field imaging. The development of a hand-held device and a real-time image analysis ease its use intra-operatively (Figure 6a) (Courtesy of Microscan™, Microvision Medical, Amsterdam, The Netherlands). Example of cortical SDF imaging showing the flow of erythrocytes (Figure 6b).

Figure 7: Indocyanine green video angiography (ICG-VA). Right middle cerebral artery aneurysm previously coiled presenting with a significant recurrence at his neck and treated surgically by clipping (Figure 7a). Intraoperative ICG-VA confirms the absence of aneurysmal sac residue and the qualitative preservation of the flow in the parent vessel and its branches (Figure 7b).

Figure 8: Example of an intraoperative BOLD-CVR study of a patient with a left-sided carotid occlusion that underwent EC-IC bypass revascularization. The BOLD-CVR image is depicted in an axial orientation with color-coding of the CVR values (ranging from red -normal/positive CVR- towards blue -impaired/negative CVR-). One can appreciate that already on this intraoperative study immediately after bypass anastomosis, CVR improvements in the left hemisphere can be seen (yellow and red areas). BOLD-CVR is calculated as %BOLD signal change/mmHg change in CO₂.

Figure 9: Comparative overview of cerebral blood flow monitoring technologies focusing on depth of analysis, spatial and temporal resolutions, integration to the surgical workflow and possibility of quantitative measurements.

IV - PATHOGENIE DE L'ŒDEME PERITUMORAL DANS LES MENINGIOMES INTRA-CRANIENS

Publié dans Neurosurgical Review

Pathogenesis of peri-tumoral edema in intracranial meningiomas.

Berhouma M, Jacquesson T, Jouanneau E, Cotton F.

Neurosurg Rev. 2019 Mar;42(1):59-71

Résumé

Les méningiomes constituent la 2^{ème} tumeur intracrânienne la plus fréquente après les gliomes, représentant environ 20% de l'ensemble des tumeurs intracrâniennes. 85% des méningiomes intéressent le compartiment sus-tentoriel avec un sexe ratio de 2:1. Les méningiomes sont classés en 3 grades selon la dernière classification de l'OMS : Méningiomes bénins (80%, 9 sous-types histologiques), méningiomes atypiques (15-20%, 3 sous-types) et méningiomes anaplasiques (1-3%, 3 sous-types). Quand il est possible, la résection chirurgicale complète demeure le traitement de référence. La radiothérapie ou la radiochirurgie peuvent également être proposés soit en première intention dans les méningiomes inopérables soit en complément de la chirurgie en cas de méningiome atypique ou anaplasique.

Les méningiomes intracrâniens s'accompagnent d'un œdème péritumoral dans 38 à 67% des cas. Cet œdème peut impacter la morbidité et la mortalité en accentuant l'effet de masse et la pression intracrânienne. L'œdème péritumoral est également associé à un risque plus élevé d'hémorragie cérébrale post-opératoire, de crise comitiale péri-opératoire et de déficit neurologique. Sans résultat clair et significatif, différentes études ont tenté de retrouver des facteurs de risque de développement d'un œdème péritumoral dans les méningiomes

intracrâniens : âge, sexe, topographie tumorale, type histologique, volume tumoral,... La pathogénie de l'œdème péritumoral reste inconnue, reposant sur 4 théories principales : Théorie compressive (méningiomes de gros volumes comprimant le parenchyme cérébral, à l'origine de phénomènes ischémiques et d'œdème cytotoxique), théorie sécrétoire-excrétoire (liée à certains sous-types histologiques spécifiques produisant des inclusions éosinophiliques et PAS-positives), théorie veineuse (méningiome obstruant le réseau veineux), et la théorie hydrodynamique (ischémie tumorale engendrant la sécrétion de facteurs angiogéniques à l'origine d'altérations de la matrice extra-cellulaire et de fuites de protéines). Notre travail reprend l'ensemble de ces théories en approfondissant l'implications de certains facteurs spécifiques et discutant les possibles cibles thérapeutiques.

REVIEW

Pathogenesis of peri-tumoral edema in intracranial meningiomas

Moncef Berhouma^{1,2}  · Timothee Jacquesson¹ · Emmanuel Jouanneau¹ · François Cotton^{2,3}

Received: 8 May 2017 / Revised: 23 July 2017 / Accepted: 18 August 2017
© Springer-Verlag GmbH Germany 2017

Abstract Peri-tumoral edema in intracranial meningiomas occurs frequently and obviously impacts the morbidity and mortality of these predominantly benign neoplasms. Several causative factors (age, gender, volume, location...) have been unsuccessfully investigated. Despite recent progresses in metabolic imaging and molecular biology, the pathogenesis of peri-tumoral edema remains debated. Hypotheses include vascular endothelial growth factor, metalloproteinases and interleukins among many others. It is probable that this pathogenesis encompasses all these factors with different levels. The current review aims to shed the light on the investigated factors involved in the pathogenesis of peri-tumoral edema in meningiomas and identify the potential therapeutic targets.

Keywords Meningioma · Peri-tumoral brain edema · Vasogenic edema · Cytotoxic edema · Vascular endothelial growth factor · Metalloproteinases · Aquaporins · Interleukins · Mast cells · Hypoxia-inducible factor

Abbreviations

PTBE	Peri-tumoral brain edema
BBB	Blood-brain barrier
VEGF	Vascular endothelial growth factor
BNP	Brain natriuretic peptide
AQP	Aquaporin
MMP	Metalloproteinases
HIF	Hypoxia-inducible factor
IL	Interleukin
WHO	World Health Organization

Introduction

Meningiomas are the second most frequent intracranial neoplasm following gliomas. They represent about one fifth of intracranial neoplasms [26, 102]. Eighty-five percent of these occur in the supratentorial compartment [114]. Female to male ratio reaches 2:1 [114]. Meningiomas are classified into three types in the WHO classification: benign (80% and 9 histological subtypes), atypical (15 to 20% and 3 subtypes), and anaplastic (1 to 3% and 3 subtypes) [112]. Gross total resection still remains the gold standard treatment, while radiotherapy and radiosurgery play a significant role in the management either as primary treatment or following surgery.

The occurrence of peri-tumoral brain edema (PTBE) is not rare in intracranial meningiomas, except for suprasellar locations, affecting between 38 and 67% of patients harboring an intracranial meningioma [39, 45]. This PTBE may raise the morbidity and mortality [3, 31, 136] by increasing brain shift and intracranial pressure [79], making the surgical removal challenging and it also is a predisposing factor to perioperative epilepsy [70, 139]. Moreover PTBE has been associated with a higher risk of postoperative intracranial hematoma [126] as

✉ Moncef Berhouma
berhouma.moncef@gmail.com

¹ Skull Base Surgery Unit, Department of Neurosurgery B, University Hospital of Lyon, Hospices Civils de Lyon, Lyon, France

² Laboratory CREATIS - CNRS UMR5220 - INSERM U1206 – Lyon 1 University – INSA, Lyon, France

³ Department of Imaging, Lyon Sud Hospital, Hospices Civils de Lyon, Lyon, France

well as neurological deficits [1, 139]. The pathogenesis of PTBE in meningiomas is still unclear and implicates to varying degrees *inter alia* vascular endothelial growth factor A (VEGF-A) [50, 75, 85, 109, 121], aquaporin 4 [65, 88, 129, 142], and matrix metalloproteinase 9 (MMP-9) [50, 92, 94]. During the last two decades, main studies have focused on the molecular characteristics of meningiomas through research concerning signal transduction pathways. It is now well established that meningiomas express receptors for epidermal growth factor [55, 64], dopamine [21, 137], platelet-derived growth factor [124], prolactin [82], and somatostatin [101]. In contrast relatively little is known about the role of extracellular matrix and PTBE in tumor-associated angiogenesis, invasion, cell signaling, and migration.

We herein review the pathogenesis of the PTBE as some specific treatments may relieve this edema prior to the meningioma's treatment and therefore impact morbidity and mortality as well. A better understanding of this pathogenesis will probably open new insights into targeted therapies in meningiomas.

Methods

A bibliographic search until June 2016 via Medline, Sciedirect, and Scopus databases was performed with the keywords "meningioma," "peri-tumoral brain edema," "VEGF," "matrix metalloproteinase," and "aquaporin." The abstracts of identified publications were reviewed and only relevant papers were considered excluding case reports. There were no language restrictions.

Clinical evidence

Up to 67% of intracranial meningiomas harbor a certain amount of peri-tumoral edema [45]. Several studies attempted to correlate PTBE with various clinical and pathological factors including sex, age, tumor location, tumor size, histological subtypes, and venous obstruction. None of these correlations was statistically significant and definitely conclusive.

No study demonstrated any correlation or trend regarding sex and age. Concerning the impact of the volume of the meningioma, there is a trend toward a greater incidence of PTBE in larger tumors. In Bitzer et al. study, the incidence of PTBE was 20.7% in tumors inferior to 10 ml in contrast to an incidence of 92.3% of PTBE in tumors larger than 10 ml [12]. This trend was also reported significantly in other studies confirming the hypothesis that a larger surface of brain compressed by the tumor volume leads to more frequent hypoxic consequences and brain/tumor adhesion issues [122].

Other studies reported the correlation between a shorter course of the symptoms reflecting a rapid growth of the tumor, and the incidence and importance of PTBE [128]. Even if

supratentorial locations were thought to be more generative of PTBE, the majority of studies dealing with location as a specific factor of PTBE revealed that suprasellar meningiomas were quite never associated with PTBE, probably because of the multiple arachnoid layers in this region.

Bitzer et al. and de Vries et al. noted a significant correlation between WHO grade II and III meningiomas and a more extensive PTBE [12, 140]. Elsewhere, a specific subtype of meningiomas, known as secretory meningiomas, is commonly associated with very large PTBE [103], as well as microcystic and angiomatous patterns.

In a recent series of 61 patients with benign meningiomas, Simis et al. noted that the extent of PTBE in meningiomas had a positive correlation with the presence of irregular margins of the tumor and higher recurrence rates, as well as with a larger volume of the meningioma on the basis of a bivariate analysis [125]. The authors conclude that larger meningiomas may disrupt the arachnoid membrane leading to leakage of edemogenic factors in the adjacent brain. Multivariate analysis confirmed the association between PTBE and the volume of the meningioma and revealed a correlation between the extent of PTBE and the risk of seizures. In the same paper, Simis et al. verified the existence of a positive statistical correlation between an irregular shape and the extent of PTBE, reinforcing the hypothesis that an irregular interface brain/meningioma favors brain invasion and edema development [39, 71, 84, 122]. In their prospective series of 135 patients that underwent total removal of intracranial meningiomas, Mantle et al. [77] noted a correlation between the extent of PTBE and the recurrence risk, as did Simis et al. Nakano et al. found that hyperintense meningiomas on T2WI were frequently accompanied by large PTBE, probably because of the larger water content of these tumors [83].

In fine, there is no clear cut positive correlation between any clinical, histological, or imaging factor and the existence of PTBE, but there is a trend toward the development of marked PTBE in large meningiomas (except for secretory, microcystic, and angiomatous histological subtypes), those developing on the supratentorial convexity particularly the middle fossa, those with irregular margins, and those with a marked pial vascular recruitment.

Pathogenesis

The pathogenesis of PTBE still remains subject to debate. Historically, Klatzo classified cerebral edema as vasogenic and cytotoxic types [61–63]. He defined vasogenic edema as secondary to an increase of capillary permeability, resulting in protein and fluid extravasations into the extracellular space particularly into the white matter. The gray matter is theoretically spared because of its intricately woven cellular architecture limiting considerably the free movement of fluids in the

extracellular space. In contrast, during cytotoxic edema, the fluid is accumulated in the intracellular compartment mainly within the glial cells including the gray matter. Four main theories on PTBE pathogenesis can be individualized:

- The brain parenchyma compression theory: Tumor size may play an important role in the genesis of PTBE. Large meningiomas lead to compression, ischemia, and cytotoxic edema [36, 39, 76]. This theory cannot be generalized as sometimes very small meningiomas cause extensive PTBE. There was no clear significant correlation between tumor size and the importance of edema in many recent case series [47, 68, 76, 93] (Fig. 1a, b). According to this theory, the incidence of PTBE in large meningiomas occurring in the elderly should be lower than in the general population of patients with intracranial meningiomas because of age-related brain atrophy, but even this statement has not been statistically demonstrated.
- The secretory-excretory theory: Some specific histological subtypes of meningiomas, particularly secretory ones [105], produce eosinophilic and periodic acid-Schiff (PAS) positive inclusions secreted along the perivascular spaces and therefore generate PTBE mainly through an osmotic mechanism [2, 18, 19, 127]. Although secretory meningiomas are usually surrounded by extensive PTBE [141], the frequency of this histological subtype (less than 3% of all meningiomas) cannot explain the overall incidence of PTBE in meningiomas [103] (Fig. 2a–c).
- The venous compression theory: Tumoral obstruction of veins and sinuses hinder the venous outflow around the meningioma. This theory was not clearly proven in large angiographic series even if in specific cases venous obstruction may represent an aggravating factor [10, 11].
- The hydrodynamic theory: The concept of intra-tumoral congestion. Tanaka et al. in 2006 found a significant relationship between PTBE and hypoplastic efferent tumoral veins using superselective angiography [130]. The

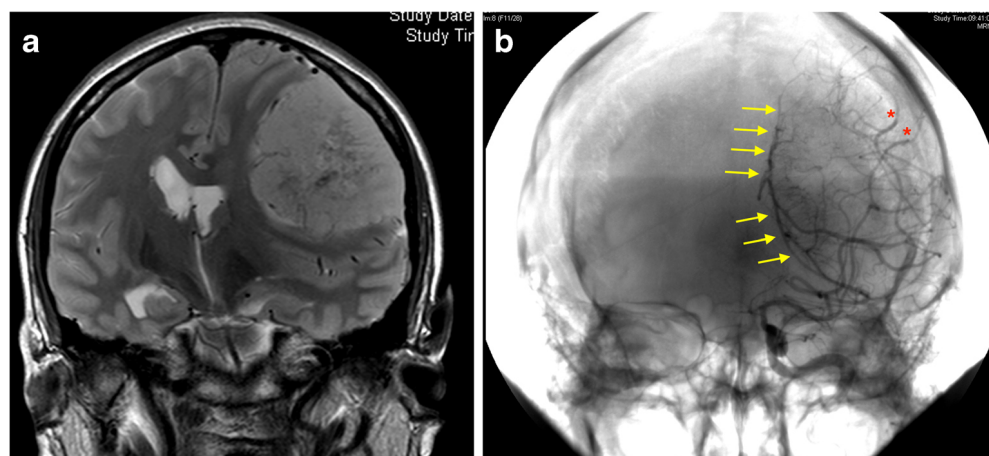
hydrodynamic theory states that when tumoral blood supply becomes insufficient, meningiomas secrete angiogenic factors resulting in immature highly permeable neovessels and therefore to leakage of plasma proteins within the tumor [85, 86]. These angiogenic factors include mainly VEGF-A but also endothelin-1 and caveolin-1 [4, 123, 146]. If the meningioma-brain interface is permeable (absence of arachnoid interface), these angiogenic factors diffuse in the surrounding brain parenchyma and vasogenic substances lead to the development of PTBE [30]. Similarities between peri-tumoral edema in meningiomas and experimentally induced vasogenic edema have been noted, reinforcing this vasogenic theory [36].

Angiogenesis, vascular permeability, and inflammation

Role of vascular endothelial growth factor

Initially described as vascular permeability factors (VPF), vascular endothelial growth factors (VEGF) are key polypeptides regulators of vessel formation during embryogenesis and in wound healing as well as vessel homeostasis. Different variants of VEGF have been recently described, but the most studied remains VEGF-A which activates numerous signaling pathways through VEGF receptor-2 and modulates vessels morphogenesis through VEGF receptor-1 with the help of various factors such as platelet-derived growth factors, angiopoietins, transforming growth factor beta, and basic fibroblast growth factor [7, 52, 54, 97]. During the first stages of angiogenesis, VEGF modulates vascular dilation, vascular leakage, and endothelial cell formation while during the late stages it regulates maturation and stabilization [8, 40, 146]. VEGF connects to endothelial cells via two receptors, the tyrosine kinase receptors flt-1 (VEGFR-1) and Flk-1KDR (VEGFR-2), both widely expressed on endothelial cells.

Fig. 1 Left hemispheric convexity grade II meningioma (a coronal T2WI and b coronal left internal carotid angiogram). Very minimal peri-tumoral edema is noted despite the WHO histological grade and the extent of pial arterial vessels recruitment from the left middle cerebral arteries (arrows). The meningeal arterial feeding is commonly assured by branches of the middle meningeal artery (*)



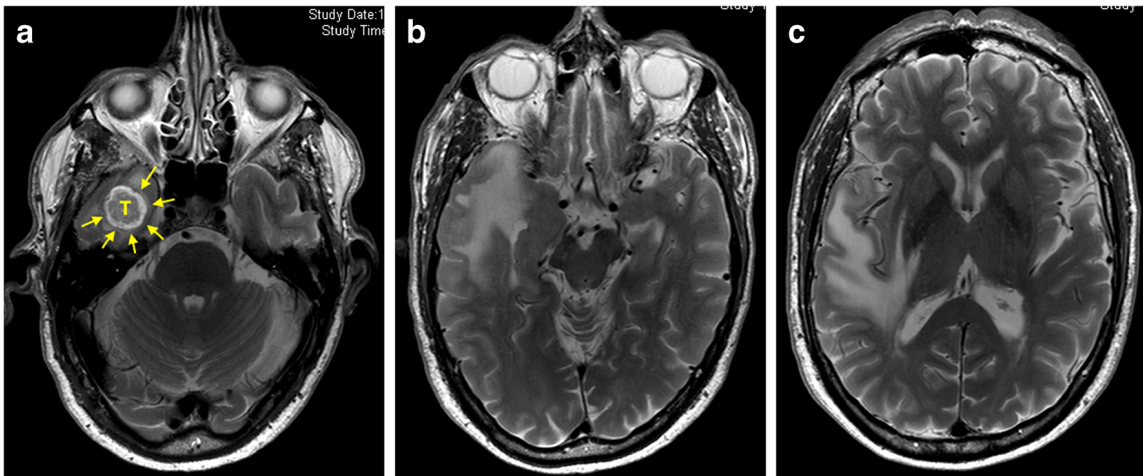


Fig. 2 Right temporal fossa secretory meningioma generating extensive temporo-parietal edema (a–c axial T2WI). Note the meningioma (T) is very well demarcated from the adjacent temporal lobe (arrows) (a)

Concerning the development of peri-tumoral brain edema in meningiomas, VEGF is thought to play a major role both in the regulation of vascular permeability (by opening of tight junctions through a phosphorylation of occludin) and the modulation of angiogenesis [74, 90, 98, 123]. In addition to other growth factors that induce VEGF secretion (epidermal growth factor, basic fibroblast growth factor), hypoxia is a powerful stimulator of VEGF secretion [9, 138]. In meningiomas, VEGF is synthesized both in tumoral cells and in the endothelium of tumor vessels [33], but not produced directly within the peri-tumoral matrix [30]. Meningiomas displaying intense VEGF immunostaining presented with a higher peri-tumoral edema incidence and edema index than in meningiomas VEGF-negative [9, 40, 58]. As a corollary, a high VEGF expression associated with the presence of a large PTBE has been proposed as predictors of recurrence in low-grade meningiomas [77, 145]. Nassehi [86] found peri-tumoral edema in 43/101 meningiomas with a statistically significant correlation with VEGF expression, as confirmed by Hou et al. and Markovic et al. [45, 78, 85]. In addition to PTBE, the tumor size and its proliferative index is correlated with VEGF expression. Dharmalingam et al. noted that 65% of grade I meningiomas displayed VEGF expression in contrast to 100% of grades II and III [28]. Markovic et al. studied the influence of the severity of PTBE and the intensity of expression of VEGF on morbidity and mortality, noting that the treatment outcome was significantly better when VEGF expression was below 50%. In the same study, the postoperative complications were more frequent in the group with PTBE, as well as the longer duration of intensive care treatment [78]. The vascular pattern of meningiomas has also been linked to VEGF expression: Pistolesi et al. identified small microvessel architecture in grade II and III meningiomas with a high VEGF expression in contrast to few larger vessels in grade I meningiomas with lower VEGF expression [99]. This data suggest that vascular architecture can also constitute a prognostic factor. Finally,

other growth factors have been investigated unsuccessfully in their possible correlation with PTBE in meningiomas such as VEGF-B, scatter factor/hepatocyte growth factor, placenta growth factor, and fibroblast growth factor-2 [66].

Mast cells, hypoxia-inducible factor-1 (HIF-1) and meningiomas

Meningiomas can be infiltrated by a variety of cells, predominantly of the immune environment such as mast cells, macrophages, and CD8 lymphocytes [15, 115]. This raises the question whether this represents an innate immune reaction toward the tumor itself or constitutes a growth environment participating to the tumorigenesis process [100]. A few authors reported a possible correlation between meningioma grade and the presence of mast cells, but the results are unclear [51, 107, 108]. The role of mast cells in the growth of meningiomas has also been suggested [37, 110]. Mast cells are multi-effector cells originating from a bone marrow progenitor. They participate to allergic reactions, immunity either innate or adaptative, inflammatory processes and autoimmunity as well. These cells have been described in various locations particularly within the central nervous system particularly choroid plexuses, meninges, hypothalamus, pituitary stalk, and pineal gland [29, 133]. Reszec et al. evaluated mast cells in a series of meningiomas using tryptase immunostaining [107, 108]. Meningiomas were classified in two groups: low grade including WHO grade I, and high grade encompassing WHO grades II and III. In this study, 31.8% of low-grade meningiomas displayed mast cells all of them presenting with marked PTBE, while 86% of high-grade meningiomas were positive for mast cells with 100% PTBE. Mast cells were found in the perivascular spaces but also within the tumor tissue. In their second study, Reszec et al. evaluated the expression of HIF-1 in addition to mast cells [108]. HIF-1 is a transcriptional factor that may, under

hypoxic conditions, induce the transcription of different genes implicated in tumor angiogenesis, invasion, cell survival, and glucose metabolism [53]. Overexpression of HIF-1 has been shown in various cancers to be correlated to grade and tumoral progression including in glioblastomas [108]. Tryptase expression which reflects the presence of mast cells was observed in 40.4% of grade I meningiomas and in 90% of high-grade meningiomas (WHO grades II and III) while HIF-1 was present in 55.7% of low grade and in 84% of high-grade meningiomas [108]. In this recent study, the presence of PTBE statistically correlated with tryptase and HIF-1 expression. The authors suggested that hypoxia generates mast cell activation and HIF-1 overexpression leading to blood-brain barrier rupture and therefore PTBE. In another study, Tirakotai et al. found that secretory meningiomas (WHO grade I), known to produce large PTBE, are highly infiltrated by mast cells [134]. The same findings were observed in chordoid meningiomas (WHO grade II) [34, 132]. Mast cells may also play a role in the cystic changes observed in one out of ten meningiomas [100]. Finally, it has been hypothesized that mast cells may be implicated in the pathogenesis of headaches associated with small meningiomas, secondary to interactions between meningeal mast cells and neurons [43].

Interpretation of tenascin expression

In meningiomas, the expression of different angiogenic factors has been demonstrated: platelet-derived growth factor, VEGF and fibroblast growth factor-2 [13, 14, 66]. Interactions between these factors within the extracellular matrix in the immediate environment of the tumor involve other key molecules. Tenascin is an extracellular matrix glycoprotein involved in embryogenesis, wound healing and tumor-associated angiogenesis [20, 59, 69, 96]. It is now established that there is a strong relationship between tenascin expression and tumoral angiogenesis [25, 73]. Indeed tenascin stimulates the proliferation and the motility of endothelial cells [147]. Kilic et al. established that there is a clear correlation between tenascin expression and VEGF expression in meningioma hypothesizing that tenascin may be a nonspecific angiogenic matrix molecule directly involved in meningioma angiogenesis [59]. The latter study showed also a correlation between tenascin expression and PTBE in meningiomas: among the 12 meningiomas not expressing tenascin 6 showed absent or minimal edema and 6 moderate edema, while of the 13 meningiomas with moderate tenascin expression, 9 showed marked PTBE [59]. Kilic et al. suggested that tenascin not only plays the role of an extracellular matrix modulating adhesion, migration and proliferation of endothelial and meningioma cells, but also participates to the process of brain invasion by the meningioma [59].

Influence of matrix metalloproteinases

Matrix metalloproteinases (MMP) are proteolytic enzymes involved in the degradation of extracellular matrix constituent, and are part of the physiological process of tissue remodeling. Among these, MMP-9 appears to be involved in tumor invasion process and angiogenesis [5, 50, 109]. MMP-9 is able to degrade the architecture of the extracellular matrix including the basement membrane and can interfere in the MAP kinase pathway resulting in the activation of cell proliferation. In meningiomas, intra-tumoral expression of MMP-9 seems to correlate with PTBE [28, 42, 46] and cell proliferation [5, 22]. Reszec et al. showed significant expression of MMP-9 in both low- and high-grade meningiomas but a clear trend toward significant expression in atypical, recurrent and malignant meningiomas was observed [109]. In this study, all meningiomas presenting with PTBE strongly expressed MMP-9. Jung et al. confirmed that MMP-9 levels were significantly associated with the intensity of PTBE [57]. It has been also noted that MMP-9 expression was directly related to VEGF expression and pial blood supply of meningiomas, through disruption of the surrounding arachnoid membrane [50]. The role of MMP-9 has been demonstrated in microcystic meningiomas: PTBE is frequently associated with this subtype and MMP-9 expression is very high. Paek et al. confirmed that an increased ratio of MMP-9 to TIMP-1 (tissue inhibitors of matrix metalloproteinases) might be associated with a microcystic degeneration of the meningioma and the formation of PTBE [94]. Nevertheless, other studies did not confirm these findings. In a canine study of intracranial meningiomas, Beltran et al. did not find any statistically significant relationship between MMP-9 and MMP-2 expression and the severity of PTBE [6].

Role of interleukine-6

Interleukin-6 (IL-6) is a multifunctional cytokine with stimulatory effects on immune response. It has been identified as a B cell differentiating factor but it is also involved as a mediator of inflammation, cellular differentiation, and immune response [35, 60, 131]. An increased expression of IL-6 in the brain has been noted in various situations including HIV-encephalopathy, multiple sclerosis, and Alzheimer disease [41, 44]. An overexpression has also been demonstrated in glioblastomas as a promoter of autocrine growth, pituitary adenomas, and meningiomas [16, 23, 135]. The role of IL-6 in meningiomas is still debated as it may act as a growth stimulator in approximately 60% of meningiomas whereas it can act as an inhibitor of tumor cell proliferation as well [17, 56, 135]. Outside the central nervous system, IL-6 is associated with local edema formation by induction of inflammation and an increase in capillary permeability, particularly in pulmonary edema [91, 113]. Par et al. found that IL-6 mRNA expression was more than 7 times higher in the moderate-to-severe peri-

meningioma edema than in those without or with very limited edema [95]. The mechanism of action of IL-6 is not clear but it appears to influence directly the integrity of the blood-brain barrier and may induce changes in the morphology and permeability of endothelial cells [80, 120]. In addition, IL-6 can simulate other substances involved in the pathogenesis of perimenigioma edema such as VEGF and MMP-9 [11, 122].

Involvement of E-cadherin and beta-catenins

E-cadherin is an epithelial Ca^{2+} -dependent cell adhesion molecule that plays a primordial role in embryonic development and morphogenesis. This molecule can be detected in epithelial tissues and cancers as well as in arachnoid villi and meningiomas. Beta-catenin is a multifunctional protein that interacts directly with E-cadherin forming the E-cadherin/catenin complex, a component of the adherens junction and an indirect modulator of tumoral cell signaling and proliferation [27, 49]. Changes of the tumor suppressor gene E-cadherin (CDH1) may play a significant role in the determination of meningioma aggressiveness and the severity of PTBE. Zhou et al. showed that the expression levels of E-cadherin and beta-catenin decreased significantly when the meningioma grade increased to reach almost null values in malignant meningiomas [148]. These authors noted a correlation between the expression levels of these molecules and the extent of PTBE and hypothesized that the harm of the cell-to-cell junctions damages the tumor-brain interface, facilitating the invasion of the adjacent brain by meningioma cells.

Role of water-electrolyte balance regulation

Aquaporins

Aquaporins are a group of 14 water channel proteins. These small size membrane-spanning proteins are expressed at plasma membranes in various tissues including brain parenchyma, particularly aquaporins 1, 4 and 9 in the latter location. Specifically, aquaporin 4 is predominantly expressed in the peri-vascular astrocytic foot processes and is suspected to be involved in the pathogenesis of chronic hydrocephalus and brain edema. Elsewhere in normal baseline conditions, aquaporin 4 may be involved in the clearance mechanism of the interstitial brain compartment also known as the glymphatic system. Recent studies have shown that an increased expression of aquaporin 4 is associated with PTBE in meningiomas [88, 142]. The inhibition of these water channel proteins may be a therapeutic option in the multimodal management of edematous meningiomas. More recently aquaporin 5 (AQP5) has been investigated. Lambertz et al. showed that AQP5 is expressed in meningiomas, with a role in cerebral water homeostasis but also in tumor cell proliferation, opening

new research pathways for recurrent or inoperable meningiomas [65].

Brain natriuretic peptide (BNP)

The heart ventricles as a consequence of left ventricle stretching secrete the brain natriuretic peptide (BNP) intended to maintain hydro-electrolytic homeostasis by downregulating the sympathetic nervous system as well as the renin-angiotensin loop, increasing smooth muscle relaxation and peripheral vascular resistance, and stimulating natriuresis. The level of BNP in the plasma is used routinely in the clinical practice as a marker of heart failure but also renal failure or hypoxia. BNP receptors have been found throughout the central nervous system and BNP level in the plasma suggested as a brain injury marker [143]. This level has also been correlated to the mass effect caused by brain tumors or brain edema in stroke [81, 118, 119]. Recently, Ruggieri et al. demonstrated that serum BNP levels are positively correlated to the volume of PTBE in patients with brain tumors [119]. Their prospective observational study integrated 110 patients including 40.9% of meningiomas, 30% of gliomas and 29.1% of metastases. The level of serum BNP seems to be directly related to the amount of PTBE rather than to the volume of the tumor itself. This brain source of BNP should not be confounded with the cardiac source that may complicate some neurological acute conditions mainly subarachnoid hemorrhages known as Takotsubo syndrome [89]. The mechanism of this phenomenon is still debated and whether BNP is only an epiphenomenon of peri-tumoral brain edema or participates to its production is still questioned. Therefore, Ruggieri et al. added PTBE to the list of known factors associated with high levels of serum BNP, i.e., gender, body mass index and intracranial pressure. They also proposed the serum level of BNP in patients with brain tumors as an indicator for the selection of patients who would more benefit from anti-edematous therapies (steroids, mannitol, diuretics) [119].

Influence of the brain-meningioma interface

As meningiomas are usually well-circumscribed extra-axial tumors, there is often a clear plane composed of connective tissues (pia-arachnoid mater and tumor stroma) that theoretically may limit the influence of intra-tumoral factors (VEGF, MMP...) on the adjacent peri-tumoral brain (Fig. 3a–c). Therefore the study of this interface and particularly the identification of the factors that may disrupt this interface are of paramount importance in the understanding of the pathogenesis of PTBE. Nakasu et al. studied 50 surgical cases of meningiomas [84]. They identified 20 cases with an individualized capsule categorized as thin ($n = 13$) and thick ($n = 7$). None of the atypical or anaplastic meningiomas displayed a

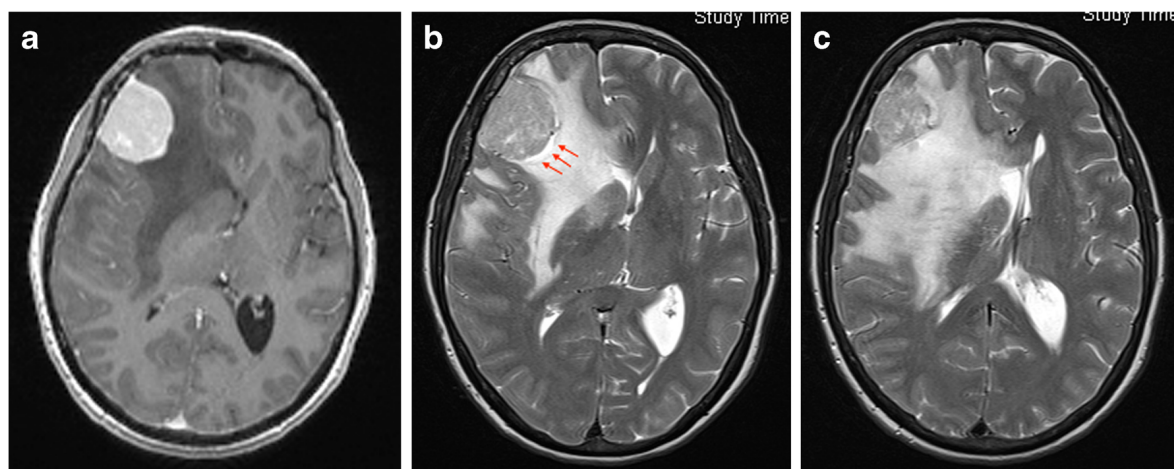


Fig. 3 Right frontal convexity grade I meningioma with extensive hemispheric edema. Note the apparent hyperintense rim surrounding the tumor that may suggest a clear plane of cleavage, in a patient presenting with status epilepticus (**a** axial T1WI with gadolinium and **b, c** axial T2WI)

capsule. They did not note any correlation between the extent of PTBE and the capsule thickness. Nevertheless and surprisingly, 6/7 of benign meningiomas with a thick capsule displayed PTBE whereas 5/13 thin-capsule meningiomas and 6/20 no-capsule meningiomas harbored PTBE. They concluded that the thick capsule significantly correlated with the extent of PTBE ($P = 0.024$). In this same study, the authors showed a clear correlation between PTBE and arachnoid disruption, and pial blood supply confirming the hypotheses of previous studies. Data including those of previous studies did not prove the positive correlation between MMP expression, particularly MMP-2 and MMP-9, and neither the disruption of the brain-tumor interface nor the brain invasion [50, 92, 94, 109].

the neuronal dysfunction and cell loss. The decrease of choline may reflect the destruction of astrocytes in the PTBE whereas the lactate peak results from ischemic changes. A precise metabolic characterization of the PTBE may predict the clinical presentation and potential sequelae. Indeed, Kamada et al. demonstrated strong correlations between the residual motor functions and NAA/choline and lactates/choline ratios. Further studies involving PET/MRI may better characterize PTBE and predict the risk of definitive neurological sequelae or epilepsy when ischemic changes are predominant. The role of elastography and specific MR sequences (such as brain surface motion imaging—BMSI) is still under investigation [106, 144]. These sequences appear promising for the exploration of the complex interactions between the meningioma and the surrounding brain parenchyma.

Multimodal imaging of PTBE in meningiomas

Recent imaging studies explored the possibilities of characterization of PTBE in brain tumors in general and meningiomas in particular to determinate the nature of edema as vasogenic and/or cytotoxic. Except ongoing works involving hybrid PET-MR, the noteworthy studies used proton magnetic resonance spectroscopy (^1H -MRS) [24, 32]. The most significant modifications in the PTBE were a decrease of N-acetylaspartate (NAA) content and a frequent lactate peak [111]. Chernov et al. reported that the severity of metabolic abnormalities in the PTBE depends upon three interrelated factors: tumor growth and invasive patterns, extensive PTBE, and large volume of the meningioma [24]. The disruption of the arachnoid and pial membrane around the meningioma leads to the direct influence of active substances like VEGF-A and MMP-9 stimulating the pial vasculature and thus vasogenic edema. This is also accompanied by ischemic alterations resulting from the direct compression of the adjacent brain from large tumors. The reduction of NAA reflects

Management of PTBE in meningiomas

Steroids remain the most frequently used agents for the management of PTBE in intra- and extra-axial intracranial tumors including meningiomas. The widespread use of synthetic steroids since the mid-1950s such as prednisone and dexamethasone, known to have a potent glucocorticoid activity, have shown an outstanding and prompt efficacy on vasogenic edema [48]. The possibilities of oral use and one daily administration facilitated this use in clinical practice. Nevertheless, the use of steroids, particularly long-term, can be associated with a noteworthy toxicity including hyperglycemia, arterial hypertension, osteoporosis, myopathy, psychiatric disorders (insomnia, mood disorders and psychosis), thromboembolic events as well as immunosuppression. In edematous forms of meningiomas, steroids may be administrated perioperatively beginning a few days before surgery. Steroids are thought to modulate the permeability of the blood-brain barrier frequently altered by various cytokines such as VEGF. This modulation is assured

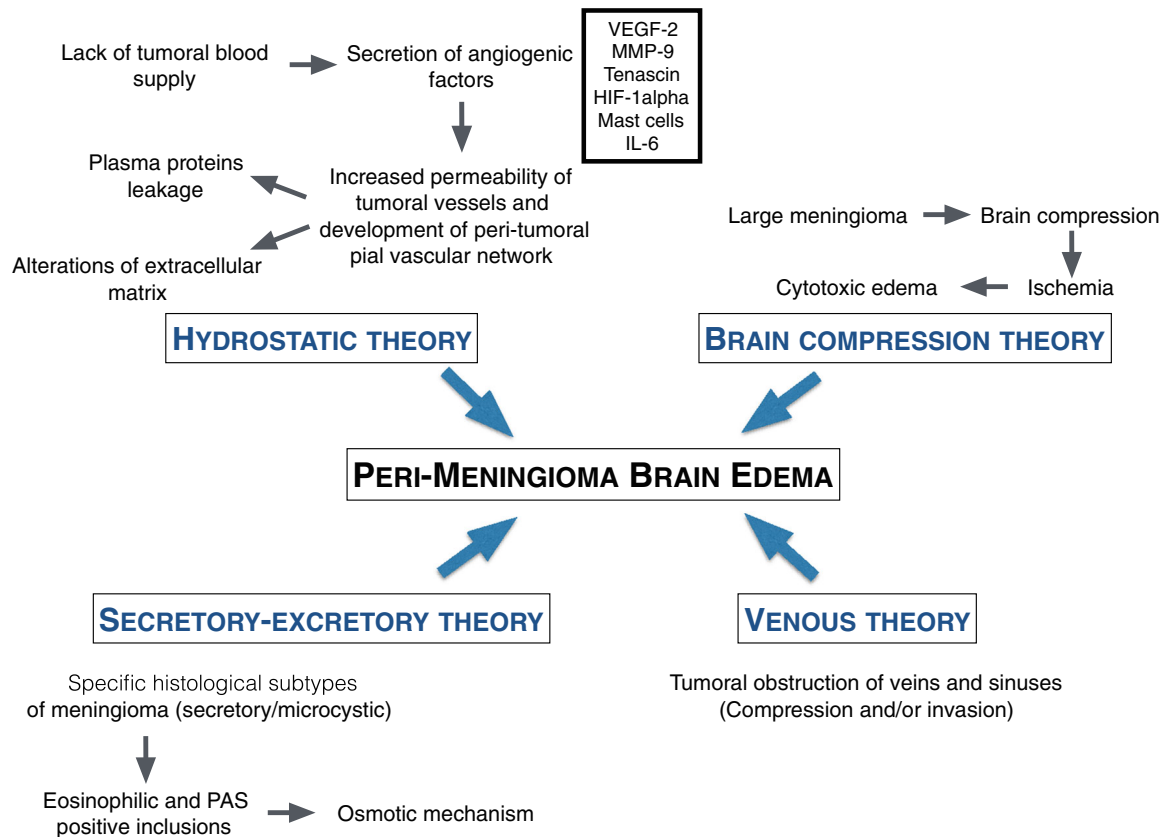


Fig. 4 Theories on the pathogenesis of PTBE in intracranial meningiomas. VEGF vascular endothelial factor, MMP metalloproteinase, HIF hypoxia-inducible factor, PAS periodic acid-Schiff

through different mechanisms involving claudins, zona occludens (ZO)-1, vascular endothelial-cadherin, and occludin [116, 117]. Limitations of steroid treatment are the risk of impairment in the quality of life because of potentially serious side

effects and the transitory anti-edematous effect. Other agents may be used in the daily practice especially if steroids are contraindicated, such as mannitol and hypertonic saline but which are associated with a risk of electrolytic disturbances.

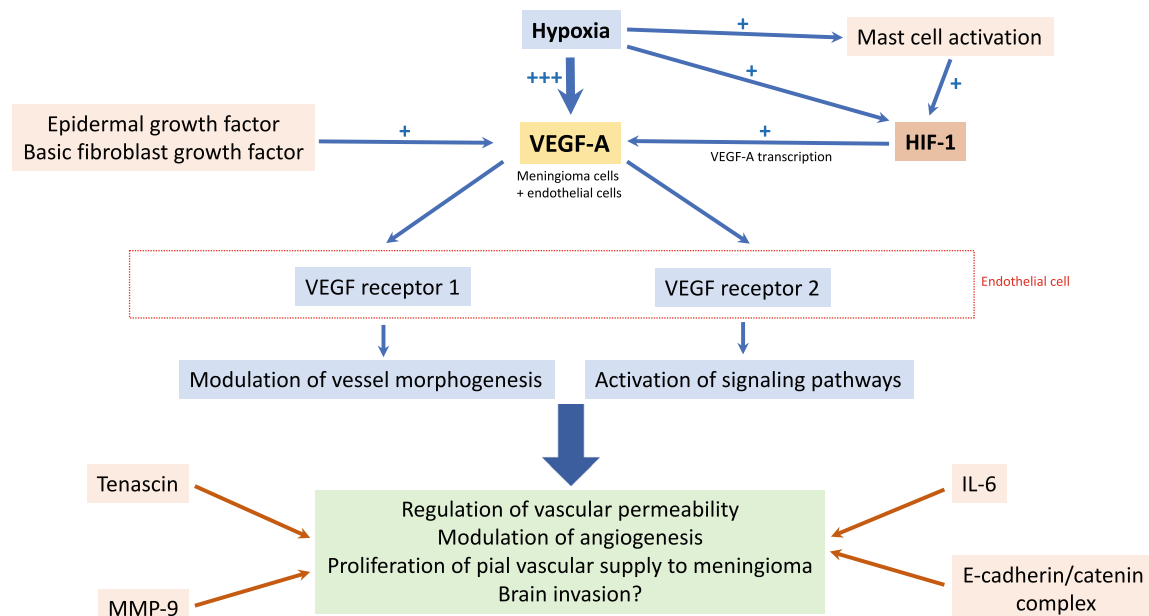


Fig. 5 Summary of the interrelated molecular mechanisms highlighting the role of hypoxia in the genesis of PTBE in intracranial meningiomas. VEGF vascular endothelial factor, MMP metalloproteinase, HIF hypoxia-inducible factor, IL interleukine

Elsewhere, corticotropin-releasing factor (CRF) appears to significantly reduce PTBE by a direct action on CRF-1 and CRF-2 receptors on blood vessels. More recently, studies on the effect of cyclooxygenase-2 inhibitors appear interesting despite cardiological risks [38].

Future research pathways

VEGF remains one of the most studied targets in neuro-oncology as it concerns various neoplasms. Very rare studies have involved a VEGF-directed therapy in meningiomas [42, 67]. Bevacizumab is a humanized monoclonal antibody that inhibits VEGF activity by binding to VEGF and inhibits VEGF receptor binding, thereby preventing the growth and maintenance of tumor blood vessels. Puchner et al. published the first report using bevacizumab in an anaplastic meningioma [104]. It was used as a salvage therapy after the recurrence of anaplastic meningioma following gross total removal and radiotherapy, with a partial remission. Rare studies involving meningiomas followed with similar results. Interestingly, one of these reported by Nayak et al. in addition to the stability or shrinkage of the enhancing tumor, 40% of patients exhibited a significant reduction of PTBE [87]. Even though the published data is very limited concerning the anti-tumoral and anti-edemagenic activities of bevacizumab in meningiomas, a trend toward efficacy exists. Various ongoing trials using hydroxyurea, temozolomide, bevacizumab, interferon-alpha, irinotecan, imatinib, tamoxifen, mifepristone and octreotide for recurrent and anaplastic meningiomas revealed a median PFS ranging from 2 to 15 months [45, 72]. PTBE as evaluated on T2WI on MRI decreased by 40% with a clinical benefit in all these cases. The association of everolimus, a mammalian target of rapamycin inhibitor, in anaplastic and recurrent meningiomas is being evaluated. In selected patients with severe PTBE, targeted treatments may help improve the perioperative morbidity.

Conclusion

The accurate comprehension of the multifarious pathogenesis of PTBE in meningiomas is of paramount importance as the extent and severity of edema may impact the neurological outcome. Obviously, none of these different hypotheses can explain by itself the genesis of PTBE; this latter may result from a conjunction of the different mechanisms (Fig. 4). The concept of a purely extra-axial tumor has to be revisited taking into account the interaction with the peri-tumoral brain tissue through the production of VEGF, metalloproteinases, pial irrigation development, and extracellular matrix reorganization (Fig. 5). Future trials of targeted treatments directed ideally

toward both meningioma proliferation and surrounding edema are expected.

Funding No required funding.

Compliance with ethical standards

Conflict of interest The authors declare that they have no conflicts of interest.

Ethical approval Not required.

Informed consent Not required.

References

1. Alaywan M, Sindou M (1993) Prognostic factors in the surgery for intracranial meningioma. Role of the tumoral size and arterial vascularization originating from the pia mater. Study of 150 cases. Neurochirurgie 39:337–347
2. Alguacil-Garcia A, Pettigrew NM, Sima AA (1986) Secretory meningioma. A distinct subtype of meningioma. Am J Surg Pathol 10:102–111
3. Arienta C, Caroli M, Crottì F, Villani R (1990) Treatment of intracranial meningiomas in patients over 70 years old. Acta Neurochir 107:47–55
4. Barresi V (2011) Angiogenesis in meningiomas. Brain Tumor Pathol 28:99–106. <https://doi.org/10.1007/s10014-010-0012-2>
5. Barresi V, Alafaci C, Caffo M, Barresi G, Tuccari G (2012) Clinicopathological characteristics, hormone receptor status and matrix metallo-proteinase-9 (MMP-9) immunohistochemical expression in spinal meningiomas. Pathol Res Pract 208:350–355. <https://doi.org/10.1016/j.prp.2012.02.013>
6. Beltran E, Matiasek K, De Risio L, de Stefani A, Feliu-Pascual AL, Matiasek LA (2013) Expression of MMP-2 and MMP-9 in benign canine rostroventral meningiomas is not correlated to the extent of peritumoral edema. Vet Pathol 50:1091–1098. <https://doi.org/10.1177/0300985813481610>
7. Benjamin LE, Hemo I, Keshet E (1998) A plasticity window for blood vessel remodelling is defined by pericyte coverage of the preformed endothelial network and is regulated by PDGF-B and VEGF. Development 125:1591–1598
8. Berkman RA, Merrill MJ, Reinhold WC, Monacci WT, Saxena A, Clark WC, Robertson JT, Ali IU, Oldfield EH (1993) Expression of the vascular permeability factor/vascular endothelial growth factor gene in central nervous system neoplasms. J Clin Invest 91:153–159. <https://doi.org/10.1172/JCI116165>
9. Bitzer M, Opitz H, Popp J, Morgalla M, Gruber A, Heiss E, Voigt K (1998) Angiogenesis and brain oedema in intracranial meningiomas: influence of vascular endothelial growth factor. Acta Neurochir 140:333–340
10. Bitzer M, Topka H, Morgalla M, Friese S, Wöckel L, Voigt K (1998) Tumor-related venous obstruction and development of peritumoral brain edema in meningiomas. Neurosurgery 42:730–737
11. Bitzer M, Wöckel L, Luft AR, Wakhloo AK, Petersen D, Opitz H, Sievert T, Ermemann U, Voigt K (1997) The importance of pial blood supply to the development of peritumoral brain edema in meningiomas. J Neurosurg 87:368–373. <https://doi.org/10.3171/jns.1997.87.3.0368>
12. Bitzer M, Wöckel L, Morgalla M, Keller C, Friese S, Heiss E, Meyermann R, Grote E, Voigt K (1997) Peritumoural brain

- oedema in intracranial meningiomas: influence of tumour size, location and histology. *Acta Neurochir* 139:1136–1142
13. Black P, Carroll R, Zhang J (1996) The molecular biology of hormone and growth factor receptors in meningiomas. *Acta Neurochir Suppl* 65:50–53
 14. Black PM, Carroll R, Glowacka D, Riley K, Dashner K (1994) Platelet-derived growth factor expression and stimulation in human meningiomas. *J Neurosurg* 81:388–393. <https://doi.org/10.3171/jns.1994.81.3.0388>
 15. Bø L, Mørk SJ, Nyland H (1992) An immunohistochemical study of mononuclear cells in meningiomas. *Neuropathol Appl Neurobiol* 18:548–558
 16. Borg SA, Kerr KE, Royds JA, Battersby RD, Jones TH (2005) Correlation of VEGF production with IL1 alpha and IL6 secretion by human pituitary adenoma cells. *Eur J Endocrinol* 152:293–300. <https://doi.org/10.1530/eje.1.01843>
 17. Boyle-Walsh E, Hashim IA, Speirs V, Fraser WD, White MC (1994) Interleukin-6 (IL-6) production and cell growth of cultured human meningiomas:-interactions with interleukin-1 beta (IL-1 beta) and interleukin-4 (IL-4) in vitro. *Neurosci Lett* 170:129–132
 18. Bradac GB, Ferszt R, Bender A, Schörner W (1986) Peritumoral edema in meningiomas. A radiological and histological study. *Neuroradiology* 28:304–312
 19. Bradac GB, Riva A, Giordana MT, Sales S, Bergui M (1997) A case of meningioma with exceptionally extensive oedema. *Neuroradiology* 39:273–275
 20. Brösicke N, Faissner A (2015) Role of tenascins in the ECM of gliomas. *Cell Adhes Migr* 9:131–140. <https://doi.org/10.1080/19336918.2014.1000071>
 21. Carroll RS, Schrell UM, Zhang J, Dashner K, Nomikos P, Fahlbusch R, Black PM (1996) Dopamine D1, dopamine D2, and prolactin receptor messenger ribonucleic acid expression by the polymerase chain reaction in human meningiomas. *Neurosurgery* 38:367–375
 22. Chambers AF, Matrisian LM (1997) Changing views of the role of matrix metalloproteinases in metastasis. *J Natl Cancer Inst* 89: 1260–1270
 23. Chang C-Y, Li M-C, Liao S-L, Huang Y-L, Shen C-C, Pan H-C (2005) Prognostic and clinical implication of IL-6 expression in glioblastoma multiforme. *J Clin Neurosci* 12:930–933. <https://doi.org/10.1016/j.jocn.2004.11.017>
 24. Chernov MF, Nakaya K, Kasuya H, Kato K, Ono Y, Yoshida S, Nakamura R, Suzuki T, Muragaki Y, Iseki H, Kubo O, Hori T, Takakura K (2009) Metabolic alterations in the peritumoral brain in cases of meningiomas: 1H-MRS study. *J Neurol Sci* 284:168–174. <https://doi.org/10.1016/j.jns.2009.05.015>
 25. Chiquet-Ehrismann R (1995) Tenascins, a growing family of extracellular matrix proteins. *Experientia* 51:853–862
 26. Claus EB, Bondy ML, Schildkraut JM, Wiemels JL, Wrensch M, Black PM (2005) Epidemiology of intracranial meningioma. *Neurosurgery* 57:1088–1095
 27. Curtis MW, Johnson KR, Wheelock MJ (2008) E-cadherin/catenin complexes are formed cotranslationally in the endoplasmic reticulum/Golgi compartments. *Cell Commun Adhes* 15:365–378. <https://doi.org/10.1080/15419060802460748>
 28. Dharmalingam P, Roopesh Kumar VR, Verma SK (2013) Vascular endothelial growth factor expression and angiogenesis in various grades and subtypes of meningioma. *Indian J Pathol Microbiol* 56:349–354. <https://doi.org/10.4103/0377-4929.125286>
 29. Dimitriadou V, Rouleau A, Trung Tuong MD, Newlands GJ, Miller HR, Luffau G, Schwartz JC, Garbarg M (1997) Functional relationships between sensory nerve fibers and mast cells of dura mater in normal and inflammatory conditions. *Neuroscience* 77:829–839
 30. Ding Y-S, Wang H-D, Tang K, Hu Z-G, Jin W, Yan W (2008) Expression of vascular endothelial growth factor in human meningiomas and peritumoral brain areas. *Ann Clin Lab Sci* 38:344–351
 31. Djindjian M, Caron JP, Athayde AA, Février MJ (1988) Intracranial meningiomas in the elderly (over 70 years old). A retrospective study of 30 surgical cases. *Acta Neurochir* 90:121–123
 32. Domingo Z, Rowe G, Blamire AM, Cadoux-Hudson TA (1998) Role of ischaemia in the genesis of oedema surrounding meningiomas assessed using magnetic resonance imaging and spectroscopy. *Br J Neurosurg* 12:414–418
 33. Dvorak HF, Sioussat TM, Brown LF, Berse B, Nagy JA, Sotrel A, Manseau EJ, Van de Water L, Senger DR (1991) Distribution of vascular permeability factor (vascular endothelial growth factor) in tumors: concentration in tumor blood vessels. *J Exp Med* 174: 1275–1278
 34. Epari S, Sharma MC, Sarkar C, Garg A, Gupta A, Mehta VS (2006) Chordoid meningioma, an uncommon variant of meningioma: a clinicopathologic study of 12 cases. *J Neuro-Oncol* 78: 263–269. <https://doi.org/10.1007/s11060-005-9092-y>
 35. Gadien RA, Otten UH (1997) Interleukin-6 (IL-6)—a molecule with both beneficial and destructive potentials. *Prog Neurobiol* 52: 379–390
 36. Gilbert JJ, Paulseth JE, Coates RK, Malott D (1983) Cerebral edema associated with meningiomas. *Neurosurgery* 12:599–605
 37. Gilfillan AM, Austin SJ, Metcalfe DD (2011) Mast cell biology: introduction and overview. *Adv Exp Med Biol* 716:2–12. https://doi.org/10.1007/978-1-4419-9533-9_1
 38. Girisig H, Palmeri B, Croci N, Soustrat M, Plotkine M, Marchandise Leroux C (2013) Effects of selective and non-selective cyclooxygenase inhibition against neurological deficit and brain oedema following closed head injury in mice. *Brain Res* 1491:78–87. <https://doi.org/10.1016/j.brainres.2012.10.049>
 39. Go KG, Wilmink JT, Molenaar WM (1988) Peritumoral brain edema associated with meningiomas. *Neurosurgery* 23:175–179
 40. Goldman CK, Bharara S, Palmer CA, Vitek J, Tsai JC, Weiss HL, Gillespie GY (1997) Brain edema in meningiomas is associated with increased vascular endothelial growth factor expression. *Neurosurgery* 40:1269–1277
 41. Gray F, Bélec L, Chrétien F, Dubreuil-Lemaire ML, Ricolfi F, Wingertsmann L, Poron F, Gherardi R (1998) Acute, relapsing brain oedema with diffuse blood-brain barrier alteration and axonal damage in the acquired immunodeficiency syndrome. *Neuropathol Appl Neurobiol* 24:209–216
 42. Hawasli AH, Rubin JB, Tran DD, Adkins DR, Waheed S, Hullar TE, Gutmann DH, Evans J, Leonard JR, Zipfel GJ, Chicoine MR (2013) Antiangiogenic agents for nonmalignant brain tumors. *J Neurol Surg B Skull Base* 74:136–141. <https://doi.org/10.1055/s-0033-1338262>
 43. Héron A, Dubayle D (2013) A focus on mast cells and pain. *J Neuroimmunol* 264:1–7. <https://doi.org/10.1016/j.jneuroim.2013.09.018>
 44. Holmin S, Söderlund J, Biberfeld P, Mathiesen T (1998) Intracerebral inflammation after human brain contusion. *Neurosurgery* 42:291–299
 45. Hou J, Kshettry VR, Selman WR, Bambakidis NC (2013) Peritumoral brain edema in intracranial meningiomas: the emergence of vascular endothelial growth factor-directed therapy. *Neurosurg Focus* 35:E2. <https://doi.org/10.3171/2013.8.FOCUS13301>
 46. Huang Q, Zhao S-L, Tian X-Y, Li B, Li Z (2013) Increased co-expression of macrophage migration inhibitory factor and matrix metalloproteinase 9 is associated with tumor recurrence of meningioma. *Int J Med Sci* 10:276–285. <https://doi.org/10.7150/ijms.5185>

47. Inamura T, Nishio S, Takeshita I, Fujiwara S, Fukui M (1992) Peritumoral brain edema in meningiomas— influence of vascular supply on its development. *Neurosurgery* 31:179–185
48. Ingraham FD, Matson DD, McLaurin RL (1952) Cortisone and ACTH as an adjunct to the surgery of craniopharyngiomas. *N Engl J Med* 246:568–571. <https://doi.org/10.1056/NEJM195204102461502>
49. Ishiyama N, Ikura M (2012) The three-dimensional structure of the cadherin-catenin complex. *Subcell Biochem* 60:39–62. https://doi.org/10.1007/978-94-007-4186-7_3
50. Iwado E, Ichikawa T, Kosaka H, Otsuka S, Kambara H, Tamiya T, Kondo S, Date I (2012) Role of VEGF and matrix metalloproteinase-9 in peritumoral brain edema associated with supratentorial benign meningiomas. *Neuropathology* 32:638–646. <https://doi.org/10.1111/j.1440-1789.2012.01312.x>
51. Jabini R, Moradi A, Afsharnezhad S, Ayatollahi H, Behravan J, Raziee HR, Mosaffa F (2014) Pathodiagnostic parameters and evaluation of O⁶-methyl guanine methyl transferase gene promoter methylation in meningiomas. *Gene* 538:348–353. <https://doi.org/10.1016/j.gene.2013.12.039>
52. Javerzat S, Auguste P, Bikfalvi A (2002) The role of fibroblast growth factors in vascular development. *Trends Mol Med* 8:483–489
53. Jensen RL (2009) Brain tumor hypoxia: tumorigenesis, angiogenesis, imaging, pseudoprogression, and as a therapeutic target. *J Neuro-Oncol* 92:317–335. <https://doi.org/10.1007/s11060-009-9827-2>
54. Jones N, Iljin K, Dumont DJ, Alitalo K (2001) Tie receptors: new modulators of angiogenic and lymphangiogenic responses. *Nat Rev Mol Cell Biol* 2:257–267. <https://doi.org/10.1038/35067005>
55. Jones NR, Rossi ML, Gregorios M, Hughes JT (1990) Epidermal growth factor receptor expression in 72 meningiomas. *Cancer* 66:152–155
56. Jones TH, Justice SK, Timperley WR, Royds JA (1997) Effect of interleukin-1 and dexamethasone on interleukin-6 production and growth in human meningiomas. *J Pathol* 183:460–468. [https://doi.org/10.1002/\(SICI\)1096-9896\(199712\)183:4<460::AID-PATH961>3.0.CO;2-Z](https://doi.org/10.1002/(SICI)1096-9896(199712)183:4<460::AID-PATH961>3.0.CO;2-Z)
57. Jung S, Moon K-S, Kim S-T, Ryu H-H, Lee Y-H, Jeong Y-I, Jung T-Y, Kim I-Y, Kim K-K, Kang S-S (2007) Increased expression of intracystic matrix metalloproteinases in brain tumors: relationship to the pathogenesis of brain tumor-associated cysts and peritumoral edema. *J Clin Neurosci* 14:1192–1198. <https://doi.org/10.1016/j.jocn.2006.11.009>
58. Kalkanis SN, Carroll RS, Zhang J, Zamani AA, Black PM (1996) Correlation of vascular endothelial growth factor messenger RNA expression with peritumoral vasogenic cerebral edema in meningiomas. *J Neurosurg* 85:1095–1101. <https://doi.org/10.3171/jns.1996.85.6.1095>
59. Kılıç T, Bayri Y, Ozduman K, Acar M, Diren S, Kurtkaya O, Ekinci G, Buğra K, Sav A, Ozek MM, Pamir MN (2002) Tenascin in meningioma: expression is correlated with anaplasia, vascular endothelial growth factor expression, and peritumoral edema but not with tumor border shape. *Neurosurgery* 51:183–192
60. Kishimoto T (1989) The biology of interleukin-6. *Blood* 74:1–10
61. Klatzo I (1985) Brain oedema following brain ischaemia and the influence of therapy. *Br J Anaesth* 57:18–22
62. Klatzo I (1987) Pathophysiological aspects of brain edema. *Acta Neuropathol* 72:236–239
63. Klatzo I (1994) Evolution of brain edema concepts. *Acta Neurochir Suppl (Wien)* 60:3–6
64. Kuratsu JI, Seto H, Kochi M, Ushio Y (1994) Expression of PDGF, PDGF-receptor, EGF-receptor and sex hormone receptors on meningioma. *Acta Neurochir* 131:289–293
65. Lambert N, Hindy NE, Adler C, Rump K, Adamzik M, Keyvani K, Bankfalvi A, Siffert W, Erol Sandalcioglu I, Bachmann HS (2013) Expression of aquaporin 5 and the AQP5 polymorphism A(-1364)C in association with peritumoral brain edema in meningioma patients. *J Neuro-Oncol* 112:297–305. <https://doi.org/10.1007/s11060-013-1064-z>
66. Lamszus K, Lengler U, Schmidt NO, Stavrou D, Ergün S, Westphal M (2000) Vascular endothelial growth factor, hepatocyte growth factor/scatter factor, basic fibroblast growth factor, and placenta growth factor in human meningiomas and their relation to angiogenesis and malignancy. *Neurosurgery* 46:938–948
67. Le Rhun E, Taillibert S, Chamberlain MC (2016) Systemic therapy for recurrent meningioma. *Expert Rev Neurother*. <https://doi.org/10.1080/14737175.2016.1184087>
68. Lee K-J, Joo W-J, Rha H-K, Park H-K, Chough J-K, Hong Y-K, Park C-K (2008) Peritumoral brain edema in meningiomas: correlations between magnetic resonance imaging, angiography, and pathology. *Surg Neurol* 69:350–355; discussion 355. <https://doi.org/10.1016/j.surneu.2007.03.027>
69. Liao H, Bu W, Wang T-H, Ahmed S, Xiao Z-C (2005) Tenascin-R plays a role in neuroprotection via its distinct domains that coordinate to modulate the microglia function. *J Biol Chem* 280:8316–8323. <https://doi.org/10.1074/jbc.M412730200>
70. Lieu AS, Howng SL (2000) Intracranial meningiomas and epilepsy: incidence, prognosis and influencing factors. *Epilepsy Res* 38:45–52
71. Lobato RD, Alday R, Gómez PA, Rivas JJ, Domínguez J, Cabrera A, Madero S, Ayerbe J (1996) Brain oedema in patients with intracranial meningioma. Correlation between clinical, radiological, and histological factors and the presence and intensity of oedema. *Acta Neurochir (Wien)* 138:485–494
72. Lou E, Sumrall AL, Turner S, Peters KB, Desjardins A, Vredenburgh JJ, McLendon RE, Herndon JE, McSherry F, Norfleet J, Friedman HS, Reardon DA (2012) Bevacizumab therapy for adults with recurrent/progressive meningioma: a retrospective series. *J Neuro-Oncol* 109:63–70. <https://doi.org/10.1007/s11060-012-0861-0>
73. Lowy CM, Oskarsson T (2015) Tenascin C in metastasis: a view from the invasive front. *Cell Adhes Migr* 9:112–124. <https://doi.org/10.1080/19336918.2015.1008331>
74. Machein MR, Kullmer J, Fiebich BL, Plate KH, Warnke PC (1999) Vascular endothelial growth factor expression, vascular volume, and, capillary permeability in human brain tumors. *Neurosurgery* 44:732–741
75. Machein MR, Plate KH (2000) VEGF in brain tumors. *J Neuro-Oncol* 50:109–120
76. Maiuri F, Gangemi M, Cirillo S, Delehaye L, Gallicchio B, Carandente M, Giamundo A (1987) Cerebral edema associated with meningiomas. *Surg Neurol* 27:64–68
77. Mantle RE, Lach B, Delgado MR, Baeza S, Bélanger G (1999) Predicting the probability of meningioma recurrence based on the quantity of peritumoral brain edema on computerized tomography scanning. *J Neurosurg* 91:375–383. <https://doi.org/10.3171/jns.1999.91.3.0375>
78. Markovic M, Antunovic V, Milenkovic S, Zivkovic N (2013) Prognostic value of peritumoral edema and angiogenesis in intracranial meningioma surgery. *J BUON* 18:430–436
79. Marmarou A, Takagi H, Shulman K (1980) Biomechanics of brain edema and effects on local cerebral blood flow. *Adv Neurol* 28:345–358
80. Maruo N, Morita I, Shirao M, Murota S (1992) IL-6 increases endothelial permeability in vitro. *Endocrinology* 131:710–714. <https://doi.org/10.1210/endo.131.2.1639018>
81. Modrego PJ, Boned B, Berlanga JJ, Serrano M (2008) Plasmatic B-type natriuretic peptide and C-reactive protein in hyperacute stroke as markers of CT-evidence of brain edema. *Int J Med Sci* 5:18–23

82. Muccioli G, Ghè C, Faccani G, Lanotte M, Forni M, Ciccarelli E (1997) Prolactin receptors in human meningiomas: characterization and biological role. *J Endocrinol* 153:365–371
83. Nakano T, Asano K, Miura H, Itoh S, Suzuki S (2002) Meningiomas with brain edema: radiological characteristics on MRI and review of the literature. *Clin Imaging* 26:243–249
84. Nakasu S, Fukami T, Jito J, Matsuda M (2005) Microscopic anatomy of the brain-meningioma interface. *Brain Tumor Pathol* 22: 53–57. <https://doi.org/10.1007/s10014-005-0187-0>
85. Nassehi D (2013) Intracranial meningiomas, the VEGF-A pathway, and peritumoral brain oedema. *Dan Med J* 60:B4626
86. Nassehi D, Dyrbye H, Andresen M, Thomsen C, Juhler M, Laursen H, Broholm H (2011) Vascular endothelial growth factor A protein level and gene expression in intracranial meningiomas with brain edema. *APMIS* 119:831–843. <https://doi.org/10.1111/j.1600-0463.2011.02764.x>
87. Nayak L, Iwamoto FM, Rudnick JD, Norden AD, Lee EQ, Drappatz J, Omuro A, Kaley TJ (2012) Atypical and anaplastic meningiomas treated with bevacizumab. *J Neuro-Oncol* 109:187–193. <https://doi.org/10.1007/s11060-012-0886-4>
88. Ng WH, Hy JW, Tan WL, Liew D, Lim T, Ang BT, Ng I (2009) Aquaporin-4 expression is increased in edematous meningiomas. *J Clin Neurosci* 16:441–443. <https://doi.org/10.1016/j.jocn.2008.04.028>
89. Nguyen TH, Neil CJ, Sverdlov AL, Mahadavan G, Chirkov YY, Kucia AM, Stansborough J, Beltrame JF, Selvanayagam JB, Zeitz CJ, Struthers AD, Frenneaux MP, Horowitz JD (2011) N-terminal pro-brain natriuretic protein levels in takotsubo cardiomyopathy. *Am J Cardiol* 108:1316–1321. <https://doi.org/10.1016/j.amjcard.2011.06.047>
90. Nishikawa R, Cheng SY, Nagashima R, Huang HJ, Cavenee WK, Matsutani M (1998) Expression of vascular endothelial growth factor in human brain tumors. *Acta Neuropathol* 96:453–462
91. Noma H, Minamoto A, Funatsu H, Tsukamoto H, Nakano K, Yamashita H, Mishima HK (2006) Intravitreal levels of vascular endothelial growth factor and interleukin-6 are correlated with macular edema in branch retinal vein occlusion. *Graefes Arch Clin Exp Ophthalmol* 244:309–315. <https://doi.org/10.1007/s00417-004-1087-4>
92. Nordqvist AC, Smurawa H, Mathiesen T (2001) Expression of matrix metalloproteinases 2 and 9 in meningiomas associated with different degrees of brain invasiveness and edema. *J Neurosurg* 95:839–844. <https://doi.org/10.3171/jns.2001.95.5.0839>
93. Paek SH, Kim C-Y, Kim YY, Park IA, Kim MS, Kim DG, Jung H-W (2002) Correlation of clinical and biological parameters with peritumoral edema in meningioma. *J Neuro-Oncol* 60:235–245
94. Paek SH, Kim DG, Park C-K, Phi JH, Kim YY, Im SY, Kim JE, Park S-H, Jung H-W (2006) The role of matrix metalloproteinases and tissue inhibitors of matrix metalloproteinase in microcystic meningiomas. *Oncol Rep* 16:49–56
95. Park K-J, Kang S-H, Chae Y-S, Yu M-O, Yoo M-O, Cho T-H, Suh J-K, Lee H-K, Chung Y-G (2010) Influence of interleukin-6 on the development of peritumoral brain edema in meningiomas. *J Neurosurg* 112:73–80. <https://doi.org/10.3171/2009.4.JNS09158>
96. Pas J, Wyszko E, Rolle K, Rychlewski L, Nowak S, Zukiel R, Barciszewski J (2006) Analysis of structure and function of tenascin-C. *Int J Biochem Cell Biol* 38:1594–1602. <https://doi.org/10.1016/j.biocel.2006.03.017>
97. Pepper MS (1997) Transforming growth factor-beta: vasculogenesis, angiogenesis, and vessel wall integrity. *Cytokine Growth Factor Rev* 8:21–43
98. Pietsch T, Valter MM, Wolf HK, von Deimling A, Huang HJ, Cavenee WK, Wiestler OD (1997) Expression and distribution of vascular endothelial growth factor protein in human brain tumors. *Acta Neuropathol* 93:109–117
99. Pistolesi S, Fontanini G, Camacci T, De Ieso K, Boldrini L, Lupi G, Padoleccchia R, Pingitore R, Parenti G (2002) Meningioma-associated brain oedema: the role of angiogenic factors and pial blood supply. *J Neuro-Oncol* 60:159–164
100. Polyzoidis S, Koletsas T, Panagiotidou S, Ashkan K, Theoharides TC (2015) Mast cells in meningiomas and brain inflammation. *J Neuroinflammation* 12:170. <https://doi.org/10.1186/s12974-015-0388-3>
101. Prat R, Banzo J, Diaz FJ (1997) Somatostatin receptors in meningioma: diagnostic and therapeutic value. *Rev Neurol* 25:2002–2005
102. Preston-Martin S (1996) Epidemiology of primary CNS neoplasms. *Neurol Clin* 14:273–290
103. Probst-Cousin S, Villagrán-Lillo R, Lahli R, Bergmann M, Schmid KW, Gullotta F (1997) Secretory meningioma: clinical, histologic, and immunohistochemical findings in 31 cases. *Cancer* 79:2003–2015
104. Puchner MJA, Hans VH, Harati A, Lohmann F, Glas M, Herrlinger U (2010) Bevacizumab-induced regression of anaplastic meningioma. *Ann Oncol* 21:2445–2446. <https://doi.org/10.1093/annonc/mdq634>
105. Regelsberger J, Hagel C, Emami P, Ries T, Heese O, Westphal M (2009) Secretory meningiomas: a benign subgroup causing life-threatening complications. *Neuro-Oncology* 11:819–824. <https://doi.org/10.1215/15228517-2008-109>
106. Reiss-Zimmermann M, Streitberger K-J, Sack I, Braun J, Arlt F, Fritzsch D, Hoffmann K-T (2015) High resolution imaging of viscoelastic properties of intracranial tumours by multi-frequency magnetic resonance elastography. *Clin Neuroradiol* 25:371–378. <https://doi.org/10.1007/s00062-014-0311-9>
107. Reszec J, Hermanowicz A, Kochanowicz J, Turek G, Mariak Z, Chyczewski L (2012) Mast cells evaluation in meningioma of various grades. *Folia Histochem Cytobiol* 50:542–546. <https://doi.org/10.5603/14744>
108. Reszec J, Hermanowicz A, Rutkowski R, Bernaczyk P, Mariak Z, Chyczewski L (2013) Evaluation of mast cells and hypoxia inducible factor-1 expression in meningiomas of various grades in correlation with peritumoral brain edema. *J Neuro-Oncol* 115:119–125. <https://doi.org/10.1007/s11060-013-1208-1>
109. Reszec J, Hermanowicz A, Rutkowski R, Turek G, Mariak Z, Chyczewski L (2015) Expression of MMP-9 and VEGF in meningiomas and their correlation with peritumoral brain edema. *Biomed Res Int* 2015:e646853. <https://doi.org/10.1155/2015/646853>
110. Ribatti D, Crivellato E (2012) Mast cells, angiogenesis, and tumor growth. *Biochim Biophys Acta* 1822:2–8. <https://doi.org/10.1016/j.bbadi.2010.11.010>
111. Ricci R, Bacci A, Tognoli V, Battaglia S, Maffei M, Agati R, Leonardi M (2007) Metabolic findings on 3T 1H-MR spectroscopy in peritumoral brain edema. *AJR Am J Neuroradiol* 28:1287–1291. <https://doi.org/10.3174/ajnr.A0564>
112. Riemenschneider MJ, Perry A, Reifenberger G (2006) Histological classification and molecular genetics of meningiomas. *Lancet Neurol* 5:1045–1054. [https://doi.org/10.1016/S1474-4422\(06\)70625-1](https://doi.org/10.1016/S1474-4422(06)70625-1)
113. Rixen D, Siegel JH (2000) Metabolic correlates of oxygen debt predict posttrauma early acute respiratory distress syndrome and the related cytokine response. *J Trauma* 49:392–403
114. Rohringer M, Sutherland GR, Louw DF, Sima AA (1989) Incidence and clinicopathological features of meningioma. *J Neurosurg* 71: 665–672. <https://doi.org/10.3171/jns.1989.71.5.0665>
115. Rossi ML, Cruz Sanchez F, Hughes JT, Esiri MM, Coakham HB (1988) Immunocytochemical study of the cellular immune response in meningiomas. *J Clin Pathol* 41:314–319
116. Roth P, Happold C, Weller M (2015) Corticosteroid use in neuro-oncology: an update. *Neurooncol Pract* 2:6–12. <https://doi.org/10.1093/nop/npu029>

117. Roth P, Regli L, Tonder M, Weller M (2013) Tumor-associated edema in brain cancer patients: pathogenesis and management. *Expert Rev Anticancer Ther* 13:1319–1325. <https://doi.org/10.1586/14737140.2013.852473>
118. Ruggieri F, Gemma M, Calvi MR, Nicelli E, Agarossi A, Beretta L (2012) Perioperative serum brain natriuretic peptide and cardiac troponin in elective intracranial surgery. *Neurocrit Care* 17:395–400. <https://doi.org/10.1007/s12028-012-9684-2>
119. Ruggieri F, Noris A, Beretta L, Mortini P, Gemma M (2016) Serum B-type natriuretic peptide is affected by neoplastic edema in patients with a brain tumor. *World Neurosurg* 85:193–196. <https://doi.org/10.1016/j.wneu.2015.08.074>
120. Saija A, Princi P, Lanza M, Scalese M, Aramnejad E, De Sarro A (1995) Systemic cytokine administration can affect blood-brain barrier permeability in the rat. *Life Sci* 56:775–784
121. Salokorpi N, Yrjänä S, Tuominen H, Karttunen A, Heljasvaara R, Pihlajaniemi T, Heikkinen E, Koivukangas J (2013) Expression of VEGF and collagen XVIII in meningiomas: correlations with histopathological and MRI characteristics. *Acta Neurochir*. <https://doi.org/10.1007/s00701-013-1699-8>
122. Salpietro FM, Alafaci C, Lucerna S, Iacopino DG, Todaro C, Tomasello F (1994) Peritumoral edema in meningiomas: micro-surgical observations of different brain tumor interfaces related to computed tomography. *Neurosurgery* 35:638–642
123. Samoto K, Ikezaki K, Ono M, Shono T, Kohno K, Kuwano M, Fukui M (1995) Expression of vascular endothelial growth factor and its possible relation with neovascularization in human brain tumors. *Cancer Res* 55:1189–1193
124. Shamah SM, Alberta JA, Giannobile WV, Guha A, Kwon YK, Carroll RS, Black PM, Stiles CD (1997) Detection of activated platelet-derived growth factor receptors in human meningioma. *Cancer Res* 57:4141–4147
125. Simis A, Pires de Aguiar PH, Leite CC, Santana PA Jr, Rosemberg S, Teixeira MJ (2008) Peritumoral brain edema in benign meningiomas: correlation with clinical, radiologic, and surgical factors and possible role on recurrence. *Surg Neurol* 70:471–477; discussion 477. <https://doi.org/10.1016/j.surneu.2008.03.006>
126. Sindou MP, Alaywan M (1998) Most intracranial meningiomas are not cleavable tumors: anatomic-surgical evidence and angiographic predictability. *Neurosurgery* 42:476–480
127. Smith HP, Challa VR, Moody DM, Kelly DL (1981) Biological features of meningiomas that determine the production of cerebral edema. *Neurosurgery* 8:428–433
128. Stevens JM, Ruiz JS, Kendall BE (1983) Observations on peritumoral oedema in meningioma. Part II: mechanisms of oedema production. *Neuroradiology* 25:125–131
129. Tan WL, Wong JHY, Liew D, Ng IHB (2004) Aquaporin-4 is correlated with peri-tumoural oedema in meningiomas. *Ann Acad Med Singap* 33:S87–S89
130. Tanaka M, Imhof HG, Schucknecht B, Kollias S, Yonekawa Y, Valavanis A (2006) Correlation between the efferent venous drainage of the tumor and peritumoral edema in intracranial meningiomas: superselective angiographic analysis of 25 cases. *J Neurosurg* 104:382–388. <https://doi.org/10.3171/jns.2006.104.3.382>
131. Tanaka T, Kishimoto T (2014) The biology and medical implications of interleukin-6. *Cancer Immunol Res* 2:288–294. <https://doi.org/10.1158/2326-6066.CIR-14-0022>
132. Tena-Suck ML, Collado-Ortíz MA, Salinas-Lara C, García-López R, Gelista N, Rembaño-Bojorquez D (2010) Chordoid meningioma: a report of ten cases. *J Neuro-Oncol* 99:41–48. <https://doi.org/10.1007/s11060-009-0097-9>
133. Theoharides TC, Stewart JM, Panagiotidou S, Melamed I (2016) Mast cells, brain inflammation and autism. *Eur J Pharmacol* 778: 96–102. <https://doi.org/10.1016/j.ejphar.2015.03.086>
134. Tirakotai W, Mennel H-D, Celik I, Hellwig D, Bertalanffy H, Riegel T (2006) Secretory meningioma: immunohistochemical findings and evaluation of mast cell infiltration. *Neurosurg Rev* 29:41–48. <https://doi.org/10.1007/s10143-005-0402-9>
135. Todo T, Adams EF, Rafferty B, Fahlbusch R, Dingermann T, Werner H (1994) Secretion of interleukin-6 by human meningioma cells: possible autocrine inhibitory regulation of neoplastic cell growth. *J Neurosurg* 81:394–401. <https://doi.org/10.3171/jns.1994.81.3.0394>
136. Trittmacher S, Traupe H, Schmid A (1988) Pre- and postoperative changes in brain tissue surrounding a meningioma. *Neurosurgery* 22:882–885
137. Trott G, Pereira-Lima JFS, Leães CGS, Ferreira NP, Barbosa-Coutinho LM, Oliveira MC (2015) Abundant immunohistochemical expression of dopamine D2 receptor and p53 protein in meningiomas: follow-up, relation to gender, age, tumor grade, and recurrence. *Braz J Med Biol Res* 48:415–419. <https://doi.org/10.1590/1414-431X20144163>
138. Tsai JC, Hsiao YY, Teng LJ, Shun CT, Chen CT, Goldman CK, Kao MC (1999) Regulation of vascular endothelial growth factor secretion in human meningioma cells. *J Formos Med Assoc* 98: 111–117
139. Vignes JR, Sesay M, Rezajooi K, Gimbert E, Liguoro D (2008) Peritumoral edema and prognosis in intracranial meningioma surgery. *J Clin Neurosci* 15:764–768. <https://doi.org/10.1016/j.jocn.2007.06.001>
140. de Vries J, Wakhloo AK (1993) Cerebral oedema associated with WHO-I, WHO-II, and WHO-III-meningiomas: correlation of clinical, computed tomographic, operative and histological findings. *Acta Neurochir* 125:34–40
141. Wang D-J, Xie Q, Gong Y, Wang Y, Cheng H-X, Mao Y, Zhong P, Huang F-P, Zheng K, Wang Y-F, Bao W-M, Yang B-J, Chen H, Xie L-Q, Zheng M-Z, Tang H-L, Zhu H-D, Chen X-C, Zhou L-F (2013) Secretory meningiomas: clinical, radiological and pathological findings in 70 consecutive cases at one institution. *Int J Clin Exp Pathol* 6:358–374
142. Wang P, Ni RY, Chen MN, Mou KJ, Mao Q, Liu YH (2011) Expression of aquaporin-4 in human supratentorial meningiomas with peritumoral brain edema and correlation of VEGF with edema formation. *Genet Mol Res* 10:2165–2171. <https://doi.org/10.4238/vol10-3gmr1212>
143. Wijdicks EF, Schievink WI, Burnett JC (1997) Natriuretic peptide system and endothelin in aneurysmal subarachnoid hemorrhage. *J Neurosurg* 87:275–280. <https://doi.org/10.3171/jns.1997.87.2.0275>
144. Yamada S, Taoka T, Nakagawa I, Nishimura F, Motoyama Y, Park YS, Nakase H, Kichikawa K (2013) A magnetic resonance imaging technique to evaluate tumor-brain adhesion in meningioma: brain-surface motion imaging. *World Neurosurg*. <https://doi.org/10.1016/j.wneu.2013.02.015>
145. Yamasaki F, Yoshioka H, Hama S, Sugiyama K, Arita K, Kurisu K (2000) Recurrence of meningiomas. *Cancer* 89:1102–1110
146. Yoshioka H, Hama S, Taniguchi E, Sugiyama K, Arita K, Kurisu K (1999) Peritumoral brain edema associated with meningioma: influence of vascular endothelial growth factor expression and vascular blood supply. *Cancer* 85:936–944
147. Zagzag D, Friedlander DR, Dosik J, Chikramane S, Chan W, Greco MA, Allen JC, Dorovini-Zis K, Grumet M (1996) Tenascin-C expression by angiogenic vessels in human astrocytomas and by human brain endothelial cells in vitro. *Cancer Res* 56: 182–189
148. Zhou K, Wang G, Wang Y, Jin H, Yang S, Liu C (2010) The potential involvement of E-cadherin and beta-catenins in meningioma. *PLoS One* 5:e11231. <https://doi.org/10.1371/journal.pone.0011231>

V - ANOMALIES DE LA MICROCIRCULATION DANS L'OEDEME PERITUMORAL : APPLICATION PEROPERATOIRE DE LA VIDEOMICROSCOPIE SIDESTREAM DARK FIELD AUX MENINGIOMES INTRACRANIENS

Publié le 22/08/2020 dans Neuro-Oncology Advances (Oxford University Press) :
<https://doi.org/10.1093/noajnl/vdaa108>

Résumé

Comme détaillé dans le chapitre IV, la pathogénie de l'œdème péritumoral dans les méningiomes intracrâniens reste débattue, alors que son impact sur la morbidité est maintenant bien établi (HTIC, comitialité, hématome post-opératoire, déficit neurologique). Parmi les éléments impliqués dans cette pathogénie et selon plusieurs études, les facteurs vasculaires semblent prégnants. Des travaux utilisant des techniques d'imagerie macroscopiques de perfusion (Scanner/IRM de perfusion, scanner au xénon, SPECT, angiographie cérébrale) ont permis de mettre en évidence des anomalies de perfusion au sein de l'œdème péritumoral. Jusque-là l'absence de technologie permettant une étude de la microcirculation péritumorale a limité la possibilité de mieux comprendre ces anomalies de perfusion à l'échelle microcirculatoire. Le but de notre travail était d'une part d'évaluer la faisabilité de l'imagerie par vidéomicroscopie *sidestream dark field* en per-opératoire et d'autre part de confirmer, pour la première fois *in vivo*, l'existence d'altérations significatives de la microcirculation péritumorale dans les méningiomes œdémateux.

Matériel et méthodes

Entre janvier et Septembre 2019, notre étude a inclus 15 patients porteurs d'une tumeur intracrânienne de la convexité compatible avec un méningiome de grade I de l'OMS. Ont été exclus les méningiomes de garde II, III et les récidives. L'œdème péritumoral a été classé selon les grades de Trittmacher : grade 0 (pas d'œdème ou discret halo

péritumoral), grade 1 (œdème péri-tumoral modéré) et grade 2 (œdème péri-tumoral diffusant à l'hémisphère cérébral affecté). Tous les patients ont pu bénéficier d'une exérèse microchirurgicale complète sous neuronavigation. Seuls 2 patients ont nécessité une corticothérapie péri-opératoire du fait de céphalées significatives. Les paramètres hémodynamiques et ventilatoires (PaCO₂) ont été contrôlés durant l'intervention pour être maintenus dans les normes. L'imagerie peropératoire de la microcirculation a été réalisée à l'aide d'un vidéomicroscope *sidestream dark field* (MicroscanTM, Microvision Medical, Amsterdam, The Netherlands) avant et après la résection du méningiome. Six régions d'intérêt sont choisies sur la surface corticale autour du méningiome : 5 régions immédiatement au contact du méningiome correspondant à l'enregistrement de la zone péri-tumorale, et un 6^{ème} point le plus à distance possible du méningiome tel que le permet la craniotomie (servant de référence). Pour chaque zone d'intérêt, 3 clips vidéo ont été réalisés en prenant soin à ne pas exercer de pression sur le cortex. Les enregistrements ont été analysés à l'aide d'un logiciel dédié (AVA 3.0 software, AMC, *University of Amsterdam, the Netherlands*). Différents paramètres de microcirculation ont été recueillis en se basant sur les recommandations internationales :

- Score de De Backer : nombre de vaisseaux croisant 3 lignes horizontales et 3 lignes verticales équidistantes divisé par la longueur totale des lignes (évaluation de la densité vasculaire)
- Index de perfusion microvasculaire : l'image est divisée en 4 quadrants égaux et le type prédominant de flux est caractérisé de manière semi-quantitative dans chaque quadrant : Absence de flux (0), flux intermittent (1), flux lent (2), flux normal (3).
- Densité vasculaire totale : Rapport entre la longueur totale des vaisseaux visibles et la surface totale analysée.
- Densité de vaisseaux perfusés : Rapport entre la longueur totale des vaisseaux perfusés (vaisseaux ayant un index de perfusion microvasculaire supérieur ou égal à 2) et la surface totale analysée.

- Proportion de vaisseaux perfusés : pourcentage de tous les vaisseaux visibles ayant un index de perfusion d'au moins 2

Résultats

Trois patients ont été exclus du fait d'un diagnostic histologique définitif de méningiome de grade II. Les 12 patients restants ont été répartis en 2 groupes en fonction de la présence ou non d'un œdème péritumoral. Le groupe « Œdème » incluait 6 patients présentant un œdème péritumoral significatif (Trittmacher grades 1 et 2). Il n'y avait pas de différence significative concernant les caractéristiques cliniques et IRM des deux groupes.

Avant la résection :

Dans le groupe « Sans œdème », les paramètres microcirculatoires étaient légèrement altérés de manière non significative. Dans le groupe « Œdème », la microcirculation était très altérée avec une baisse de près de 50% des différents paramètres microcirculatoires : Les valeurs de densité microvasculaire en particulier des petits vaisseaux de diamètre inférieur à $20 \mu\text{m}$ étaient réduites de près de 68% par rapport à la microcirculation corticale normale. Les paramètres de perfusion étaient également très diminués avec une baisse de 46%, 76,5% et 48,6% pour l'index de perfusion microvasculaire, la densité de vaisseaux perfusés, et la proportion de vaisseaux perfusés, respectivement.

Après la résection :

Dans le groupe « Sans œdème », la résection du méningiome a permis une quasi-normalisation des paramètres microcirculatoires, probablement en rapport avec la levée de l'effet de masse sur le parenchyme cérébral péritumoral. Dans le groupe « Œdème », les valeurs de microcirculation (densité vasculaire et perfusion) après résection se sont nettement améliorées de manière statistiquement significative, tout en demeurant bien inférieures aux valeurs de références particulièrement concernant la densité des petits vaisseaux de diamètre inférieur à $20 \mu\text{m}$. Cette différence résiduelle pourrait être le fait de l'œdème péritumoral lui-même.

Discussion

Jusqu'à présent, seules des études utilisant des imageries macroscopiques ont permis de mettre en évidence des anomalies de perfusion, le plus souvent difficiles à interpréter en l'absence d'une résolution suffisante : Conséquences de l'œdème vasogénique, angiogenèse tumorale et ischémie secondaire à l'effet de masse. Notre étude démontre pour la 1^{ère} fois *in vivo* des anomalies significatives de la densité et la perfusion vasculaire dans la région péritumorale particulièrement en cas d'œdème, soulignant le concept de fragilité microvasculaire de cette région anatomique avec des risques ischémiques potentiels en cas de manipulation chirurgicale intempestive ou lors d'utilisation d'un écarteur cérébral. Il demeure difficile de savoir si les altérations de la microcirculation péritumorale, tant la baisse de la densité microvasculaire que les anomalies de la microperfusion cérébrale, résultent des phénomènes ischémiques dus à l'effet de masse ou sont secondaire à l'œdème péritumoral. Les deux phénomènes sont probablement concomitants et la prédominance de l'un ou l'autre peut expliquer le pronostic fonctionnel post-opératoire et la réponse à la corticothérapie péri-opératoire. L'imagerie par vidéomicroscopie per-opératoire pourrait éventuellement permettre de prédire le pronostic de récupération fonctionnelle en fonction de la sévérité des altérations microcirculatoires constatées.

Perspectives et limites

Le but premier de notre étude était la faisabilité de cette modalité d'imagerie de la microcirculation durant une procédure neurochirurgicale. Une étude similaire incluant plus de patients, avec en plus une imagerie pré-opératoire de perfusion avec une meilleure résolution que ce que permettent les technologies actuelles, devrait confirmer nos résultats et permettre de mieux comprendre les phénomènes ischémiques péri-tumoraux. L'influence des facteurs systémiques (PaCO₂, PAM, drogues vasoactives) sur les paramètres microcirculatoires pourrait également être évalué.

Une des limites de cette technologie d'imagerie SDF consiste en l'impossibilité d'évaluer les zones plus profondes (substance blanche), sachant que la distribution de l'œdème péritumoral est rarement homogène et superficielle.

La vidéomicroscopie SDF reste une imagerie de contact donc très sensible à la pression exercée sur le tissu mesuré et à la présence d'éventuels liquides d'interface.

Conclusion

Notre étude a confirmé la possibilité d'utiliser la vidéomicroscopie SDF en peropératoire pour l'imagerie/monitoring de la microcirculation cérébrale. Elle a également mis en évidence des anomalies significatives de la densité et de la perfusion microvasculaire au sein de l'œdème péritumoral dans les méningiomes intracrâniens, anomalies dont la valeur pronostique reste à explorer.

Neuro-Oncology Advances

2(1), 1–11, 2020 | doi:10.1093/noajnl/vdaa108 | Advance Access date 27 August 2020

Alterations of cerebral microcirculation in peritumoral edema: feasibility of *in vivo* sidestream dark-field imaging in intracranial meningiomas

Moncef Berhouma, Thiebaud Picart, Chloe Dumot, Isabelle Pelissou-Guyotat, David Meyronet, François Ducray, Jerome Honnorat, Omer Eker, Jacques Guyotat, Anne-Claire Lukaszewicz, and François Cotton

Department of Neurosurgical Oncology and Vascular Neurosurgery, Pierre Wertheimer Neurological and Neurosurgical Hospital, Hospices Civils de Lyon, Lyon, France (M.B., T.P., C.D., I.P.-G., J.G.); Creatis Lab, CNRS UMR 5220, INSERM U1206, Lyon 1 University, INSA Lyon, Lyon, France (M.B., O.E., F.C.); Department of Pathology, Pierre Wertheimer Neurological and Neurosurgical Hospital, Hospices Civils de Lyon, Lyon, France (D.M.); Centre de Recherche en Cancérologie de Lyon INSERM U1052 CNRS 5286, Lyon 1 University, Lyon, France (D.M.); Department of Neurooncology, Pierre Wertheimer Neurological and Neurosurgical Hospital, Hospices Civils de Lyon, Lyon, France (F.D., J.H.); Department of Neuroradiology, Pierre Wertheimer Neurological and Neurosurgical Hospital, Hospices Civils de Lyon, Lyon, France (O.E.); Department of Neuroanesthesia and Neurocritical Care, Pierre Wertheimer Neurological and Neurosurgical Hospital, Hospices Civils de Lyon, Lyon, France (A.-C.L.); Department of Neuroimaging, Centre Hospitalier Lyon Sud, Hospices Civils de Lyon, Pierre-Bénite, France (F.C.)

Corresponding Author: Moncef Berhouma, MD, MSc, Department of Neurosurgical Oncology and Vascular Neurosurgery, Pierre Wertheimer Neurological and Neurosurgical Hospital, University of Lyon, Hospices Civils de Lyon, 59 Boulevard Pinel, 69394 Lyon Cedex 03, France (berhouma.moncef@gmail.com; moncef.berhouma@chu-lyon.fr).

Abstract

Background. Intracranial meningiomas display a variable amount of peritumoral brain edema (PTBE), which can significantly impact perioperative morbidity. The role of microcirculatory disturbances in the pathogenesis of PTBE is still debated. The aim of this study was to microscopically demonstrate and intraoperatively quantify, for the first time, the alterations to microcirculation in PTBE using sidestream dark-field (SDF) imaging.

Methods. Adult patients with WHO grade I meningiomas were recruited over a 9-month period and divided into 2 groups depending on the absence (NE group) or the presence (E group) of PTBE. *In vivo* intraoperative microcirculation imaging was performed in the peritumoral area before and after microsurgical resection.

Results. Six patients were included in the NE group and 6 in the E group. At the baseline in the NE group, there was a minor decrease in microcirculatory parameters compared to normal reference values, which was probably due to the mass effect. In contrast, microcirculatory parameters in the E group were significantly altered, affecting both vessel density and blood flow values, with a drop of approximately 50% of normal values. Surgical resection resulted in a quasi-normalization of microcirculation parameters in the NE group, whereas in the E group, even if all parameters statistically significantly improved, post-resection values remained considerably inferior to those of the normal reference pattern.

Conclusion. Our study confirmed significant alterations of microcirculatory parameters in PTBE in meningiomas. Further *in vivo* SDF imaging studies may explore the possible correlation between the severity of these microcirculatory alterations and the postoperative neurological outcome.

Key Points

- *In vivo* analysis of peritumoral microcirculation is possible with sidestream dark-field imaging.
- Microcirculation parameters are significantly altered in the peritumoral edema in meningiomas.

Importance of the Study

Intracranial meningiomas regularly display peritumoral edema. The responsibility of microcirculation disturbances and perfusion anomalies in the pathogenesis of this peritumoral edema is still debated. Using sidestream dark-field imaging, we demonstrated and quantified for the first time *in vivo* the existence of significant alterations of microcirculation parameters including blood flow and vessel density in the peritumoral edema

in meningiomas. We confirmed the persistence of significant microcirculation alterations after surgical resection and mass effect withdrawal. Our results support the concept of vascular vulnerability of the peritumoral brain edema. Future studies using sidestream dark-field imaging may help to establish *in vivo* a correlation between the intraoperative severity of peritumoral microcirculation alterations and the neurological outcome.

Meningiomas represent the second most common intracranial tumor in adults, accounting for approximately 20% of all intracranial tumors.¹ Approximately 38–67% of meningiomas exhibit a variable amount of peritumoral brain edema (PTBE). PTBE impacts the surgical management of intracranial meningiomas and is associated with a higher morbidity² due to an increased risk of perioperative raised intracranial pressure, seizures,³ postoperative hematoma, and neurological deficits.^{4,5} In addition to apparent diffusion coefficient and tumor sphericity, PTBE represents one of the radiologic and radiomic characteristics that may predict meningioma grade and outcome.⁶ Numerous studies have attempted to identify specific risk factors for the development of PTBE (age, sex, histological grading and subtype, vascularity, blood supply, tumor size, expression of sex hormones, and vascular endothelial growth factor [VEGF] expression), but their results have been inconsistent.^{2,7–13} Hence, the pathogenesis of PTBE is still a matter of debate and relies on 4 main theories, which are probably associated at different levels: the compression theory (large meningiomas compressing the adjacent brain, leading to ischemia and cytotoxic edema), the secretory-excretory theory (specific histological secretory subtypes producing eosinophilic and periodic acid-Schiff positive inclusions), the venous compression theory (meningiomas obstructing venous outflow), and the hydrodynamic theory (tumor hypoxia leading to the secretion of angiogenic factors with leakage of plasma proteins and alterations of extracellular matrix).

Recent histopathological studies have highlighted the critical role of angiogenic factors (VEGF, hypoxia-inducible factor-1, platelet-derived growth factor, etc.) in the alterations of the peritumoral microcirculation network, emphasizing the responsibility of the hydrodynamic theory in the pathogenesis of PTBE in meningiomas. In parallel, perfusion and vascular macroscopic imaging studies resulted in questions about whether the impact of ischemic foci within the PTBE was secondary to the brain compression by a large meningioma or to the PTBE itself. The lack of adequate techniques to investigate the microcirculation *in vivo* has been a major limitation to explore and confirm these anomalies at the microscopic level. Only macroscopic imaging techniques (perfusion CT/MRI, xenon-enhanced CT, single-photon emission computed tomography, angiography, etc.) were used to investigate the

peritumoral vascular network in meningiomas pointing some perfusion anomalies.^{7,10,11,14–23} Nevertheless, these macroscopic alterations of peritumoral circulation may not reflect the anomalies at the level of the microcirculation.^{24,25} The recent development of handheld noninvasive videomicroscopic techniques has offered new possibilities in the investigation of microcirculation.^{26,27}

The aim of this study was to explore *in vivo* the peritumoral cerebral microcirculation and determine whether specific alterations of the microcirculation in PTBE are present in patients with intracranial meningiomas in terms of vessel density and blood flow. The effect of microsurgical resection on the peritumoral microcirculatory parameters and hence the responsibility of mass effect versus edema on peritumoral microcirculation was also investigated. To our knowledge, this is the first study showing firsthand evidence of alterations of the peritumoral cerebral microcirculation using *in vivo* sidestream dark-field (SDF) imaging.

Material and Methods

Patient Population

The intraoperative use of SDF imaging was approved by the Local Ethics Committee, and written informed consent was obtained from each patient. Our study population included 15 adult patients who were diagnosed with suspected intracranial convexity WHO grade I meningioma between January 2019 and September 2019. We included only meningiomas that developed on the skull convexity to allow the exposition of the adjacent cortical brain surface for microcirculation intravital imaging. To ensure patient homogeneity, recurrent meningiomas were excluded as well as WHO grade II and III meningiomas.

Neuroimaging

The tumor volume was evaluated on T1-weighted sequences with gadolinium using the formula for a spheroid ($V = 4/3 \pi abc$). PTBE was evaluated on T2-weighted sequence and was classified in terms of extension into 3 levels according to the Trittmacher criteria²⁸ (Figure 1):

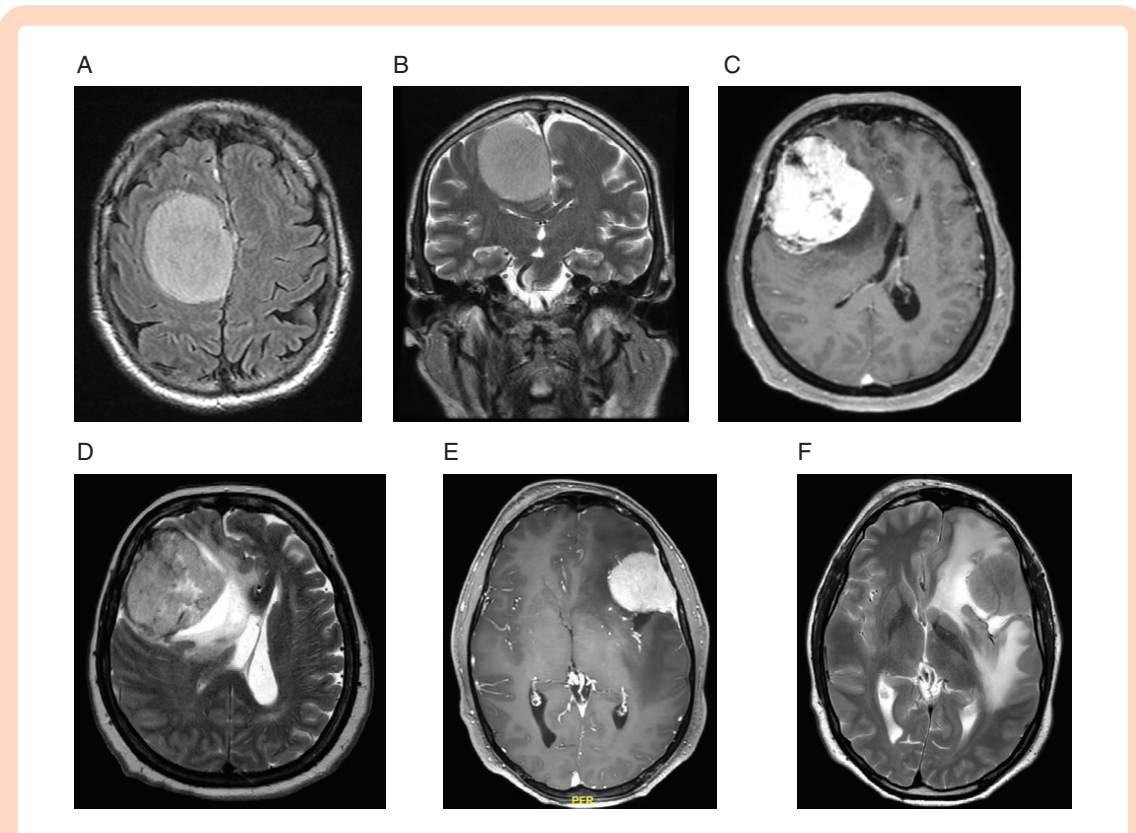


Figure 1. Peritumoral edema was classified according to Trittmacher criteria: grade 0 (A, axial Flair sequence and B, coronal T2-weighted sequence); grade 1 (C, axial T1-weighted sequence with gadolinium and D, axial T2-weighted sequence); grade 2 (E, axial T1-weighted sequence with gadolinium and F, axial T2-weighted sequence).

grade 0 represents the absence of edema or the presence of a small halo around it; grade 1, moderate edema around the tumor; and grade 2, spread of edema involving the white matter of the affected hemisphere. Patients were split into 2 groups depending upon the presence of peritumoral edema (grades 1 and 2, E group) or the absence of peritumoral edema (grade 0, NE group).

Operative Procedure

All patients underwent microsurgical gross total removal under neuronavigation by the same senior neurosurgeon (M.B.). Only 2 patients, who had grade 2 edema, received perioperative corticosteroids because of the presence of severe headaches. All patients neither underwent preoperative endovascular embolization nor received hyperosmolar solutions during the surgical procedure. Anesthetic operative parameters were maintained as stable as possible during the microcirculation imaging in all patients with objectives of normocapnia and a normal mean arterial pressure. All patients had preoperative hematocrit levels within a normal range, and none required transfusion during surgery. No static brain retraction was used in any patient.

Microcirculation Registration

In all our patients, we assessed the peritumoral microcirculation parameters with SDF imaging (Microscan; Microvision Medical) before and after surgical resection. SDF imaging relies on a stroboscopic light-emitting diode ring-based modality integrated in a handheld device (Figure 2A).^{24,29–32} This device is composed of a light guide with a magnifying lens and an analogue embedded camera. The illumination comes from a green light with a 530 nm wavelength that is specifically absorbed by hemoglobin. Hence, the red blood cells appear as dark globules surrounding the vessels in a white/gray background. This technique provides visualization of the microcirculation at a depth of approximately 500 μm. We placed the tip of the device in a specifically designed sterile transparent plastic cap. The probe was stabilized in a self-retaining adjustable Leyla retractor arm to avoid hand-related micro-movements during registration and coupled with neuronavigation to select the peritumoral areas where the edema reaches the brain surface.

The craniotomy was performed in a standard fashion. Microcirculation evaluation was performed according to the consensus recommendations for the assessment of microcirculation.³³ Six regions of interest (ROIs)

were identified on the cortical surface around the meningioma and correlated to the neuronavigation data on T2 sequences: 5 ROIs immediately adjacent to the tumor and corresponding to the peritumoral region, and one control ROI was as far from the meningioma limit as the craniotomy allowed and where the edema is absent according to neuronavigation, to serve as "normal/control" microcirculation reference (Figure 2B). An SDF probe was placed at the contact of the cortex before any arachnoidal opening for pre-resection measurements ("baseline data") and then at the end of the resection using the same ROIs ("post-resection data"). For each ROI, 3 video clips of 20 seconds were obtained. Particular attention was required to avoid any pressure artifact on the cortex and limit the quantity of fluid (either CSF or saline serum irrigation)

between the cortical surface and the lens. During registration, the device was automatically adjusted as to have an optimal contrast and focus as well as a constant zoom for all registrations. The final on-screen magnification of the images was 325 times that of the original, corresponding to a field size of $1280 \mu\text{m} \times 960 \mu\text{m}$. AVA 3.0 software (AMC, University of Amsterdam, the Netherlands) was used to calculate the microcirculatory parameters:

- De Backer score (/mm): Number of vessels crossing 3 horizontal and 3 vertical equidistant lines (Figure 3A) divided by the total length of the lines, thus evaluating vessel density.
- Microvascular flow index (MFI): This index reflects the perfusion quality. The image is divided into 4 quadrants (Figure 3B) and the prominent type of flow is semi-quantitatively assessed by the observer using an ordinal scale in each quadrant (absent = 0, intermittent = 1, sluggish = 2, and normal = 3). MFI results from the average of the 4 quadrants. Absent flow corresponds to the complete lack of any flow throughout the video sequence. Intermittent flow is defined by at least half of the

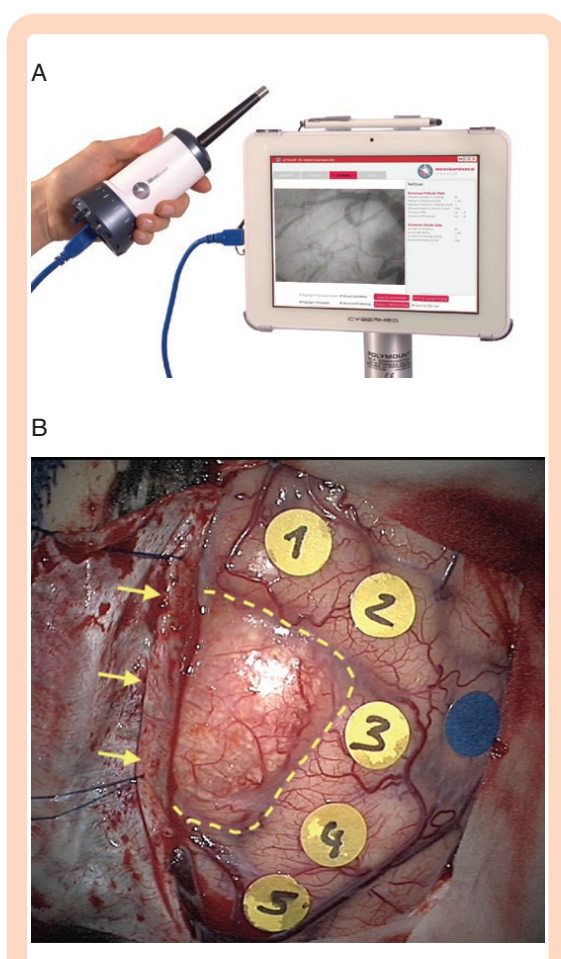


Figure 2. SDF imaging device used intraoperatively with a sterile draping (courtesy of Microscan; Microvision Medical) (A). Operative view of a parasagittal right frontal meningioma (dotted yellow line). The dura is opened and reflected on the sagittal sinus (yellow arrows). Five cortical spots (1–5) are identified within the adjacent peritumoral area corresponding to the peritumoral edema in accordance with the neuronavigation guidance. The blue spot is chosen as far from the tumor as the craniotomy allowed and served as a reference point for SDF imaging (B).

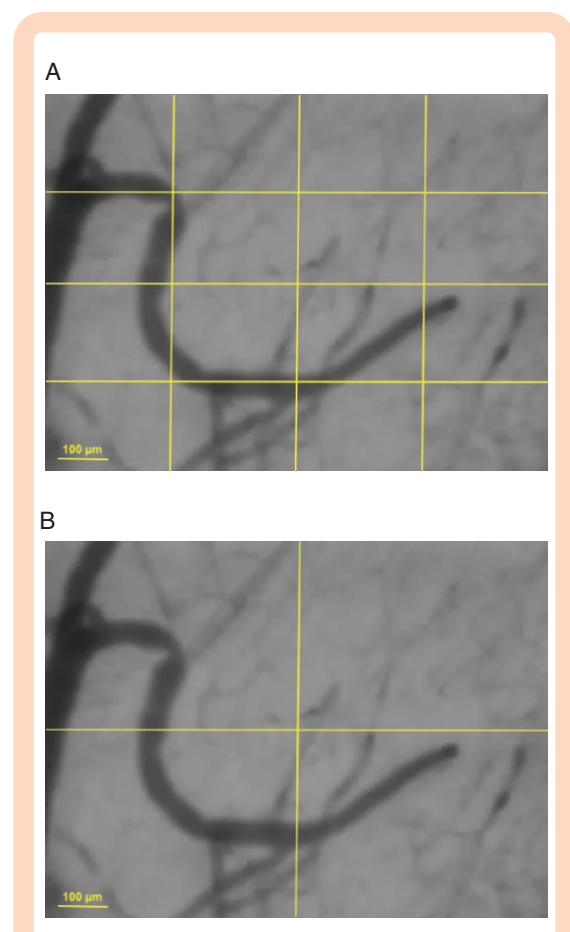


Figure 3. Determination of De Backer's score (A) and microvascular flow index (B).

- sequence without any flow. Sluggish is a continuous but very slow flow ([Supplementary Video 1](#)).
- Total vessel density (TVD/mm.mm²): The total length of the vessels divided by the total surface area of the analyzed image. A similar measurement was applied to small vessels with a diameter $\leq 20 \mu\text{m}$, corresponding to the small vessel density (SVD).
 - Perfusion vessel density (PVD/mm.mm²): This value corresponds to the functional vessel density and is calculated from the total length of perfused vessels (MFI score ≥ 2) divided by the surface area of the analyzed image.
 - Proportion of perfused vessels (PPV): Defined as the percentage of all visible vessels with at least a sluggish flow ($100 \times \text{number of perfused vessels}/\text{total number of vessels}$).

Statistical Analysis

Data on microcirculatory parameters are presented as the mean \pm SD for each group of patients unless otherwise stated. Fisher's exact test was used when appropriate. Differences between groups were compared using a paired Student's *t* test if the data were normally distributed; otherwise, a Mann-Whitney *U* test was used. A Wilcoxon signed-rank test with continuity correction was used specifically for MFI and PPV. A *P* value of less than .05 was considered significant. Statistical analyses were conducted using R software version 3.5.1.

Results

Patient Characteristics

Three patients were excluded after pathological examination confirmed WHO grade II meningiomas. The 12 remaining patients with confirmed WHO grade I meningiomas were split into 2 groups of 6 patients each. The E group included patients with meningiomas with peritumoral edema (4 patients with Trittmacher grade 1 edema and 2 patients with grade 2 edema), and the NE group comprised meningiomas without peritumoral edema (Trittmacher grade 0). There were no significant differences between the characteristics of the 2 groups, except for the duration of symptoms (defined as the interval between the first symptoms and the imaging diagnosis), with 43.33 ± 13.54 days (mean \pm SD) for the NE group and 14.16 ± 5.69 for the E group (*P* = .0033). The mean age was comparable in both groups, 55.16 ± 9.37 years old versus 50 ± 14.13 years old for the NE and E groups, respectively (*P* = .5133). The sex ratio (M:F) was 4:2 in the NE group and 3:3 in the E group. The tumor volume ranged from 8 to 45.98 cm^3 , and there was no significant difference between the groups ($21.73 \pm 7.4 \text{ cm}^3$ for the NE group and $21.07 \pm 12.61 \text{ cm}^3$ for the E group, *P* = .922). Clinical presentation included significant unusual headaches in 8 patients (66.6%), mainly in the E group; motor deficits in 3 patients (25%: 2 patients with severe hemiparesis and 1 patient with left arm monoparesis); cognitive decline in 2 patients

(16.6%); and one inaugural generalized seizure in 1 patient (8.3%) treated with oral Levetiracetam (500 mg twice daily). Neuroimaging data were representative of common grade I meningiomas: 50% of tumors were hypo-T2, 33% iso-T2, and 17% hyper-T2. Diffusion and perfusion data were without particularities (mean relative cerebral blood volume [rCBV] 7.4 ± 4.2 in the NE group vs 6.8 ± 2.4 in the E group, excluding one patient in whom perfusion data were not interpretable because of artifacts). A gross total microsurgical resection was possible in all patients. The brain-tumor interface was smooth in all patients in the NE group, while it was irregular and without an arachnoid plane in 33% of patients in the E group. The postoperative course was uneventful for all patients. The neurological outcome was excellent in all patients with resolution of increased intracranial pressure symptoms and complete recovery of any preoperative neurological deficits within 2 postoperative months. No patients had suffered postoperative seizures including the one who presented with an inaugural generalized seizure (Engel class I) in whom Levetiracetam has been progressively stopped at the sixth postoperative month. Pathological examination confirmed WHO grade I meningiomas in all patients without any particular distribution (50% meningotheelial, 33.3% transitional, 8.3% fibrous, and 8.3% angiomyomatous).

Microcirculatory Data at Baseline

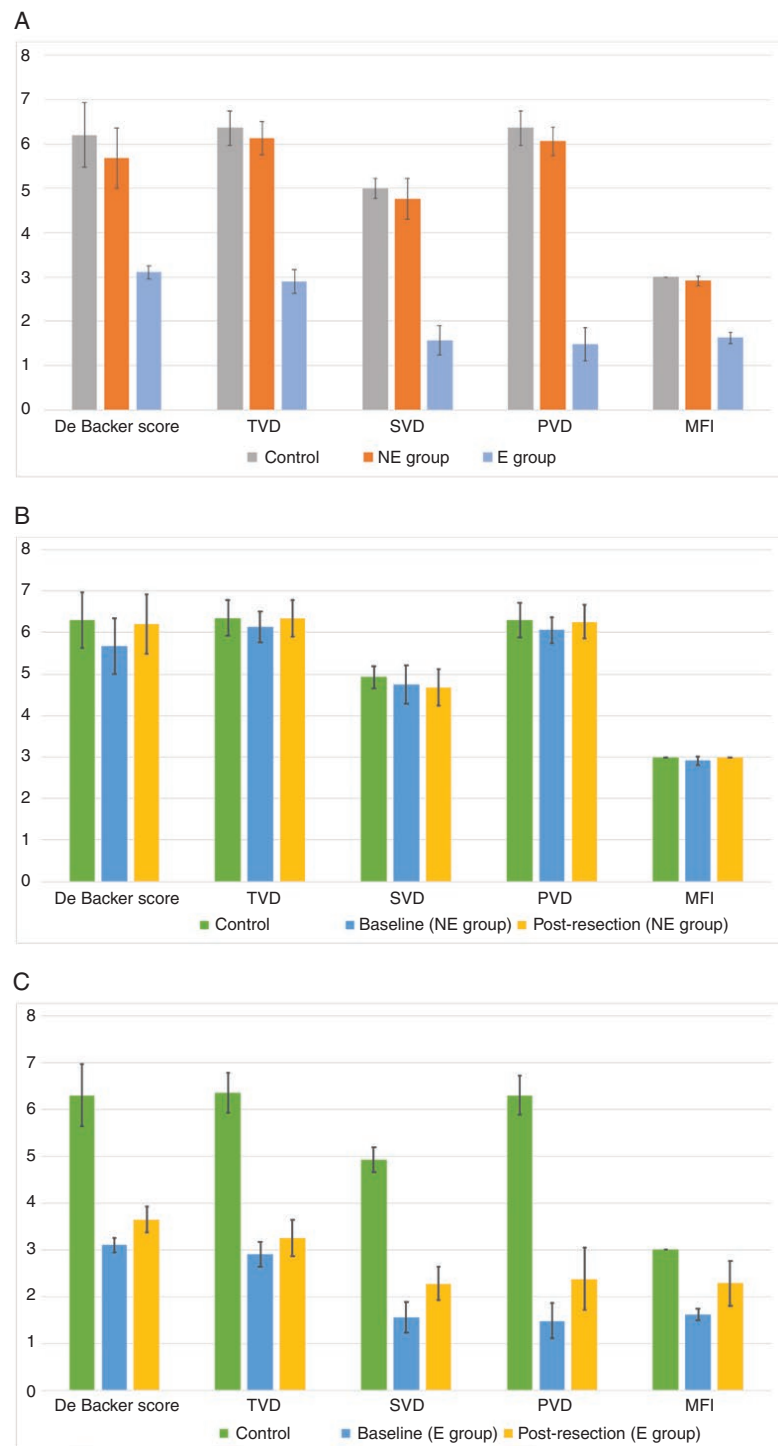
Microcirculatory measurements at the reference point as far as possible from the meningioma were similar in both the NE and E groups at baseline (ie, before surgical resection). Thus, the mean values of reference points of the 2 groups were considered as representing "normal" cerebral cortical microcirculation and served as control values for subsequent comparisons.

In the NE group ([Supplementary Table S1](#)), we observed a statistically minor nonsignificant decrease in all microcirculatory parameters, particularly vessel density (De Backer score, TVD/SVD). Only MFI reached statistical significance (*P* = .048), whereas the other perfusion parameters did not (PVD and PPV).

In contrast, all microcirculatory parameters in the E group were significantly affected in the PTBE area with an approximately 50% drop compared to control ([Supplementary Table S2](#)). Vessel density was particularly reduced for small vessels (diameter $< 20 \mu\text{m}$) with a decline of more than 68% of SVD values compared to control. Perfusion parameters were also very altered in PTBE with a drop of 46%, 76.5%, and 48.6% in the values of MFI, PVD, and PPV, respectively.

Globally, microcirculatory patterns of the peritumoral area in the absence of edema (NE group) were almost similar to normal cortical microcirculation (apart from a slight decrease that may be due to mass effect), whereas all parameters (including perfusion and vessel density) were statistically significantly collapsed in PTBE ([Figure 4A](#)).

In no patient did we observe any pattern of angiogenic architecture in the limits of the 5 ROIs chosen for SDF imaging, namely, no irregular and tortuous vessels and no vascular conglomerates between normal microcirculation areas.³⁴



Figures 4. (A) Microcirculatory parameters in peritumoral area at baseline in NE and E groups. Control group corresponds to microcirculatory parameters at the reference point considered as normal cortical microcirculation. De Backer score is expressed in per millimeter. MFI: mean flow index (from 0 to 3), TVD: total vessel density (/mm.mm²), SVD: small vessel density (/mm.mm²), PVD: perfused vessel density (/mm.mm²). Mean ± SD.

Microcirculatory Data After Tumoral Resection

In the NE group, surgical resection of the meningioma allowed for minor improvement of almost all microcirculatory parameters in the peritumoral area ([Supplementary Table S3](#)); however, they were not statistically significant, except for the De Backer score, which reached the value of the control reference measurement ($6.21 \pm 0.71/\text{mm}$). This evolution may be interpreted as the direct effect of the elimination of the tumoral mass effect on the adjacent brain tissue ([Figure 4B](#)).

In the E group, the removal of the tumoral mass effect provoked a statistically significant increase of all microcirculation parameters ([Supplementary Table S4](#)), but the post-resection values remained considerably inferior to the normal reference pattern, reflecting only the consequence of the withdrawal of mass effect. The substantial residual difference between post-resection microcirculatory parameters and normal values ([Figure 4C](#)) may be the result of the peritumoral edema itself, confirming its prevalent role in the alterations of microcirculatory parameters in PTBE when compared to the mass effect alone, particularly when considering the SVD.

Discussion

Until now, preoperative imaging techniques have revealed only macroscopic perfusion anomalies within the edema surrounding intracranial meningiomas, but there was no evidence of any vascular density or perfusion anomalies at the microcirculatory scale. Our study demonstrates for the first time *in vivo* substantial alterations of the microcirculatory parameters in the immediate environment of intracranial meningiomas, particularly when peritumoral edema exists. Hence, the significant decrease in both perfusion and vessel density in the PTBE as shown confirms the microvascular fragility of this area, and the necessity to preserve it from any excessive surgical manipulation and brain retraction to avoid ischemic damage.

Imaging of Brain Microcirculation

Microcirculation is defined as a vast vascular network of small vessels with a diameter of less than $100\text{ }\mu\text{m}$ (capillaries, venules, and arterioles), ensuring not only the transport of vital substrates to tissues and clearing their waste products but also playing a critical role in vascular hemodynamics and resistance, blood coagulation, inflammation, and immunity.^{27,34–41} Direct visualization of the microcirculatory network has been described in 1987 by Slaaf

et al.,⁴² and then it was improved in 1999 by Groner et al.⁴³ with the development of orthogonal polarization spectral (OPS) imaging, the precursor to SDF imaging. The first human studies were focusing mainly on the alterations of microcirculation during sepsis by measurement on the sublingual mucosa.^{25,39,40} SDF was developed by Goedhart et al.³⁰ in 2007 to overcome the drawbacks of OPS imaging, which was mainly the limited visualization of small capillaries due to blurring. Moreover, SDF imaging uses low-power LED, allowing for a better autonomy and portability for clinical and operative use. SDF imaging offers a precise estimation of the functional capillary density.

The development of handheld compact devices for OPS imaging and then SDF imaging has opened a large field of possibilities, including for the investigation of cerebral microcirculation.⁴³ In 2000, Uhl et al.³⁴ confirmed the feasibility of OPS imaging in a series of 12 patients (4 incidental aneurysms serving as control group, 3 patients with aneurysmal subarachnoid hemorrhage [SAH], and 5 patients with brain tumors). They were able to visualize vasospasm in small arterioles (diameter $\leq 150\text{ }\mu\text{m}$) in patients with SAH undergoing normal transcranial Doppler imaging and in the absence of clinical signs of vasospasm. Pennings et al.⁴⁴ showed with OPS imaging the increased arteriolar contractility in response to hyperventilation in 16 patients who underwent an operation for aneurysmal SAH. After the introduction of SDF imaging in 2007,³⁰ very few human brain microcirculation studies were published ([Table 1](#)). In 2011, Pérez-Bárcena et al.²⁹ applied SDF imaging to the evaluation of cortical microcirculation in malignant stroke patients requiring decompressive craniectomy. They were able to confirm a significant blood flow reduction in the cortical microcirculation and decreased vascular density in patients with stroke. To our knowledge, our study demonstrates for the first time *in vivo* specific microcirculation alterations within the PTBE. Until now, preoperative imaging techniques have revealed only perfusion anomalies within the edema surrounding intracranial meningiomas, but there was no evidence of any vascular density anomaly as well. We were able to confirm at the microscopic level the alterations of vascular density in the PTBE likewise perfusion anomalies. The very significant decrease in both the perfusion and vessel density in the PTBE as shown confirms the vulnerability of this zone toward any surgical manipulation, particularly the use of a self-retaining retractor on the peritumoral brain tissue during the resection. This microcirculatory vulnerability of the PTBE as quantified in our study also raises the question of the necessity of exploring the influence of the systemic hemodynamic parameters during surgery, as well as the impact of vasoactive factors (mean arterial pressure, ETCO_2 , intravenous noradrenaline, etc.) on peritumoral microcirculation.

(B) Evolution of microcirculatory parameters of PTBE after surgical resection of meningiomas in the NE group, as compared to baseline (pre-resection parameters) and to the control group (normal cortical microcirculation). De Backer score is expressed in per millimeter. MFI: mean flow index (from 0 to 3), TVD: total vessel density ($/\text{mm} \cdot \text{mm}^2$), SVD: small vessel density ($/\text{mm} \cdot \text{mm}^2$), PVD: perfused vessel density ($/\text{mm} \cdot \text{mm}^2$). Mean \pm SD. (C) Evolution of microcirculatory parameters of PTBE after surgical resection of meningiomas in E group, as compared to baseline (pre-resection parameters) and to the control group (normal cortical microcirculation). De Backer score is expressed in per millimeter. MFI: mean flow index (from 0 to 3), TVD: total vessel density ($/\text{mm} \cdot \text{mm}^2$), SVD: small vessel density ($/\text{mm} \cdot \text{mm}^2$), PVD: perfused vessel density ($/\text{mm} \cdot \text{mm}^2$). Mean \pm SD.

Table 1. Main Applications of OPS and SDF Techniques for Imaging the Brain Microcirculation

Authors (year)	Technique	Context	Patient Population	Main Conclusions
Uhl et al. (2000)	OPS	Study of the feasibility of OPS imaging during different neurosurgical procedures	12 patients (4 incidental aneurysms serving as control group, 3 patients with aneurysmal subarachnoid hemorrhage, and 5 patients with brain tumors)	<ul style="list-style-type: none"> Visualization of vasospasm is small arterioles (diameter $\leq 150 \mu\text{m}$) in patients with SAH having normal transcranial doppler and without a clinical sign of vasospasm Evidence of an increase in functional capillary density at the end of the surgery probably because of a decrease in intracranial pressure either by CSF release or tumor debulking
Uhl et al. (2003)	OPS	Aneurysmal surgery (without and with SAH)	10 patients with aneurysmal SAH compared to a control group of 3 patients with incidental aneurysms	<ul style="list-style-type: none"> Significant decrease of capillary density in patients with SAH ($30.5 \pm 13.8/\text{cm}^2$ in contrast with $91.5 \pm 36.5/\text{cm}^2$ for patients with incidental aneurysms) Microvasospasms on the small cortical arterioles with a reduction of diameter up to 75.1%
Pennings et al. (2004)	OPS	Aneurysmal SAH surgery	16 patients in 2 groups: early surgery group (within 48 h from bleeding) and late surgery group	<ul style="list-style-type: none"> In the early surgery group provoked hypotension resulted in a decrease of $39 \pm 15\%$ in arteriolar diameter, while in the late surgery group the decrease was estimated to $17 \pm 20\%$ compared to $7 \pm 7\%$ in controls Microvascular tonus is significantly increased after SAH, suggesting a potential role in the pathogenesis of vasospasm-induced ischemia
Pennings et al. (2006)	OPS	Imaging of the peri-nidal region in brain Arterio-Venous Malformation	2 patients with brain AVM—OPS imaging before and after surgical resection	<ul style="list-style-type: none"> Significant increase in microvascular flow in the peri-nidal brain with an MFI raising from 2 to 3.7 and FCD raising from $1.4 \pm 1.3 \text{ cm/mm}^2$ to $2.1 \pm 0.8 \text{ cm/mm}^2$ Data were consistent with the hyperperfusion syndrome and normal perfusion pressure breakthrough
Pennings et al. (2009)	OPS	Aneurysmal SAH surgery—response of brain microcirculation to topical papaverine	14 patients operated on with aneurysmal SAH versus 3 patients with deep pathology not affecting the cortical microcirculation (control group)	<ul style="list-style-type: none"> Unpredictable response to topical papaverine with both dilatation and constriction observed Risk of a rebound effect Diminished vasodilatory capacity of the cerebral microcirculation after subarachnoid hemorrhage still to be confirmed
Pérez-Bárcena et al. (2011)	SDF	Cortical microcirculation in stroke	6 patients with stroke operated on for decompressive craniectomy versus 5 neurosurgical patients without cortical microcirculation pathology (control group)	Significant blood flow reduction in the cortical microcirculation and decreased vascular density in patients with stroke
Pérez-Bárcena et al. (2015)	SDF	Cortical microcirculation in traumatic brain injury (TBI)	14 patients with TBI requiring surgery (5 subdural hematomas and 9 parenchymal lesions) versus 5 neurosurgical patients without cortical microcirculation pathology (control group)	<ul style="list-style-type: none"> PPV similar in all groups Perfused vessel density index smaller in the peri-contusional area Overall preservation of microcirculation parameters in TBI
Berhouma et al. (2020)	SDF	Microcirculation in the peritumoral brain edema in intracranial meningiomas	12 patients with intracranial WHO grade I meningiomas split into 2 groups according to the presence (E group) or absence (NE group) of peritumoral edema	<ul style="list-style-type: none"> Severe alterations of vessel density and blood flow parameters in peritumoral edema Partial recovery of microcirculatory parameters after surgical resection due to withdrawal of mass effect only Hypothesis that the severity of microcirculatory alterations may predict the presence of ischemic spots and hence the neurological outcome

Characterization of Peritumoral Perfusion

While peritumoral perfusion can be evaluated intraoperatively with several optical technologies (laser speckle contrast imaging, laser doppler imaging, intraoperative MRI, thermography, etc.), only SDF imaging provides a direct morphological assessment of vessel density and the proportion of perfused vessel in addition to a semiquantitative estimation of blood flow. Until now, the peritumoral perfusion in meningiomas has been studied preoperatively using macroscopic imaging mostly MRI. MR perfusion sequences within the peritumoral brain area remain difficult to interpret mainly because of the poor resolution and the mass effect. Thus, in our series, preoperative MR perfusion was measured only within the meningioma as we were not able to obtain interpretable macroscopic perfusion data within the peritumoral area. Very rare studies have evaluated MR perfusion within the PTBE.⁴⁵ It has been demonstrated that the rCBV is significantly increased in PTBE in WHO grade II and III meningiomas compared with grade I, which is probably because of tumor pial invasion and local brain angiogenesis.¹⁹ Based on these observations, we chose to study only WHO grade I meningiomas to avoid major imaging interference from peritumoral neo-vascularization.

In WHO grade I meningiomas, variations of rCBV in PTBE were the result of different factors, mainly vasogenic edema, angiogenesis, and ischemia secondary to tumoral mass effect. It is still unclear whether one of these factors prevails or is the consequence of the other factors in the pathogenesis of PTBE, even if ischemia appears as a secondary event. Ischemic alterations in the peritumoral brain in meningiomas have been investigated in detail and so has the role of mass effect.^{17,45} Lehmann et al.¹⁸ studied the PTBE in meningiomas with MR perfusion imaging and confirmed an increase in relative maximum signal drop with rising distance from the meningioma, suggesting the role of compression by the mass effect, as demonstrated in our study through the evolution of microcirculatory parameters before and after surgical resection. Tatagiba et al.²³ provided a study of 12 intracranial meningiomas using a xenon-enhanced CT scan. They found CBF values 28% lower in the peritumoral area compared to the ipsilateral hemisphere. According to the authors, the low peritumoral blood flow in meningiomas is not only secondary to vasogenic edema but also results from an ischemic phenomenon due to the mass effect, thus explaining the absence of response to corticosteroids and occasionally definitive postoperative deficits. In our E group, the significant residual microcirculatory alterations after surgical resection were probably secondary to the combined effect of edema and ischemic modifications. We can hypothesize that ischemic changes in the PTBE may result from both vessel density drop as well as perfusion anomalies translating into low MFI and PPV values. The proportion between irreversible ischemic changes and reversible edema in PTBE may condition the postoperative neurological outcome. In our future SDF imaging work, we aim to study the correlation between the degree of in vivo microcirculatory alteration severity within the PTBE in edematous meningiomas and the postoperative neurological outcome to verify if the in vivo peritumoral microcirculatory pattern can eventually predict

the risk of definitive neurological deficits. Furthermore, we may be able to determine if ischemic irreversible alterations are more specifically correlated with either vessel density or blood flow anomalies. These ischemic anomalies in PTBE were also confirmed at a macroscopic level in an MR study by Domingo et al.⁴⁶ The authors showed low CBV with elevated lactate in the PTBE, suggesting that local hypoperfusion and metabolic disturbances may play a potential role in the pathogenesis of PTBE. Bitzer et al.⁴⁵ explored 26 patients with 27 meningiomas and 5 gliomas with perfusion-weighted imaging. The authors concluded that there was no decrease; rather, there was a slight increase in perfusion in peritumoral brain tissue in meningiomas without edema. Though in meningiomas with edema, these perfusion parameters were significantly reduced. Therefore, Bitzer et al. raised the question of whether peritumoral edema caused decreased perfusion or if the reduction in perfusion generated edema. In their study, there were no anomalies in diffusion and perfusion in the peritumoral brain in meningiomas without edema, whereas they demonstrated areas of ischemia with a reduction of Apparent Diffusion Coefficient values in about one-third of meningiomas with edema. The authors noted that these ischemic foci were very limited in size compared to the extent of edema, and they always occurred immediately adjacent to the tumor wall. Since two-thirds of the meningiomas with edema did not exhibit these ischemic features, the authors concluded that ischemia should be regarded as a secondary event in the pathogenesis of PTBE.

Limitations and Perspectives

We aimed to assess the feasibility of intraoperative SDF imaging in meningiomas and to confirm the existence of both perfusion and vessel density alterations in PTBE. A larger series correlating in vivo SDF imaging and preoperative high-definition perfusion MR imaging should confirm our data and moreover explore the ischemic responsibility in the pathogenesis of PTBE. The influence of intraoperative systemic factors (mean arterial pressure, vasoactive drugs, and ETCO_2) on microcirculation in PTBE during surgery may also be evaluated using SDF imaging in larger series.

Notwithstanding we used neuronavigation to perform measurements at the peritumoral locations where the edema was the most superficial, we remained limited to the assessment of the peritumoral cortex, whereas deep peritumoral regions were not accessible. Therefore, our results may not reflect the whole microcirculatory environment of the tumor, which may be heterogeneous, particularly if the majority of peritumoral edema is located deep in the brain tissue not reachable by the SDF registration capacity.

SDF imaging is a contact method requiring an optimal interface with the brain's surface. Pressure-induced microcirculatory alterations are possible and may impair the accuracy of the measured parameters (Figure 5). Noncontact methods are available (laser speckle contrast imaging, thermography, etc.), allowing for the analysis of larger areas but remain sensitive to motion artifacts and do not provide morphological information at the microcirculatory scale (TVD, PPV, etc.).

Other technological refinements that may facilitate intraoperative microcirculation imaging include shorter



Figure 5. Example of SDF imaging (Patient N°4) depicting the importance of the quality of image acquisition to ensure reliable microcirculation parameters and avoid artifacts: A slight local subarachnoid hemorrhage (yellow asterisk) secondary to the craniotomy may alter the image contrast. In this case, wall vessel normally not visible in SDF imaging becomes visible (blue arrow). The presence of fluids between the lens and the cortical surface should also be avoided and may interfere with the visibility of small arterioles distorting the vessel density index (blue asterisks). Please note the sluggish flow pattern (MFI<2) resulting in very low columns of globular erythrocytes (yellow arrows).

data acquisition with automated analysis and an incident light beam probe (incident dark-field imaging) that could potentially offer a better image resolution.⁴⁷

Conclusions

Even though our study was limited to very few patients, it has clearly confirmed the feasibility of *in vivo* SDF microcirculation imaging in brain surgery and showed quantitatively severe alterations of both perfusion and vessel density parameters in PTBE, confirming the vulnerability of the peritumoral microcirculation in edematous meningiomas. Whether the severity of these alterations may correlate with ischemic foci in PTBE and thus predict the postoperative neurological outcome is still not known. Obviously, SDF imaging opens new insights in the exploration of brain microcirculation.

Supplementary Data

Supplementary data are available at *Neuro-Oncology Advances* online.

Keywords

ischemia | meningioma | microcirculation | peritumoral edema | sidestream dark-field imaging

Funding

None declared.

Conflict of interest statement. The authors declared no potential conflicts of interest with respect to the research, authorship, and/or publication of this article.

Authorship Statement. All authors have critically revised the manuscript and approved its final content. Manuscript draft, analysis, and interpretation of the data: M.B. and A.C.L. Acquisition of the data: M.B., T.P., C.D., and J.G. Conception and design of the study: M.B., J.G., I.P.G., O.E., D.M., J.H., F.D., and F.C. Interpretation of the data: M.B., A.C.L., and F.C.

References

- Claus EB, Bondy ML, Schildkraut JM, Wiemels JL, Wrensch M, Black PM. Epidemiology of intracranial meningioma. *Neurosurgery*. 2005;57(6):1088–1095; discussion 1088.
- Go KG, Wilimink JT, Molenaar WM. Peritumoral brain edema associated with meningiomas. *Neurosurgery*. 1988;23(2):175–179.
- Lieu AS, Howng SL. Intracranial meningiomas and epilepsy: incidence, prognosis and influencing factors. *Epilepsy Res*. 2000;38(1):45–52.
- Alaywan M, Sindou M. [Prognostic factors in the surgery for intracranial meningioma. Role of the tumoral size and arterial vascularization originating from the pia mater. Study of 150 cases]. *Neurochirurgie*. 1993;39(6):337–347.
- Vignes JR, Sesay M, Rezajooi K, Gimbert E, Liguoro D. Peritumoral edema and prognosis in intracranial meningioma surgery. *J Clin Neurosci*. 2008;15(7):764–768.
- Morin O, Chen WC, Nassiri F, et al. Integrated models incorporating radiologic and radiomic features predict meningioma grade, local failure, and overall survival. *Neurooncol Adv*. 2019;1(1):vdz011.
- Bitzer M, Wöckel L, Luft AR, et al. The importance of pial blood supply to the development of peritumoral brain edema in meningiomas. *J Neurosurg*. 1997;87(3):368–373.
- Goldman CK, Bharara S, Palmer CA, et al. Brain edema in meningiomas is associated with increased vascular endothelial growth factor expression. *Neurosurgery*. 1997;40(6):1269–1277.
- Yoshioka H, Hama S, Taniguchi E, Sugiyama K, Arita K, Kurisu K. Peritumoral brain edema associated with meningioma: influence of vascular endothelial growth factor expression and vascular blood supply. *Cancer*. 1999;85(4):936–944.
- Inamura T, Nishio S, Takeshita I, Fujiwara S, Fukui M. Peritumoral brain edema in meningiomas—fluence of vascular supply on its development. *Neurosurgery*. 1992;31(2):179–185.
- Bradac GB, Ferszt R, Bender A, Schörner W. Peritumoral edema in meningiomas. A radiological and histological study. *Neuroradiology*. 1986;28(4):304–312.
- Hou J, Kshettry VR, Selman WR, Bambakidis NC. Peritumoral brain edema in intracranial meningiomas: the emergence of vascular endothelial growth factor-directed therapy. *Neurosurg Focus*. 2013;35(6):E2.

13. Berhouma M, Jacquesson T, Jouanneau E, Cotton F. Pathogenesis of peri-tumoral edema in intracranial meningiomas. *Neurosurg Rev*. 2019;42(1):59–71.
14. Huang RY, Bi WL, Griffith B, et al. Imaging and diagnostic advances for intracranial meningiomas. *Neuro Oncol*. 2019;21(Suppl. 1):i44–i61.
15. Tamrazi B, Shiroishi MS, Liu CS. Advanced Imaging of Intracranial Meningiomas. *Neurosurg Clin N Am*. 2016;27(2):137–143.
16. Nassehi D, Sørensen LP, Dyrbye H, et al. Peritumoral brain edema in angiomatic supratentorial meningiomas: an investigation of the vascular endothelial growth factor A pathway. *APMIS*. 2013;121(11):1025–1036.
17. Sergides I, Hussain Z, Naik S, Good C, Miles K, Critchley G. Utilization of dynamic CT perfusion in the study of intracranial meningiomas and their surrounding tissue. *Neural Res*. 2009;31(1):84–89.
18. Lehmann P, Vallée JN, Saliou G, et al. Dynamic contrast-enhanced T2*-weighted MR imaging: a peritumoral brain oedema study. *J Neuroradiol*. 2009;36(2):88–92.
19. Zhang H, Rödiger LA, Shen T, Miao J, Oudkerk M. Perfusion MR imaging for differentiation of benign and malignant meningiomas. *Neuroradiology*. 2008;50(6):525–530.
20. Martin AJ, Cha S, Higashida RT, et al. Assessment of vasculature of meningiomas and the effects of embolization with intra-arterial MR perfusion imaging: a feasibility study. *AJNR Am J Neuroradiol*. 2007;28(9):1771–1777.
21. Kimura H, Takeuchi H, Koshimoto Y, et al. Perfusion imaging of meningioma by using continuous arterial spin-labeling: comparison with dynamic susceptibility-weighted contrast-enhanced MR images and histopathologic features. *AJNR Am J Neuroradiol*. 2006;27(1):85–93.
22. Uematsu H, Maeda M, Itoh H. Peritumoral brain edema in intracranial meningiomas evaluated by dynamic perfusion-weighted MR imaging: a preliminary study. *Eur Radiol*. 2003;13(4):758–762.
23. Tatagiba M, Mirzai S, Samii M. Peritumoral blood flow in intracranial meningiomas. *Neurosurgery*. 1991;28(3):400–404.
24. Pérez-Bárcena J, Romay E, Llompart-Pou JA, et al. Direct observation during surgery shows preservation of cerebral microcirculation in patients with traumatic brain injury. *J Neurol Sci*. 2015;353(1–2):38–43.
25. Boerma EC, van der Voort PH, Ince C. Sublingual microcirculatory flow is impaired by the vasopressin-analogue terlipressin in a patient with catecholamine-resistant septic shock. *Acta Anaesthesiol Scand*. 2005;49(9):1387–1390.
26. Eriksson S, Nilsson J, Sturesson C. Non-invasive imaging of microcirculation: a technology review. *Med Devices (Auckl)*. 2014;7:445–452.
27. Charlton M, Sims M, Coats T, Thompson JP. The microcirculation and its measurement in sepsis. *J Intensive Care Soc*. 2017;18(3):221–227.
28. Trittmacher S, Traupe H, Schmid A. Pre- and postoperative changes in brain tissue surrounding a meningioma. *Neurosurgery*. 1988;22(5):882–885.
29. Pérez-Bárcena J, Goedhart P, Ibáñez J, et al. Direct observation of human microcirculation during decompressive craniectomy after stroke. *Crit Care Med*. 2011;39(5):1126–1129.
30. Goedhart PT, Khalilzada M, Bezemer R, Merza J, Ince C. Sidestream dark field (SDF) imaging: a novel stroboscopic LED ring-based imaging modality for clinical assessment of the microcirculation. *Opt Express*. 2007;15(23):15101–15114.
31. Dostal P, Schreiberova J, Dostalova V, et al. Effects of hypertonic saline and mannitol on cortical cerebral microcirculation in a rabbit craniotomy model. *BMC Anesthesiol*. 2015;15:88.
32. Dostalova V, Schreiberova J, Dostalova V, et al. Effects of hypertonic saline and sodium lactate on cortical cerebral microcirculation and brain tissue oxygenation [published ahead of print]. *J Neurosurg Anesthesiol*. 2018;30(2):163–170.
33. De Backer D, Hollenberg S, Boerma C, et al. How to evaluate the microcirculation: report of a round table conference. *Crit Care*. 2007;11(5):R101.
34. Uhl E, Lehmberg J, Steiger H-J, Messmer K. Intraoperative detection of early microvasospasm in patients with subarachnoid hemorrhage by using orthogonal polarization spectral imaging. *Neurosurgery*. 2003;52(6):1307–1315.
35. Guven G, Hilty MP, Ince C. Microcirculation: physiology, pathophysiology, and clinical application [published online December 18]. *Blood Purif*. 2020;49(1–2):143–150.
36. Guterman David D, Chabowski Dawid S, Kadlec Andrew O, et al. The human microcirculation. *Circ Res*. 2016;118(1):157–172.
37. Vinke EJ, Eyding J, de Korte C, Slump CH, van der Hoeven JG, Hoedemaekers CWE. Quantification of macrocirculation and microcirculation in brain using ultrasound perfusion imaging. *Acta Neurochir Suppl*. 2018;126:115–120.
38. Wan Z, Ristagno G, Sun S, Li Y, Weil MH, Tang W. Preserved cerebral microcirculation during cardiogenic shock. *Crit Care Med*. 2009;37(8):2333–2337.
39. Klijn E, Den Uil CA, Bakker J, Ince C. The heterogeneity of the microcirculation in critical illness. *Clin Chest Med*. 2008;29(4):643–54, viii.
40. De Backer D, Creteur J, Preiser JC, Dubois MJ, Vincent JL. Microvascular blood flow is altered in patients with sepsis. *Am J Respir Crit Care Med*. 2002;166(1):98–104.
41. Craigie EH. The architecture of the cerebral capillary bed. *Biol Rev Camb Philos Soc*. 1945;20:133–146.
42. Slaaf DW, Tangelder GJ, Reneman RS, Jäger K, Bollinger A. A versatile incident illuminator for intravital microscopy. *Int J Microcirc Clin Exp*. 1987;6(4):391–397.
43. Groner W, Winkelman JW, Harris AG, et al. Orthogonal polarization spectral imaging: a new method for study of the microcirculation. *Nat Med*. 1999;5(10):1209–1212.
44. Pennings FA, Bouma GJ, Ince C. Direct observation of the human cerebral microcirculation during aneurysm surgery reveals increased arteriolar contractility. *Stroke*. 2004;35(6):1284–1288.
45. Bitzer M, Klose U, Geist-Barth B, et al. Alterations in diffusion and perfusion in the pathogenesis of peritumoral brain edema in meningiomas. *Eur Radiol*. 2002;12(8):2062–2076.
46. Domingo Z, Rowe G, Blamire AM, Cadoux-Hudson TA. Role of ischaemia in the genesis of oedema surrounding meningiomas assessed using magnetic resonance imaging and spectroscopy. *Br J Neurosurg*. 1998;12(5):414–418.
47. van Elteren HA, Ince C, Tibboel D, Reiss IK, de Jonge RC. Cutaneous microcirculation in preterm neonates: comparison between sidestream dark field (SDF) and incident dark field (IDF) imaging. *J Clin Monit Comput*. 2015;29(5):543–548.

Supplementary data

	Reference point (control)	Peri-tumoral area (n=6)	p
De Backer score (mm ⁻¹)	6.30 ± 0.66	5.68 ± 0.67	0.1173
MFI	3	2.91 ± 0.11	0.0481
TVD (mm.mm ⁻²)	6.35 ± 0.43	6.13 ± 0.37	0.3271
SVD (mm.mm ⁻²)	4.93 ± 0.27	4.75 ± 0.46	0.4408
PVD (mm.mm ⁻²)	6.30 ± 0.42	6.06 ± 0.32	0.2353
PPV (%)	99.35 ± 1.17	98.96 ± 1.46	0.6782

Table 1. Microcirculatory parameters at the reference point (control) at baseline compared with the peri-tumoral area in the NE group.

MFI: Mean flow index, TVD: Total vessel density, SVD: Small vessel density, PVD: Perfused vessel density, PPV: Proportion of perfused vessels

	Reference point (control)	PTBE (n=6)	p
De Backer score (mm ⁻¹)	6.30 ± 0.66	3.1 ± 0.15	<0.0001
MFI	3	1.62 ± 0.12	<0.0001
TVD (mm.mm ⁻²)	6.35 ± 0.43	2.9 ± 0.27	<0.0001
SVD (mm.mm ⁻²)	4.93 ± 0.27	1.56 ± 0.33	<0.0001
PVD (mm.mm ⁻²)	6.30 ± 0.42	1.48 ± 0.38	<0.0001
PPV (%)	99.35 ± 1.17	51.06 ± 11.62	0.0003

Table 2. Microcirculatory parameters at the reference point (control) at baseline compared with the peri-tumoral brain edema (PTBE) area in the E group.

MFI: Mean flow index, TVD: Total vessel density, SVD: Small vessel density, PVD: Perfused vessel density, PPV: Proportion of perfused vessels

	Baseline (n=6)	Post-resection (n=6)	p
De Backer score (mm ⁻¹)	5.68 ± 0.67	6.21 ± 0.71	0.0044
MFI	2.91 ± 0.11	3	0.3457
TVD (mm.mm ⁻²)	6.13 ± 0.37	6.35 ± 0.44	0.1152
SVD (mm.mm ⁻²)	4.75 ± 0.46	4.68 ± 0.45	0.4441
PVD (mm.mm ⁻²)	6.06 ± 0.32	6.26 ± 0.40	0.0667
PPV (%)	98.96 ± 1.46	98.72 ± 1.03	1

Table 3. Evolution of microcirculatory parameters in the peri-tumoral area after surgical resection in NE group.

MFI: Mean flow index, TVD: Total vessel density, SVD: Small vessel density, PVD: Perfused vessel density, PPV: Proportion of perfused vessels

	Baseline (n=6)	Post-resection (n=6)	p
De Backer score (mm ⁻¹)	3.1 ± 0.15	3.65 ± 0.28	0.0066
MFI	1.62 ± 0.12	2.29 ± 0.48	0.0590
TVD (mm.mm ⁻²)	2.9 ± 0.27	3.25 ± 0.39	0.0235
SVD (mm.mm ⁻²)	1.56 ± 0.33	2.28 ± 0.35	0.0022
PVD (mm.mm ⁻²)	1.48 ± 0.38	2.38 ± 0.67	0.0066
PPV (%)	51.06 ± 11.62	72.95 ± 17.09	0.0312

Table 4. Evolution of microcirculatory parameters in the PTBE after surgical resection in E group.
MFI: Mean flow index, TVD: Total vessel density, SVD: Small vessel density, PVD: Perfused vessel density, PPV: Proportion of perfused vessels

VI - SYNTHESE - PERSPECTIVES

La microcirculation cérébrale joue un rôle primordial dans le couplage débit sanguin/métabolisme cérébral. L'imagerie et/ou le monitoring de la microcirculation aide à mieux comprendre les mécanismes complexes de ce couplage mais permettrait également de réduire la morbidité/mortalité durant certaines interventions neurochirurgicales. Différentes technologies d'imagerie per-opératoire de la microcirculation ont été décrites (Cf. chapitre III) mais aucune ne remplit complètement tous les critères permettant de parler de technique « optimale » : analyse en temps réel, simplicité d'utilisation, excellente résolution spatiale, analyse morphologique microvasculaire et quantification du débit sanguin cérébral, et intégration parfaite dans le travail chirurgical (intégration au microscope opératoire par exemple). Parmi ces technologies, nous avons choisi la vidéomicroscopie sidestream dark field car elle permet une étude morphologique (visualisation directe de la microcirculation et estimation de la densité vasculaire) outre l'étude de la perfusion. Cette technique est également abordable par rapport à d'autres techniques moins accessibles (techniques laser, IRM peropératoire, ...). Elle n'a été essayée en peropératoire que dans de rares cas cliniques principalement en pathologie neurovasculaire. A notre connaissance, notre étude de faisabilité en pathologie tumorale cérébrale est donc originale. Pour cette étude, nous avons opté pour l'étude de la microcirculation péri-tumorale dans les méningiomes intracrâniens. En effet, dans ce domaine spécifique, plusieurs questions demeurent sans réponses en particulier concernant le rôle joué par la microcirculation péritumorale dans la pathogénie de l'œdème. Une meilleure compréhension des phénomènes microvasculaires en jeu dans la zone péritumorale est capitale, d'autant qu'il est maintenant établi que l'œdème péritumoral dans les méningiomes intracrâniens impacte la morbidité et la mortalité. Plus encore, de récentes études de radiomique [21] ont mis en évidence le caractère prédictif de cet œdème sur le grade histo-pronostique des méningiomes, en plus du coefficient de diffusion apparent et la morphologie tumorale (« sphéricité »).

- a) Évolution des techniques d'imagerie de la microcirculation cérébrale :

Étant donnée l'absence actuelle d'une technologie unique optimale permettant une étude en temps réel de la microcirculation tant sur le plan morphologique que sur le plan de la perfusion tissulaire, l'association de plusieurs technologies complémentaires dans un même appareillage peropératoire pourrait s'avérer très intéressant. L'exemple récent de l'association du laser speckle contrast imaging et de la vidéomicroscopie SDF illustre parfaitement la complémentarité entre les deux techniques intégrées dans un module compact facilitant un usage potentiel en salle opératoire (Figure 1). [22]

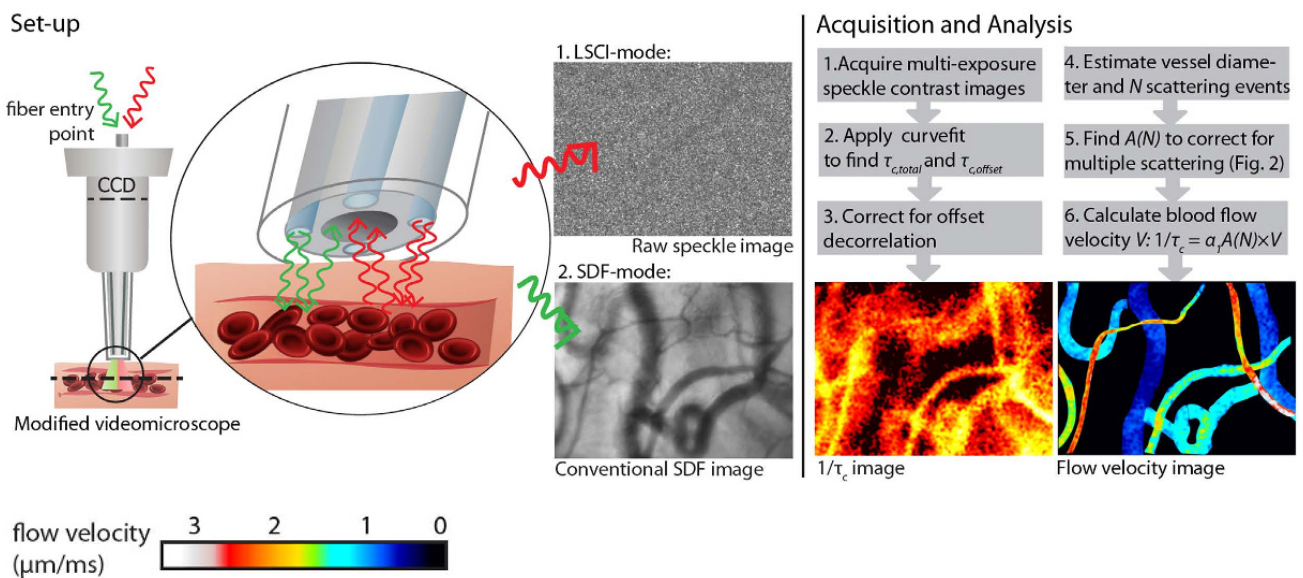


Figure 1. Dispositif associant vidéomicroscopie SDF et imagerie laser speckle. (Nadort A et al.)

L'association d'une technologie spécifiquement dédiée au monitorage du débit sanguin cérébral (laser speckle par exemple) et d'une technique de mesure du métabolisme cérébral (thermographie, near-infrared spectroscopy) permettrait en théorie de mieux appréhender la physiopathologie du couplage débit/métabolisme et probablement d'affiner la cartographie fonctionnelle cortico-sous-corticale peropératoire. [23] La miniaturisation des dispositifs, leur intégration dans le déroulement du travail chirurgical en particulier au microscope opératoire (Figure 2) [24], et la possibilité in fine d'obtenir un monitoring

morphologique et quantitatif microvasculaire devraient rendre l'usage peropératoire de ces technologies plus courant.

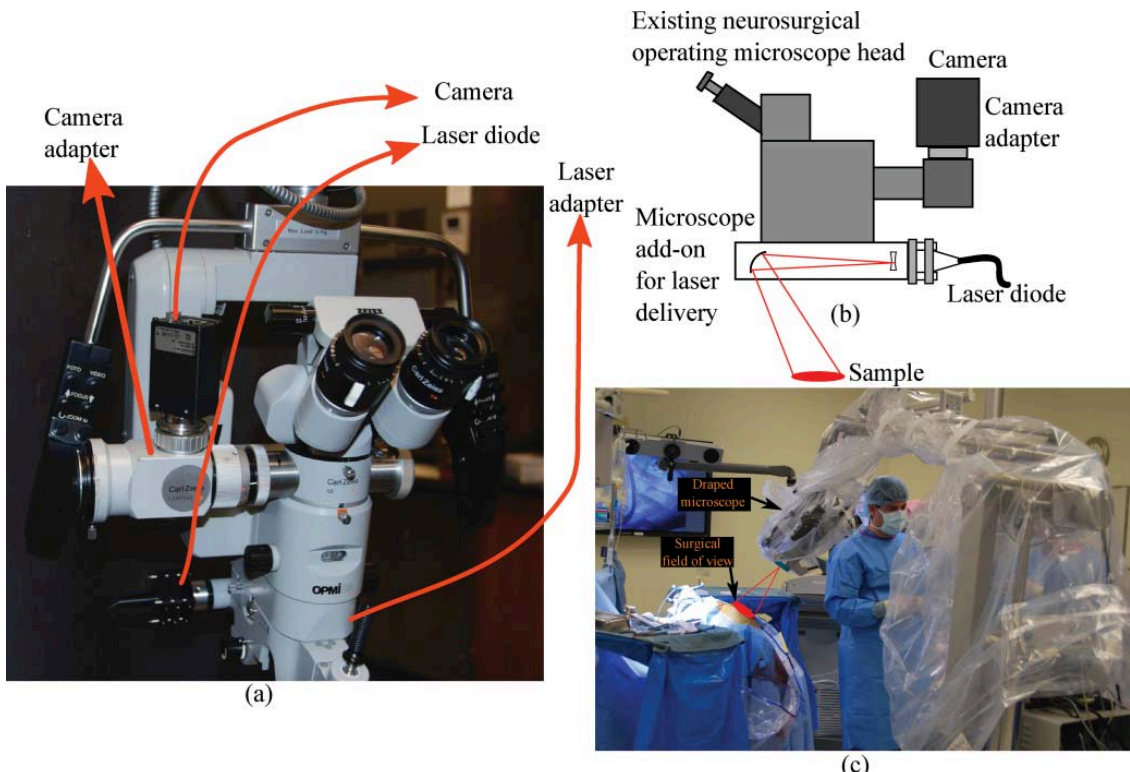


Figure 2. Prototype d'intégration d'un laser speckle au microscope opératoire (Parthasarathy AB et al.)

Telle qu'expérimentée dans notre étude, la vidéomicroscopie requiert un contact avec le tissu cérébral avec un risque d'artefact de mouvement et de pression, en particulier lorsque les mouvements pulsatiles cérébraux sont marqués chez certains patients. Ces techniques de contact, mais également les autres techniques (Laser speckle, thermographie, spectroscopie infrarouge, ...) ne permettent qu'un monitorage de la surface visible, ce qui ne reflète pas nécessairement les anomalies microcirculatoires possibles en profondeur (ce que permet l'IRM ou l'artériographie peropératoire, ou indirectement le neuromonitoring électrophysiologique des faisceaux cortico-sous-corticaux).

b) Perspectives en neuro-oncologie :

L'imagerie conventionnelle pré-opératoire (IRM en particulier) ne permet pas d'identifier clairement d'éventuelles lésions ischémiques au sein de la plage œdémateuse

péritumorale. Or l'existence de telles lésions peut conditionner le pronostic fonctionnel post-opératoire, d'où l'importance de pouvoir les caractériser soit en préopératoire à l'aide d'imageries diagnostiques précises soit plus facilement en peropératoire l'aide de technologies d'imagerie de la microcirculation. Il s'agit d'un possible projet prolongeant notre travail, dans lequel nous envisageons d'associer le laser speckle pour sa capacité à analyser des zones cérébrales plus étendues et son intégration au microscope opératoire, et la vidéomicroscopie SDF, seule technique permettant une imagerie morphologique de la microcirculation en particulier la densité vasculaire. Cette étude permettrait de rechercher une corrélation entre un seuil de perfusion et de densité microcirculatoires péri-tumorales et l'état fonctionnel post-opératoire notamment la capacité de récupération d'un déficit neurologique pré-chirurgical. Outre cette corrélation, il serait intéressant de rechercher un éventuel rapport entre ces anomalies microcirculatoires et le profil moléculaire et/ou le grading tumoral.

Par ailleurs, que ce soit dans le cadre des méningiomes intracrâniens ou d'autres types de tumeurs cérébrales, l'imagerie de la microcirculation péri-tumorale pourrait permettre d'investiguer l'éventuelle relation entre la densité microvasculaire et la réponse aux anticorps anti-VEGF tel le Bevacizumab.

Enfin, dans certaines tumeurs qui, macroscopiquement, miment parfaitement le tissu cérébral adjacent tels les gliomes de grades II de l'OMS, la visualisation d'une architecture microcirculatoire spécifique (densité, perfusion, néovascularisation...) pourrait permettre d'étendre les limites de l'exérèse chirurgicale.

Ainsi, alors que son rôle semble évident en neurochirurgie des malformations vasculaires cérébrales, l'imagerie de la microcirculation ouvre des perspectives intéressantes en neuro-oncologie tant sur le plan du diagnostic histo-moléculaire que sur la compréhension de la réponse aux traitements médicaux en particulier les anti-VEGF.

CONCLUSION

A travers l'étude des anomalies microcirculatoires dans l'œdème péri-tumoral des méningiomes intracrâniens, notre travail a confirmé la faisabilité de l'imagerie peropératoire de la microcirculation cérébrale grâce à la vidéomicroscopie sidestream dark

field. L'association de cette dernière à une technologie à résolution spatiale plus importante permettant de monitorer des surfaces corticales plus étendues (laser speckle contrast par exemple) pourrait à terme permettre de cartographier les fonctions cérébrales en complément des techniques électrophysiologiques communément utilisées ou de surveiller en temps réel l'effet d'un clampage vasculaire temporaire

REFERENCES

1. Guterman DD, Chabowski DS, Kadlec AO, Durand MJ, Freed JK, Ait-Aissa K, Beyer AM. The Human Microcirculation: Regulation of Flow and Beyond. *Circ Res.* 2016 Jan 8;118(1):157-72
2. Zlokovic BV. Neurovascular pathways to neurodegeneration in Alzheimer's disease and other disorders. *Nat Rev Neurosci.* 2011 Nov 3;12(12):723-38
3. Löscher W, Potschka H. Drug resistance in brain diseases and the role of drug efflux transporters. *Nat Rev Neurosci.* 2005 Aug;6(8):591-602
4. Miyoshi J, Takai Y. Molecular perspective on tight-junction assembly and epithelial polarity. *Adv Drug Deliv Rev.* 2005 Apr 25;57(6):815-55
5. Abbott NJ, Ronnback L and Hansson E (2006) Astrocyte-endothelial interactions at the blood-brain barrier. *Nat Rev Neurosci* 7(1):41-53
6. Sokoloff L. Relationships among local functional activity, energy metabolism, and blood flow in the central nervous system. *Fed Proc.* 1981 Jun;40(8):2311-6
7. Zhu XH, Zhang Y, Zhang N, Ugurbil K, Chen W. Noninvasive and three-dimensional imaging of CMRO₂ in rats at 9.4 T: reproducibility test and normothermia/hypothermia comparison study. *J Cereb Blood Flow Metab.* 2007 Jun;27(6):1225-34
8. Howarth C. The contribution of astrocytes to the regulation of cerebral blood flow. *Front Neurosci.* 2014 May 9;8:103
9. Caro, C.G., Fitz-Gerald, J.M. & Schroter, R.C. (1969) Arterial wall shear and distribution of early atheroma in man. *Nature*, 223, 1159-1160.

10. Ando J, Yamamoto K. Vascular mechanobiology: endothelial cell responses to fluid shear stress. *Circ J.* 2009 Nov;73(11):1983-92
11. Dupui P, Géraud G. Régulation de la circulation cérébrale. *EMC Neurologie*, 17-003-C-10, 2006
12. Iadecola C, Xu X. Nitro-L-arginine attenuates hypercapnic cerebrovasodilation without affecting cerebral metabolism. *Am J Physiol.* 1994 Feb;266(2 Pt 2):R518-25
13. Willie, C.K., Macleod, D.B., Shaw, A.D., Smith, K.J., Tzeng, Y.C., Eves, N.D., Ikeda, K., Graham, J., Lewis, N.C., Day, T.A. & Ainslie, P.N. (2012) Regional brain blood flow in man during acute changes in arterial blood gases. *The Journal of physiology*, 590, 3261- 3275.
14. Bolduc, V., Thorin-Trescases, N. & Thorin, E. (2013) Endothelium-dependent control of cerebrovascular functions through age: exercise for healthy cerebrovascular aging. *Am J Physiol Heart Circ Physiol*, 305, H620-633
15. Hamel, E. (2006) Perivascular nerves and the regulation of cerebrovascular tone. *J Appl Physiol* (1985), 100, 1059-1064.
16. Reading, S.A. & Brayden, J.E. (2007) Central role of TRPM4 channels in cerebral blood flow regulation. *Stroke*, 38, 2322-2328
17. Lassen, N.A. (1959) Cerebral blood flow and oxygen consumption in man. *Physiol Rev*, 39, 183-238.
18. Willie, C.K., Tzeng, Y.C., Fisher, J.A. & Ainslie, P.N. (2014) Integrative regulation of human brain blood flow. *J Physiol*, 592, 841-859
19. Tan, C.O. (2012) Defining the characteristic relationship between arterial pressure and cerebral flow. *Journal of applied physiology*, 113, 1194-1200
20. Hamner, J.W. & Tan, C.O. (2014) Relative contributions of sympathetic, cholinergic, and myogenic mechanisms to cerebral autoregulation. *Stroke* 45, 1771-1777
21. Morin O, Chen WC, Nassiri F, et al. Integrated models incorporating radiologic and radiomic features predict meningioma grade, local failure, and overall survival. *Neurooncol Adv.* 2019;1(1). doi:10.1093/noajnl/vdz011

22. Nadort A, Kalkman K, van Leeuwen TG, Faber DJ. Quantitative blood flow velocity imaging using laser speckle flowmetry. *Scientific Reports* 6(1):1–10 (2016)
23. Suzuki T, Oishi N, Fukuyama H. Simultaneous infrared thermal imaging and laser speckle imaging of brain temperature and cerebral blood flow in rats. *J Biomed Opt* 24(3):1–11 (2018)
24. Parthasarathy AB, Weber EL, Richards LM, Fox DJ, Dunn AK. Laser speckle contrast imaging of cerebral blood flow in humans during neurosurgery: a pilot clinical study. *J Biomed Opt* 15(6):066030 (2010)